Technical Report HL-96-14
April 1996

US Army Corps of Engineers
Waterways Experiment Station

Three-Dimensional Numerical Simulation of Seasonal Flow and Salt Transport for the C&D Canal

by Bernard B. Hsieh, David R. Richards

Prepared for U.S. Army Engineer District, Philadelphia

PRINTED ON RECYCLED PAPER

DISCLAIMER NOTICE

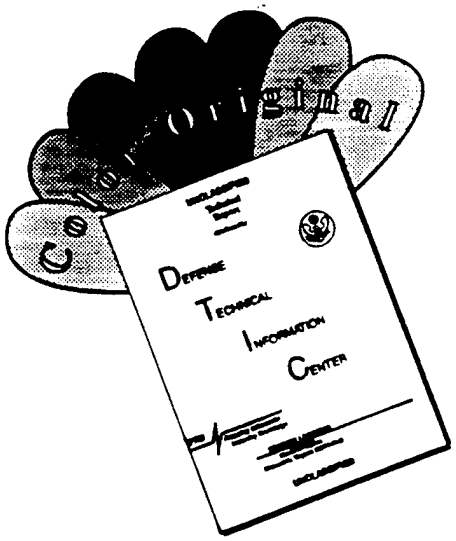

THIS DOCUMENT IS BEST QUALITY AVAILABLE. THE COPY FURNISHED TO DTIC CONTAINED A SIGNIFICANT NUMBER OF COLOR PAGES WHICH DO NOT REPRODUCE LEGIBLY ON BLACK AND WHITE MICROFICHE.

Technical Report HL-96-14
April 1996

Three-Dimensional Numerical Simulation of Seasonal Flow and Salt Transport for the C&D Canal

by Bernard B. Hsieh, David R. Richards

U.S. Army Corps of Engineers
Waterways Experiment Station
3909 Halls Ferry Road
Vicksburg, MS 39180-6199

Final report

Approved for public release; distribution is unlimited

Prepared for U.S. Army Engineer District, Philadelphia
Philadelphia, PA 19107-3390

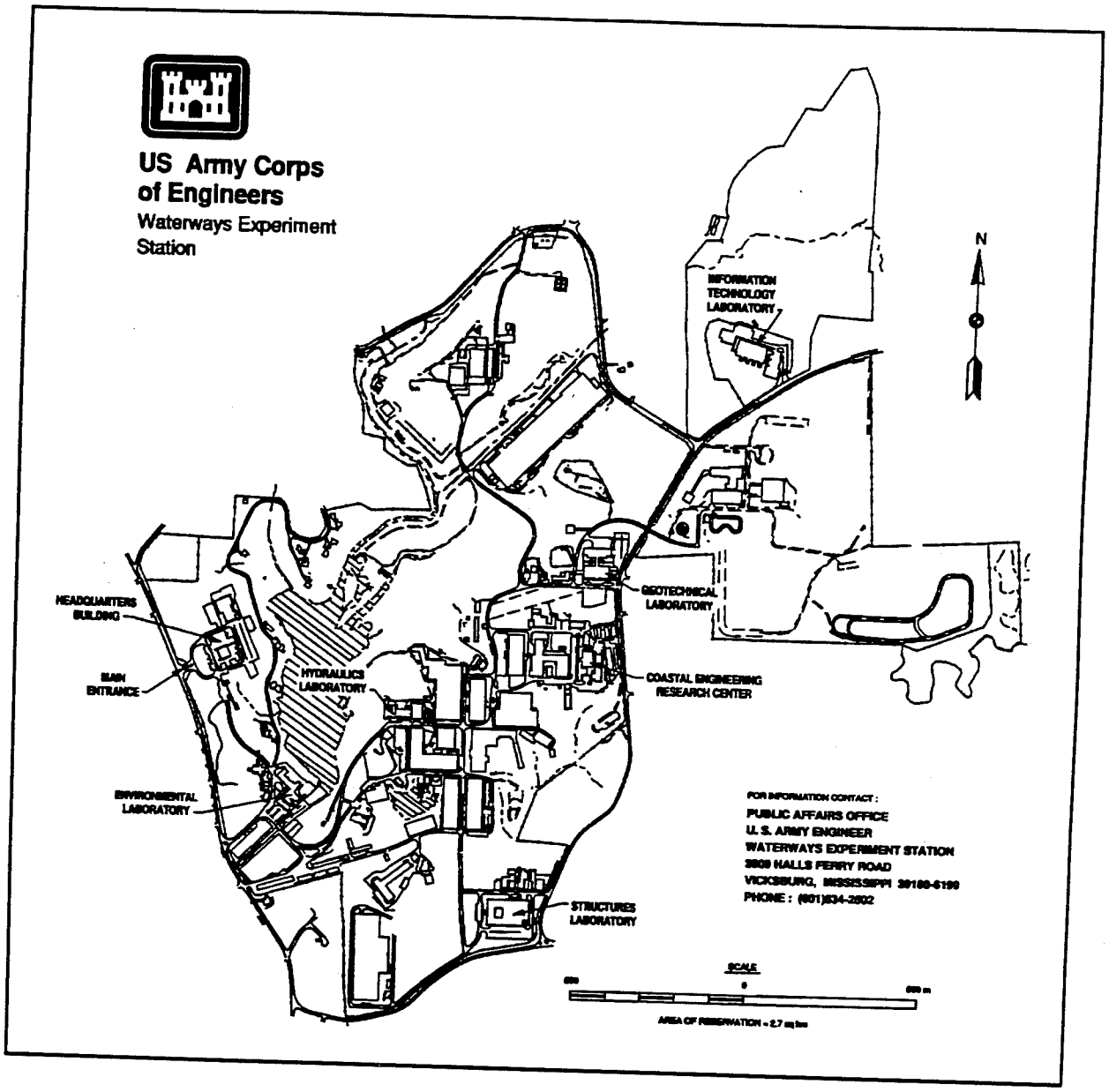

Waterways Experiment Station Cataloging-in-Publication Data

Hsieh, Bernard Bor-Nian.

Three-dimensional numerical simulation of seasonal flow and salt transport for the C&D Canal / by Bernard B. Hsieh, David R. Richards ; prepared for U.S. Army Engineer District, Philadelphia.

124 p. : ill. ; 28 cm. — (Technical report ; HL-96-14)

Includes bibliographical references.

1. Saltwater encroachment — Mathematical models. 2. Estuaries — Delaware — Delaware Bay. 3. Estuaries — Maryland — Chesapeake Bay. 4. Chesapeake and Delaware Canal (Del. and Md.) I. Richards David R. II. United States. Army. Corps of Engineers. Philadelphia District. III. U.S. Army Engineer Waterways Experiment Station. IV. Hydraulics Laboratory (U.S. Army Engineer Waterways Experiment Station) V. Title. VI. Series: Technical report (U.S. Army Engineer Waterways Experiment Station) ; HL-96-14.

TA7 W34 no.HL-96-14

Contents

Preface

This study was funded by the U.S. Army Engineer District, Philadelphia, and conducted at the U.S. Army Engineer Waterways Experiment Station (WES) by personnel of the Hydraulics Laboratory (HL) under the general direction of Messrs. F. A. Herrmann, Jr., Director, HL; R. A. Sager, Assistant Director, HL; W. H. McAnally, Chief, Estuaries Division (ED), HL; and D. R. Richards, Chief, Estuarine Simulation Branch, ED. Principal investigators and authors of this report were Dr. B. B. Hsieh and Mr. D. R. Richards, Estuarine Simulation Branch.

At the time of publication of this report, Director of WES was Dr. Robert W. Whalin. Commander was COL Bruce K. Howard, EN..

Conversion Factors, Non-SI to SI Units of Measurement

Non-SI units of measurement used in this report can be converted to SI units as follows:

Multiply	By	To Obtain
cubic feet per second	0.02831685	cubic meters
feet	0.3048	meters
miles (U.S. statute)	1.609347	kilometers

1 Introduction

Purpose and Scope of Work

The Chesapeake and Delaware (C&D) Canal (Figure 1) is a sea level, man-made canal joining two large estuarine systems. The 28 km canal extends from Reedy Point on the Delaware estuary to Welch Point on the Elk River, a tributary of the Upper Chesapeake Bay. The objective of the C&D Canal model study is to determine the net transport through the canal for various forcing conditions over two (spring and fall) seasonal periods. study the impact of increasing the authorized project depth from 35 feet MLW (existing) to 40 feet MLW (proposed) in the eastern end of the C&D Canal and the channel between Courthouse Point and Poole's Island in the Upper Chesapeake Bay.

To identify and quantify these transports, a three-dimensional hydrodynamic model was used to simulate the management concerns. Two time periods were identified as particularly important for environmental reasons and they were selected as model verification periods. The first period covered the low-flow season (from September to November) and represented the most significant period for drinking water concerns. The second period covered the high-flow season (from April to June), and represented environmental concerns because it is the most active spawning period for many living resources. This three-month period was also identified by biologists as a critical period for striped bass and other indicator species.

Review of Previous Study Findings

The most recent enlargement of the project to accommodate larger vessels began in 1963 and was completed in late 1975. The resulting cross-section has an authorized depth of 35 ft (10.7 m) below mean low water and a bottom width of 450 ft (137.2 m). A 1987 hydrographic survey indicated the average depth of the canal was 40 ft (12.2 m) except for 1.5 miles on the eastern end which was 35 ft (10.7 m).

A three-dimensional (3-D) hydrodynamic model of the C&D Canal and adjacent estuaries was developed using CH3D-WES (Hsieh, Johnson and

Richards, 1993). The finite difference numerical method was used to solve the governing equations of motion on a boundary-fitted grid. This method has a more accurate resolution of complex horizontal geometry than the traditional rectilinear finite difference grids. A special feature of the model is a simplified vertical turbulence model based on the assumption of local turbulence equilibrium.

The first phase of modeling used the field measurements from September 1984 since it had the most complete data available. The accuracy of model verification depended on accurate tidal datums and salinity values at the open model boundaries. The results indicated that in both the model calculations and the field data there was a net transport in the C&D Canal in the westward direction. Although these seem like large changes, the net effect on salinities was very small. This demonstrated that a narrow channel, such as the C&D Canal, connecting two dynamic water bodies can be successfully modeled using time-varying forcing functions even if the tidal and density forcing functions are highly variable. For further details on model development and verification information, refer to the published report by Hsieh, Johnson, and Richards, 1993.

2 Seasonal Model Verifications

Uncertainties of Boundary and Initial Conditions

Accurate boundary and initial conditions are crucial in the startup and verification of numerical simulations. Even though the salinity time histories at both ends (the Delaware Bay side and the Chesapeake Bay side) of this model domain were not known, it was still possible to construct them as described in the following paragraphs.

Statistical techniques including harmonic analysis and correlation analysis have been used to synthesize time-varying boundary salinities from very limited information. In this case estimation was difficult because salinity amplitude and phase distortion were caused by a very strong salinity gradient between the mouth of the canal and the middle part of Delaware Bay. The major driving force at the boundary is the surface elevation which is a function of tide with wind. In order to determine the water surface boundary condition at the Reedy Point side of the canal, a 33-hour low-pass filter was used to extract the subtidal component from the surface elevation record. Then a highly correlated relationship was found between tidal propagation phase and the salinity variations. A synthetic, time-varying, salinity boundary condition was developed based on available data, correlations between tidal phase propagation and salinity variations, and by using previous studies (Galperin and Mellor, 1990).

The same treatment can be used to generate the salinity boundary for the Chesapeake Bay side. However, since the boundary at the Chesapeake Bay Bridge is strongly influenced by freshwater from the upper Chesapeake Bay, the estimation process was more complicated. Since the estimation technique (Hsieh, in preparation) is still under development, the selected approach was to use the results of the 3-D Chesapeake Bay numerical model (Johnson, et. al. 1991) for the 1984-1986 simulation study. Therefore, the closest data station to the Bay Bridge was used to synthesize the boundary conditions at the Chesapeake Bay model limit.

In general, two sharp salinity gradients are found in this modeling domain. The first gradient is from the ocean source salinity near the mouth of the Delaware Bay to the upstream freshwater near Trenton, New Jersey and through the C&D Canal extends to the upper Chesapeake Bay. A second gradient extends from the ocean source salinity of the mouth of Chesapeake Bay upstream to the freshwater near Conowingo Dam. Information from a previous study by Garvine et. al., 1992, was also used to incorporate the existing data points for developing the initial salinity conditions.

Grid Refinement

In the first phase of modeling, a medium resolution 3-D numerical grid of Upper Chesapeake Bay, a coarse 3-D grid of Delaware Bay, and a fine grid of the C&D Canal and its boundary area were developed. The grid contained 873 active horizontal cells and a maximum of 12 vertical layers, resulting in 3325 computational cells. It required one minute time-steps to achieve model stability and 5.1 CRAY Y-MP CPU hours to complete a one-month simulation. Verification of the low-flow seasonal model using this medium resolution grid required 12.5 CRAY Y-MP hours. Since there were uncertainties in some input parameters and an inability of the medium resolution numerical grid to capture the salinity gradient in the lower Delaware Bay, the initial salinity verification effort showed too much salt entering the system during the latter part of the seasonal model run. This phenomena was not apparent during the previous short-term (monthly) computation.

These modeling inadequacies were eliminated by developing a refined grid, increasing the vertical resolution to 16 layers, and incorporating additional important bathymetric features. The horizontal spacing in the entire Delaware Bay, especially the lower bay, was reduced in order to capture the salinity gradient in the direction of flow. The final version of the grid resulted in 6210 computational cells with 1422 active horizontal grids (Figure 2). This improvement actually reduced the seasonal run time to 4.1 CPU hours because the time-step could be increased to 5 min.

Low-Flow Verification (Low-Flow Base)

The September 1984 model test was extended two months for low-flow verification. The model required the following input: the time-varying water surface and salinity distributions at the Annapolis, Lewes, and Cape May boundaries; an initial salinity field; and wind data from the Baltimore-Washington International (BWI) and Wilmington Airports. The freshwater inflows came from the Patapsco, Elk, Sassafras, Chester, and Susquehanna Rivers on the Chesapeake Bay side, and the Delaware, Schuylkill, Salem, Cohansey, and Maurice Rivers on the Delaware Bay side. For rivers without river flow gauges, such as Sassafras and Chester Rivers, the freshwater inflows were estimated using a neighboring station with a similar watershed area. The total number

of river boundaries for the base condition is different from the September 1984 version because it only considered major tributaries. Basic output for the model included the following: water surface elevations from Havre De Grace, Reedy Point, Philadelphia, Old Town Point, and Chesapeake City; tidal currents at Summit Bridge and Arnold Point; and salinity time series at Summit Bridge, Arnold Point, Howell Point, and Reedy Point. The geographic locations for these monitoring stations are shown in Figures 1a&b.

Boundary Conditions

In the September 1984 verification, the tidal boundary was set at Annapolis, MD for the Chesapeake Bay side (Figure 3a) and at Lewes, Del, and Cape May, NJ with linear interpolation to the surface cells between two ends for the Delaware Bay side (Figures 3b&c). The Delaware boundary shows more significant neap-spring tidal variations than the Chesapeake boundary due to less tidal damping.

Figure 4 shows the daily river inflows for the Susquehanna River at Conowingo, MD (solid line) and the Delaware River at Trenton, NJ. The weekly patterns in flow releases for the Conowingo Dam are explained by the minimum flow operation cycle required during this period.

The directional components of wind forcing at Baltimore - Washington International (BWI) shown in Figures 5a&b. In this study, the wind field over the Upper Chesapeake Bay was determined by using the BWI data. The C&D Canal and Delaware Bay wind fields were represented using Wilmington data (Figures 5d&c).

Salinity boundary and initial conditions at the Delaware Bay mouth (Figure 6a) and at the Chesapeake Bay Bridge (Figure 6b) were generated in a manner similar to the low-flow verification. The solid line represents the near surface and the dashed line represents near bottom values.

Results

For the purposes of model spinup, the model was run without salinity. The model water surface elevations and tidal currents agreed fairly well with the field data, so, salt transport was added after five days of simulation. The salinity distribution for several selected locations showed excess salt entering the system. Therefore, additional grid refinement was needed to capture the salinity gradients of the lower Delaware Bay.

The grid refinement generally improved verification, except for special events, such as the extremely low salinity of November 16-18, 1984 at Summit Bridge. The salinity level suddenly dropped to lower than 2 ppt from about 7.5 ppt. It was found, after studying the forcing functions, that there

was a very strong eastward wind and small tidal ranges during this period. Therefore, less salt entered the C&D Canal from the Delaware boundary and more freshwater was brought by the wind from the Chesapeake side. This implies that the land-water conversion factor from the wind field is sensitive to these events. Over-water winds were calculated using Hsu's (1986) formula which suggests a simple dimensional relation between the wind velocity over the sea and over the land. Also, since a time-varying and regionally constant wind field is assumed, local specification for the coefficients of the formula is necessary.

Figures 7a-e present a comparison between computed and observed water-surface elevations at five stations over a selected period. In general, the agreement between them was very good. At Havre De Grace, the phase error between these two curves was due to the model requiring a minimum of two layers (10 ft) in a very shallow Susquehanna Flat area (< 10 ft).

The comparison between computed and observed tidal currents is shown in Figures 8a-c. The Summit Bridge comparisons were good. Although the tidal current amplitudes at Arnold Point were underestimated, they still had excellent phase prediction while Summit Bridge and Reedy Point have good salinity comparisons (Figures 9a-c). Excellent prediction was seen for extreme events. The delayed response time for salinity was due to a forcing function change seen in the last few days of computation. The gauges at Arnold Point and Howell Point (Figures 9a-e) gave reasonable salinity predictions.

Average seasonal flow and salinity patterns are important results from the simulations. Figures 10a-c show average current velocities for layers 16, 13, and 10. These correspond to the surface, -15 ft, and -30 ft layers in the model. This corresponds to the near surface, mid-depth, and near bottom of the C&D Canal. Relatively weak residual circulation was found in the middle of the Chesapeake Bay while stronger circulation formed at the deepest area of the lower Delaware Bay. Since the freshwater discharge during this period for both river basins was very low, the net transport in the C&D Canal was westward.

During fall 1984, the 12 ppt isohaline intruded in the surface layer about 48 miles from the Delaware Bay entrance, which is in contrast to the 2 ppt isohaline of surface layer that reached only to the entrance of the Sassafras River in Chesapeake Bay. Figures 10a-c show the flow transport and the averaged seasonal salinity for the same layer. The colored contour plots (Figures 11a-c) indicate the salinity level at 2 ppt increments.

High-Flow Verification (High-Flow Base)

The second base test, April 1 through June 30, 1984, created a representative seasonal high-flow verification model that covered spring 1984.

Boundary Conditions

Tidal boundaries for the Chesapeake and Delaware Bay sides of the high-flow seasonal model are shown in Figures 12a-c. Figure 13 shows the daily riverflow from the Susquehanna and Delaware Rivers during this period. The similarity between these two curves indicates comparable hydrograph patterns for the two river basins in this period. There were no release regulation responses for the Susquehanna River discharge until late June. In comparing the Susquehanna River hydrograph with the surface elevation in Annapolis, MD, it was found that storm events increased the tidal ranges. Typical windfields at BWI are shown in Figures 14a and b and at Wilmington, in Figures 14c and d.

The salinity boundary conditions at both sides of the model limits were estimated in a manner similar to the low-flow seasonal base. These synthesized results are shown in Figures 15a-b. A higher vertical salinity difference (about 7 ppt) was found at the Chesapeake Bay side due to a higher volume of freshwater entering the system from the Susquehanna River and other small tributaries.

Results

The computed surface elevations were compared with field measurements at three interior gages, namely, Havre de Grace, Reedy Point, and Philadelphia (Figures 16a-c). The third month of tidal current simulation at both Summit Bridge and Arnold Point is shown in Figures 17a-d. The computed tidal currents compared very well for both amplitude and phase. Figures 18a-d compare the computed and observed salinity at the Summit Bridge, Arnold Point, and Reedy Point stations. The largest difference was at Reedy Point in late June (about 2 ppt) which could be caused by uncertainties in the land-water conversion factor for wind or the salinity boundary conditions at the mouth of the Delaware Bay.

The average currents for the verification period from near surface, middle, and near bottom layers are shown in Figures 19a-c. Since the freshwater inflows in this period were larger than in the fall season, stronger residual flows were found in the upper Chesapeake and the upper Delaware Bays. There was no significant change of circulation patterns in the lower and middle Delaware Bay. The net flow transport was eastward in the C&D Canal in this case which resulted in pushing (surface layer) the 12 ppt isohaline to about 22 river miles above the Delaware Bay entrance. On the Chesapeake Bay side, the 2 ppt isohaline was pushed to the mouth of the Chester River where a very fresh region was formed in upper Chesapeake Bay. These color contour plots are shown in Figures 20a-c.

Summary of Two Seasonal Model Verifications

In summary, two seasonal salt transport bases were constructed representing the critical periods of environmental impact (April through June) and water supply demand (September through November). The salinity boundary uncertainties were solved by using both the subtidal variation approach for Delaware Bay and the previous 3-D Chesapeake Bay Model numerical simulation results. The net transport of flow and salt are primarily dependent on the total amount and relative strength of the freshwater inflows in these two river basins. The differences in freshwater flow conditions between the two seasonal periods resulted in a 2 ppt isohaline location difference of 35 miles in Delaware Bay and 30 miles in Chesapeake Bay.

3 Base and Plan Simulations of Flow and Salt Transport

Riverflow Analysis

In this system there are two major sources of freshwater inputs, the river inflows from the Susquehanna River at Conowingo Dam and the Delaware River at Trenton. The different flow conditions were identified by studying the historical records for the most representative patterns.

Since this phase of the modeling effort concentrated on a seasonal scale, a seasonal mean for each individual year can be used to indicate the average volume of water entering a particular river system. This process works for the high-flow and low-flow year but not as well for the year of medium-flow since more than one river basin is involved.

The mean difference, total, and ratio of river flows were determined using a simple ranking analysis for the period 1957-1987. This time interval spans the total length of 31 years; therefore, a medium flow is ranked near 0 while 15 and -15 are high and low-flows, respectively.

Total volume of mean inflows, differences, and ratios were plotted as Figures 21a-c. Data were not recorded at the Conowingo Reservoir gauge, Susquehanna River, until 1967 so the Marietta gauge, the closest upstream gauge from Conowingo, was used for maintaining a continuous representative record of the Susquehanna River inflows. A conversion factor of 1.048, based on the drainage area ratio between these two gauges, was used to estimate the inflows arriving at the mouth of the river. The final selection of high-flow, medium-flow, and low-flow from a 31 year record with RI (ranking index), MT (mean total), MD (mean difference), and MR (mean ratio) is summarized as Table 1.

Table 1
Ranking Indexes from Historical Records

	High-flow	Medium-flow	Low-flow
Spring			
Year	1972	1957	1975
RI	14.9	0.3	-13.6
MT (cfs)	143645	62187	36745
MD (cfs)	93309	36987	22726
MR (cfs/cfs)	4.71	3.94	4.24
Fall			
Year	1977	1958	1964
RI	15.0	0.2	-14.9
MT (cfs)	93722	24763	4826
MD (cfs)	63322	7985	688
MD (cfs/cfs)	5.16	1.95	1.33

Simulation Test Series

After the most representative flow conditions were selected, test series were conducted by determining the simulation run composed of different boundary conditions with channel deepening alternatives. Currently, the average depth of the canal is about 40 ft except 1.5 miles on the eastern end which is 35 ft. This 40 ft deep channel also extends to Courthouse Point in the Elk River. The remaining channel from that point to Poole's Island is 35 ft deep (base). The plan condition is designed to deepen the 35 ft deep channel to 40 ft (plan 1). Modeled depth distribution for the existing channel in 5 ft increment is shown in Figure 22.

Twenty-four basic production runs (Table 2) were conducted. The flow boundaries included the base (1984), low-flow, medium-flow, high-flow, and the highest-flow difference for each season. The highest-flow difference was chosen by either low-flow in the Chesapeake Bay and the high-flow in the Delaware Bay or the converse. These cases may not exist in the real condition since riverflow in the Chesapeake Bay river basin is always higher than riverflow in the Delaware Bay basin. However, it is useful to observe these extreme synthetic conditions and their effects on flow patterns and transport. In addition, two other extreme conditions were included, the highest difference and the lowest difference, which occurred in the same historical

Table 2
Basic Production Tests[1]

Test	Inflow b.c.	Tidal b.c.	Salt b.c.	Geometry
1	low-base	84F	syn. 84F	EX
2	low-base	84F	syn. 84F	40 ft
3	low-low	84F	syn. 84F	EX
4	low-low	84F	syn. 84F	40 ft
5	low-medium	84F	syn. 84F	EX
6	low-medium	84F	syn. 84F	40 ft
7	low-high	84F	syn. 84F	EX
8	low-high	84F	syn. 84F	40 ft
9	low-Del-low/Ches-high	84F	syn. 84F	EX
10	low-Del-low/Ches-high	84F	syn. 84F	40 ft
11	low-Del-high/Ches-low	84F	syn. 84F	EX
12	low-Del-high/Ches-low	84F	syn. 84F	40 ft
13	high-base	84S	syn. 84S	EX
14	high-base	84S	syn. 84S	40 ft
15	high-low	84S	syn. 84S	EX
16	high-low	84S	syn. 84S	40 ft
17	high-medium	84S	syn. 84S	EX
18	high-medium	84S	syn. 84S	40 ft
19	high-high	84S	syn. 84S	EX
20	high-high	84S	syn. 84S	40 ft
21	high-Del-low/Ches-high	84S	syn. 84S	EX
22	high-Del-low/Ches-high	84S	syn. 84S	40 ft
23	high-Del-high/Ches-low	84S	syn. 84S	EX
24	high-Del-high/Ches-low	84S	syn. 84S	40 ft

[1]The first part of inflow boundary condition indicates the period either in the low flow season (September - November) or in the high flow season (April - June). The flow conditions which were determined by the ranking analysis for particular year was represented by the second part of the inflow boundary condition.

record year. From the results shown in Figure 21b, these conditions (Runs 3-4 and Runs 19-20) have been overlapped to basic runs. For easy comparison and to maintain a manageable data base, the tidal boundary, salinity boundary, initial salinity, and wind field were assumed the same for each particular seasonal run.

Eighteen data save locations were identified and outputs of surface elevation, velocity, and salinity were saved (Table 3). Four control points from these eighteen locations in the C&D Canal, Chesapeake City, Summit Bridge, St. Georges, and Reedy Point were used to estimate the flow and salt transport due to flow regime changes. The seasonal averaged flow and salinity for the entire computational domain were saved as long-term average conditions.

Table 3
Areas of Data Saved for the C&D Canal 3-D Numerical Model

Save points	Grid location(I,J)	Model depth
1	(15,77)	35
2	(22,18)	25
3	(22,76)	35
4	(25,80)	20
5	(25,77)	35
6	(29,81)	10
7	(29,77)	35
8	(31,84)	10
9	(33,77)	35
10	(44,76)	40
11	(50,76)	40
12	(57,76)	40
13	(63,76)	40
14	(71,76)	35
15	(73,77)	15
16	(73,75)	15
17	(75,76)	40
18	(75,102)	40

Selected Simulated Seasonal Flow and Transport

Four sets of simulated seasonal flow and transport conditions were selected as extreme conditions: 1964, the lowest low-flow; 1977, the highest low-flow; 1985, the lowest high-flow; and 1972, the highest high-flow. The remaining simulations were included in the database and used to compare the results as necessary. Average flow and salinity patterns are presented for four extreme conditions along with differences for extreme conditions.

The significant findings for these simulations are summarized as follow:

a. 1964: Extremely low flows were experienced for both river basins. Flow and salt intruded from Delaware Bay to the Chesapeake Bay through the C&D Canal. There was a weak average flow in the whole upper Chesapeake Bay. Figures 23a-d show the average flow and salt for near-surface and near- bottom layers based on the C&D channel depth (1990 existing). The 2 ppt isohalines were restricted to the Susquehanna Flats and lower Susquehanna River. The surface layer of 2 ppt isohaline was about 80 miles from the mouth of the Delaware Bay. For layer 10 (near the bottom layer of the C&D Canal), the 12 ppt isohaline reached about 5 miles from the C&D Canal's eastern entrance. The 12 ppt isohaline reached about 5 miles from the C&D Canal's eastern entrance.

b. 1977: The total river inflows were about 19 times the flows of 1964. A strong down bay flow in the upper Chesapeake Bay pushed water from the Chesapeake Bay to Delaware Bay. It also caused a stronger seaward flow above the middle of the Delaware Bay. The 2 ppt isohalines were pushed to Poole's Island on the Chesapeake side and near the eastern entrance of the C&D Canal for the Delaware Bay surface layer. The 12 ppt isohalines retreated to within 40 miles from the Delaware Bay entrance (Figures 24a-d).

c. 1972: This was the historical spring high-flow year primarily due to Hurricane Agnes. During the middle of June 1972, about 1 million cfs was released from Conowingo Reservoir. Because the flow was so strong, most of the freshwater was flushed to the lower Chesapeake Bay across almost the entire cross-section. The 12 ppt isohaline was down to 25 miles from the Delaware Boundary (Figures 25a-d).

d. 1985: During this year the averaged river flows were small, but enough to produce an eastward transport through the C&D Canal. This demonstrates that westward transport is unlikely to occur during the spring season since the year 1985 (extreme low-flow in this season) has resulted in an eastward transport. The 2 ppt isohalines occurred near Hart Miller Island in upper Chesapeake Bay and 10 miles above the eastern end of the C&D Canal in the surface layer (Figures 26a-d).

e. The difference of 1977-1964: Figure 27 a-d show the differences between the average velocity and salinity for each computational cell between 1977 and 1964. There is no significant difference between the average current patterns for the middle and lower Delaware Bay below approximately the 40 river mile mark. The greatest differences in salinity distribution occurred between the 40 to 50 river mile mark (about 10 ppt) in Delaware Bay and in the cross-section between the entrance of the Back and Magothy Rivers in the deeper water of the upper Chesapeake Bay (about 6 ppt). This indicates that the sensitivity of salinity variations due to flow changes is primarily in regions of higher gradient salinity and high geometry slope (Figures 27a-d).

f. The difference of 1972-1985: A similar analysis was conducted by taking the difference between the two extreme flow years during the spring period. While the locations of greatest difference of salinity had little the magnitudes were reduced by approximately one-half of 1972 salinity level compared to 1985 salinity value in the upper Chesapeake Bay. This demonstrates again that salinity changes during the high-flow season were less sensitive than in the low-flow season (Figures 28a-d).

Current and Salt Variations Due to Channel Deepening

The differences in flow vectors and salinity contours between the existing channel and the proposed channel conditions show the impacts of channel deepening over the model domain. In the next section, the fluxes of flow and salt through the C&D Canal will be discussed individually. Simulations of deepened proposed 40 ft conditions for four extreme flow conditions are summarized:

a. Lowest low-flow condition (1964): There was no significant change in either flow or salinity variation in Delaware Bay. More complex flow patterns and geometry exist in the upper Chesapeake Bay system. Physically, the residual circulation differences were not represented to actual circulation pattern, but related the flow variation due to accumulation for a season scale. However, the flow scale for this difference was relatively small (usually less than 2 cm/sec within a seasonal averaged). Figure 29a indicates that a difference generated clock-wise circulation occurred below Hart Miller Island and above the cross-section in Magothy River. Since the scale of this plot (1 cm/sec) is much smaller than the average velocity (10 cm/sec), the actual salinity change depends on a combination of flow change and salinity gradient integrated over the simulation period. The western end of the C&D Canal showed some change due to channel deepening. Figure 29b shows the average salt over an entire seasonal simulation. Salinity with maximum values of 0.30 ppt was carried from around

Craighill Channel to the landward direction of the Bay and was deposited up to the head of Chesapeake Bay.

b. Highest low-flow condition (1977): There was a stronger flow difference and larger circulation causing higher salinity transport to Kent Island with a maximum value of 1 ppt. The channel deepening in the C&D Canal caused a noncritical (1-2 cm/sec) but greater flow intrusion to (40 ft) Chesapeake Bay (Figures 30a-b).

c. Highest high-flow condition (1972): Higher differences of currents were expected, since the original flow in this condition was so strong. Extremely low salinity distributions existed over the upper Chesapeake Bay, and were limited up to 0.4 ppt (Figures 31a-b).

d. Lowest high-flow condition (1985): Extremely weak current differences due to deepening were found under this condition. Elk River and the western end of the C&D Canal showed a relatively larger difference with the maximum difference, not exceeding 0.1 ppt, in both the middle Chesapeake Bay and the Elk River area (Figures 32a-b).

Estimation of Flow and Salt Transport through the Canal

The flow and salt transport for the entire seasonal simulation was estimated using the outputs of computed surface elevation, currents, and salinities for each selected water column in the Canal. The control points for these calculations were Chesapeake City, Summit Bridge, St. Georges, and Reedy Point. To compute transport through the C&D Canal, the area of each computational cell for a particular cross-section was multiplied by the current speed in the channel direction and then integrated over time. The salinity concentration was incorporated when computing the salt transport. Seasonal average transport was obtained by integrating the flow field over time from the first slack-before-ebb flow to the last slack-before-ebb flow during the simulation period and divided by the elapsed time. In each of the 24 basic simulation runs, the total elapsed time was 2034 hours (161 tidal cycles). Table 4 summarizes the seasonal flow and salt transport for each simulation run at Summit Bridge.

The first 12 cases were 6 pairs of low-flow period simulations and the remaining cases were high-flow. During the low-flow period, net flow transport usually was westward unless seasonal inflows in the Susquehanna River exceeded a certain amount which is discussed later in this report. Runs 9-12 (and Runs 21-24) used historical conditions to demonstrate synthetic conditions that would give the maximum gradient of flows across the C&D Canal between the Delaware and Chesapeake basins.

Table 4
Seasonal Flow and Salt Transport at Summit Bridge

Test No.	Flow Year	Flow	Net Transport (m^3/s)			Net Salt Trans (g/sec)		
			Base	Plan	Diff	Base	Plan	Dif
1&2	1984	low-base	-22.0	-24.0	-2.0	-361	-395	-34.0
3&4	1964	low-ℓ	-35.6	-34.7	0.9	-529	-537	-8.0
5&6	1958	low-m	-13.1	-10.1	3.0	-227	-228	-1.0
7&8	1977	low-h	39.6	35.7	-3.9	-30	-37	-7.0
9&10	1977-64	low-h/low-ℓ	31.9	28.5	-3.4	248	296	48.0
11&12	1964-75	low-ℓ/low-h	-27.9	-24.3	3.6	28	5	-23.0
13&14	1984	high-base	50.0	49.0	-1.0	-31	-28	3.0
15&16	1972	high-h	89.7	88.3	-1.4	8	4	-4.0
17&18	1957	high-m	39.6	38.7	-0.9	13	8	-5.0
19&20	1985	high-ℓ	22.1	22.3	0.2	-55	-62	-7.0
21&22	1972-65	high-h/high-ℓ	97.5	95.5	-2.0	21	29	8.0
23&24	1985-84	high-ℓ/high-h	13.8	14.8	1.0	9.6	8.6	-1.0

[1]Positive sign of net flow and salt transport represents the direction from the Chesapeake side to the Delaware side.

It is because the flows come from different historical years. The high river flow in the susquehanna River basins could correspond-low river flow in the Delaware River basin at the same calendar ranking date. For example, test run 9 obtained even less easward transport than test run 7. Similar conditions occurred for the salt transport results. The salt transport most likely will be westward, although the flow transport during the low-flow period could result in an eastward transport. During the high-flow period, salt transport usually will be eastward unless a very low seasonal flow occurs, such as in the case of 1985.

Table 4 shows that the change in net flow through the canal was attributable to channel deepening was less than 4.0 m^3/s. This could be the significant change based on the integration effect of (m^3/s) (cubic meter per second) hydrologic differences in the Delaware and Chesapeake basins, particularly in the low-flow period. For salt transport, the greatest impact from channel deepening was a 48 g/sec value to the west. The significance of this variation was also attributed to the integration of salinity distribution and net flow over the entire season.

Table 5 shows the calculations for the flow and salt transport through the C&D Canal from selected flow conditions. Basically, Reedy Point has differences from the other three stations. At low-flow, the eastern end of the canal has greater westward flow but during high-flow it has a stronger eastern flow. Salt transport has the opposite effect and was more complicated because two salinity gradients exist in the canal.

Table 5
Seasonal Net Flow and Transport from Selected Locations in the C&D Canal for the Existing Conditions

Year	Flow Conditions	Chesapeake City	Summit Bridge	St. Georges	Reedy Point
	Flow Transport(m**3/sec)				
1984	low-base	-21.4	-22.0	-22.4	-24.8
1964	low-low	-35.1	-35.6	-37.0	-38.4
1958	low-medium	-12.6	-13.1	-14.5	-16.0
1977	low-high	40.1	39.6	38.3	36.4
1984	high-base	50.5	50.2	49.6	47.8
1972	high-high	90.3	89.7	89.2	88.2
1957	high-medium	40.0	39.6	39.2	37.5
1985	high-low	22.6	22.1	21.7	20.8
	Salt Transport (g/sec)				
1984	low-base	-355	-361	-359	-352
1964	low-low	-515	-529	-540	-536
1958	low-medium	-229	-227	-224	-208
1977	low-high	-37	-30	-22	-8
1984	high-base	-24	-31	-39	-49
1972	high-high	4	9	17	48
1957	high-medium	9	13	20	24
1985	high-low	-55	-55	-49	-39

[1]Positive sign of seasonal net flow and salt tranport represents the direction form the Chesapeake side to the Delaware side.

An important part of this study was to quantify the relationships between flow conditions and net transport on a seasonal scale. A nonlinear regression analysis was used to identify the approximate flows which might produce zero net transport through the canal on a seasonal scale. It was assumed that the

seasonal net flow transport in the C&D was the function of seasonal mean flow for either river basins. This analysis only gives a rough approximation, since more data points are needed to improve the accuracy of the estimation. Table 6 gives the calculation summaries with results that show the critical flow is about 27,500 cfs in the Susquehanna River and about 12,700 cfs in the Delaware River for the medium-high

Table 6
Critical Seasonal Flows of Net Transport in the C&D Canal

Year	Flow Transport (cfs)	Sus.(S) Flow (cfs)	Del.(D) Flow (cfs)
1984	-773	9813	3704
1964	-1251	2757	2069
1958	-460	16374	8398
1977	1391	78522	15200
Critical Flow Estimation	0	27500	12700

flow-season. Also, the critical flow for the high-flow season can be theoretically estimated by extrapolation. However, these values are very low and may not happen in real situations. The estimation of critical salt transport is more complicated because more parameters are involved and is not shown due to a combination of limited usefulness and complexity.

Circulation and Salinity Changes Caused by Channel Deepening

This study has described the proposed plan of channel deepening from 35 ft to 40 ft in the eastern end of the C&D Canal and the channel between Courthouse Point and Poole's Island in the Upper Chesapeake Bay. Four extreme flow conditions were studied with the discovery that the major circulation changes occur below Poole's Island and the Elk River which connects the C&D Canal and upper Chesapeake Bay. The magnitude of change depends on the strength of seasonal flow regimes and the salinity gradient during that period. The strength of a difference generated circulation differences between the existing and the plan conditions seem to be the source indicator for contributing the movement of salinity.

During the analysis of base and plan circulation results, what initially appeared to be boundary uncertainty clockwise circulation caused by over constrained boundary conditions, were observed in the results. For comparison and sensitivity of deepening reasons, in addition to the proposed plan, there were two additional channel deepening plans to investigate the flow and salt transport variations. The plan 2 restricts the channel deepening area to the Sassafras River entrance from Courthouse Point in the upper Chesapeake Bay but still includes deepening of the C&D Canal's eastern end. The plan 3 deepened the channel only in the C&D Canal portion. Eight conditions (runs 25-32) were run with the same model inputs as the original deepening plan. Therefore, some minor changes in the initial salinity conditions were required because of a bathymetry change. The results for the surface layer are summarized as follows:

a. The lowest flow condition for the low-flow period (1964): In the first channel deepening test, weak apparently artificial circulation formed near Hart Miller Island and Poole's Island. The second test, however, retained a smaller magnitude of artificial circulation. No significant flow differences were found above Poole's Island to near Courthouse Pt. If we amplify the flow vector which represents the difference, it appears on the above described difference missing area. Therefore, the "difference generated" circulation in the lower part of the upper Chesapeake Bay does exist. The changes in flow patterns might be due to the accumulation effect of changes in the geometry (Figures 33a-d).

b. The highest flow condition for the low-flow period (1977): Compared to the original plan, about the same magnitude of artificial circulation was found for the first channel deepening test. The influence of the channel deepening between Poole's Island and the entrance of Sassafras River was relatively small. The second test received a significantly smaller salinity change when the difference generated circulation became weak (Figures 34a-d).

c. The highest flow condition for the high-flow period (1972): Both plans produced similar artificial circulation in the middle of the Chesapeake Bay. Plan 3 also showed this phenomenon because the strength of flow was extremely high during this period (Figures 35a-d).

d. The lowest flow condition for the high-flow period (1985): No significant change in salinity patterns was found for both plans. The strength of flow was relatively low as was the salinity gradient in the middle of Chesapeake Bay. (Figures 36a-d).

Table 7 lists the flow and salt transport through the C&D Canal at Summit Bridge for each channel deepening test. The channel deepening between Poole's Island and the entrance to Courthouse Point has the least flow transport impact but produces higher salinity change due to higher salinity gradient.

Table 7
Flow and Salt Transport through C&D Canal for Channel Deepening Alternative and Tests at Summit Bridge, MD

Flow Year	Transport Parameter	Base	Plan 1
1964	flow (m^3/s)	-35.6	-34.7
	salt (gm/s)	-529.0	-539.0
1977	flow (m^3/s)	39.6	35.7
	salt (gm/s)	-30.0	-37.0
1972	flow (m^3/s)	89.7	88.3
	salt (gm/s)	8.0	4.0
1985	flow (m^3/s)	22.1	22.3
	salt (gm/s)	-55.0	-62.0

4 Conclusions

Three-dimensional flow and transport models were developed to study the impact of deepening the C&D Canal from 35 ft to 40 ft. Their coverage included Delaware Bay from the Atlantic Ocean upstream to the head of tide at Trenton, NJ, the C&D Canal, and the upper Chesapeake Bay from Annapolis, MD upstream to the head of tide. The boundary conditions for the models were based on two three-month seasonal periods. The models were verified with prototype data and found accurate for water surface elevations, tidal currents, and salinity distributions.

Twenty-four simulations were conducted with a wide range of boundary conditions and geometries, including combinations of freshwater inflow, tide, and salinity boundary conditions. The low-flow, medium-flow, and high-flow conditions were determined using a statistical analysis of the historical records. Extreme conditions, not likely to occur in nature, were also tested including extremely high Susquehanna flows while the Delaware River experienced very low flows, as well as the converse. The modeled geometries included the existing or base condition and three deepened or plan conditions.

The simulation during the flow condition from 1957 to 1987 (Table 4) indicated that during low riverflow, the range of net flow transport was between 35.6 cubic meters per second (m^3/sec) westward and 39.6 m^3/sec eastward. The salt transport values were between 529 g/sec westward and 30 m^3/sec eastward. During high river flow, the net flow transport was between 22.1 m^3/sec eastward and 89.7 m^3/sec westward while salt transport rates were between 55 g/sec westward and 13 g/sec eastward. This indicated that salt transport was driven more by density differences than by differences in basin hydrology.

The net flow transport change due to (proposed 40 ft) was less than 4.0 m^3/sec, it could be significant amount (23 percent change for year 1958 flow condition), particularly in the extreme low riverflow of fall season and could be related to the relative strength of tidal forcing from both directions in the C&D Canal and the length of channel deepening proposed in upper Chesapeake Bay. During high-flow conditions, the flow is dominated by riverine discharge causing more inflows from the Susquehanna River to flow down to Chesapeake Bay while during low-flow conditions, tidal forcing dominates the mechanism of water movement.

The maximum net salt transport rate for this plan in the C&D Canal was around 34 g/sec (1984 scenario). This resulted in slight salinity changes in the upper Chesapeake region. The maximum change usually occurred between the entrance of the Chester River and Hart-Miller Island. While the eastern side of this section tends to have increased salinity, the western side has decreased salinity. The maximum salinity change between the base condition and plan 1 condition is about 1.1 ppt, compared to the natural seasonal (5-8 ppt) variation in this area.

References

Galperin, B. and Mellor, G. L. "A Time-Dependent, Three-Dimensional Model of the Delaware Bay and River System Part II: Three-Dimensional Flow Fields and Residual Circulation," Estuarine, Coastal and Shelf Science 31, 255-281, Nov. 1990.

Garvine, R., McCarthy, R. and Wong, K C. "The Axial Salinity Distribution in the Delaware Estuary and its Weak Response to River Discharge," Estuarine, Coastal and Shelf Science 35,157-165. Apr. 1992.

Hsieh, B. "Houston-Galveston Navigation Channels, Texas Project; Report 5, System Simulation of Tidal Hydrodynamic Phenomena in Galveston Bay, Texas" (in preparation), U.S. Army Engineer Waterways Experiment Station, Vicksburg, MS.

Hsieh, B., Johnson, B. and Richards, D. "A Three-Dimensional Numerical Model Study for the Chesapeake and Delaware Canal and Adjacent Bays," Technical Report HL-93-4, U. S. Army Engineer Waterways Experiment Station, Vicksburg, MS. 1993.

Hsu, S. A. "Correction of Land Based Wind Data for Offshore Applications : A Further Evaluation, "Journal of Physical Oceanography 16, 390-394, 1986

Johnson, B. H. et al. "Development and Verification of a Three-Dimensional Numerical Hydrodynamic, Salinity, and Temperature Model of Chesapeake Bay; Volume I, Main Text and Appendix D," U.S. Army Engineer Waterways Experiment Station, Vicksburg, MS, 1991.

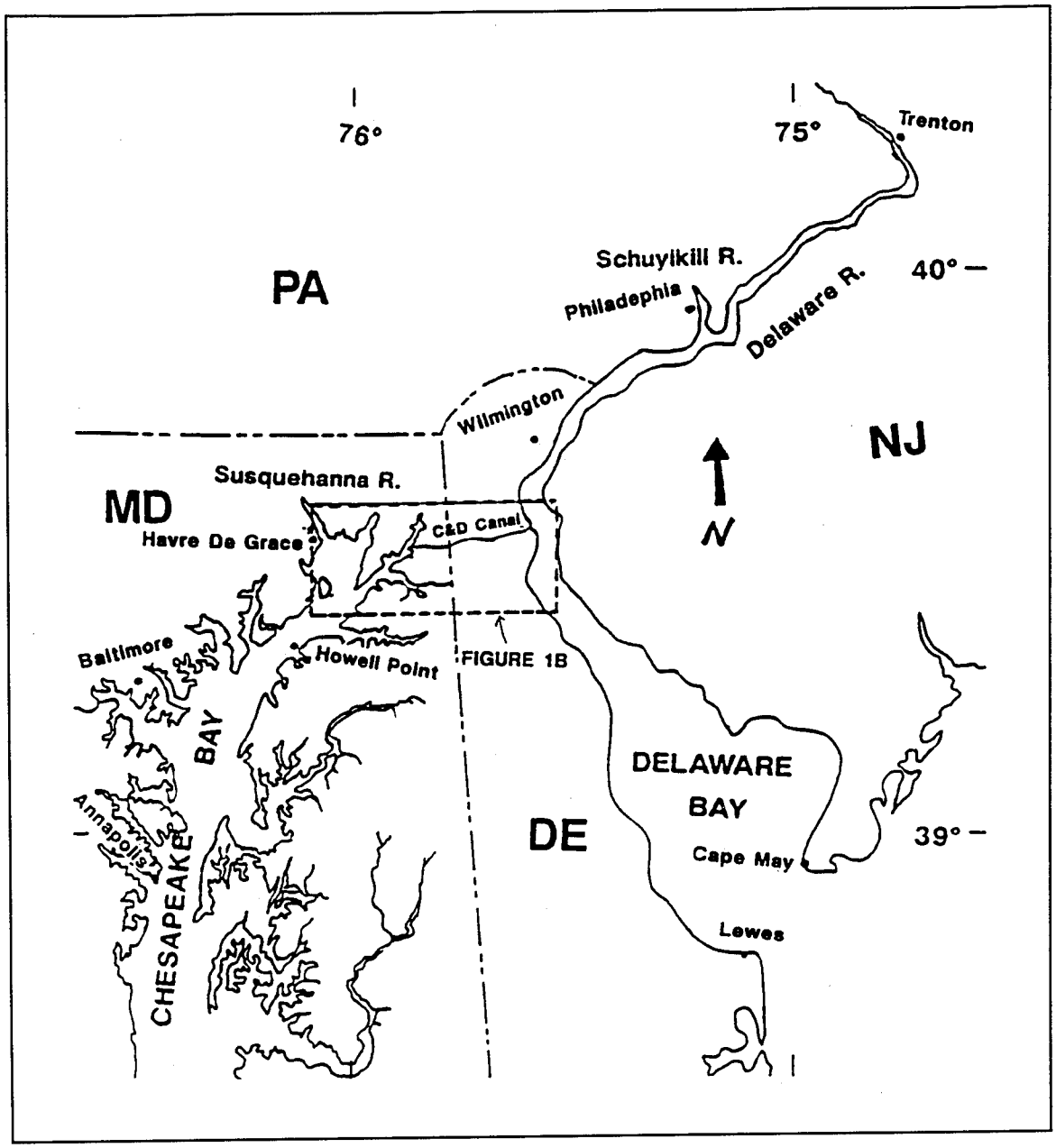

Figure 1a. C&D Canal and adjacent estuaries

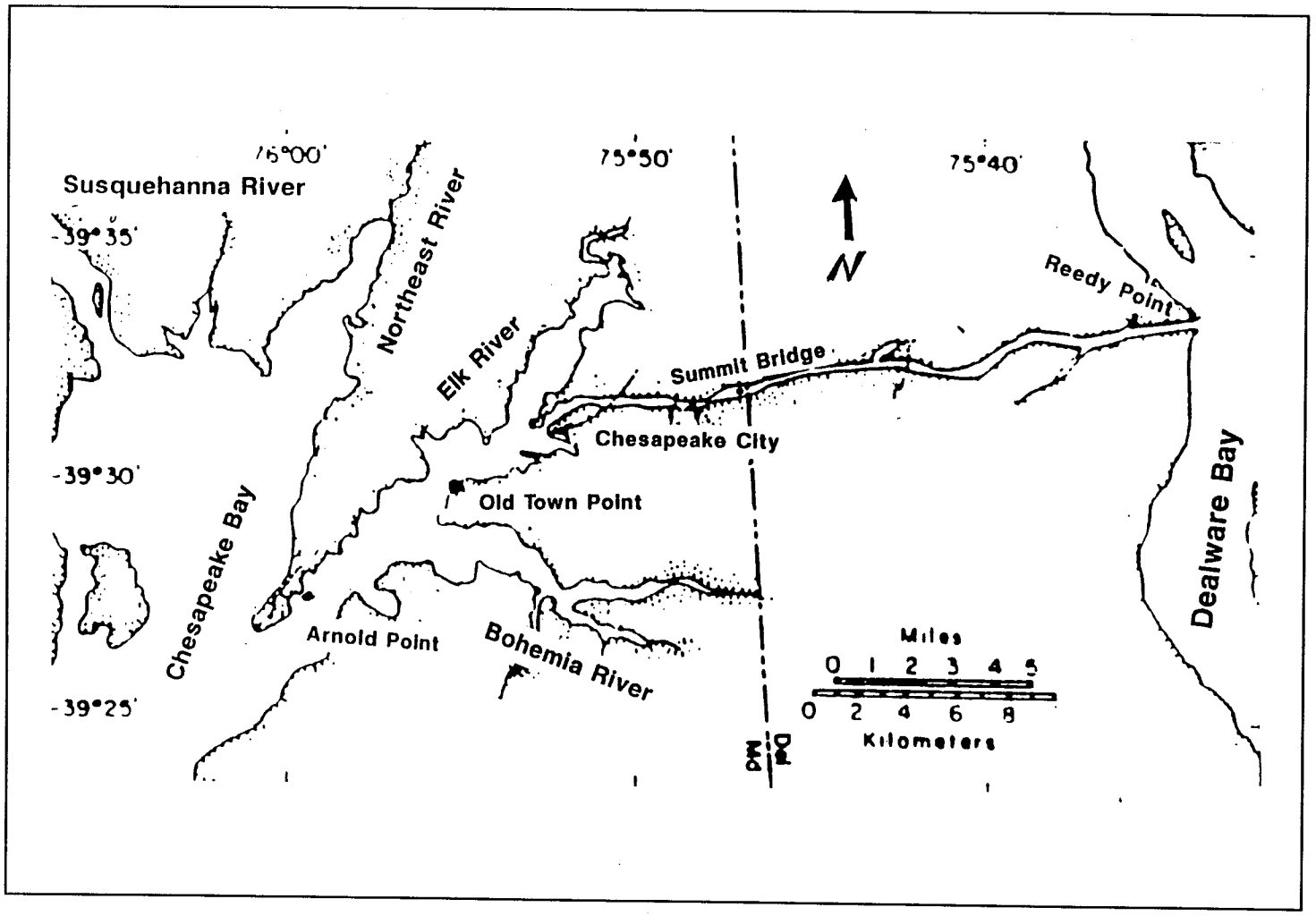

Figure 1b. C&D Canal System

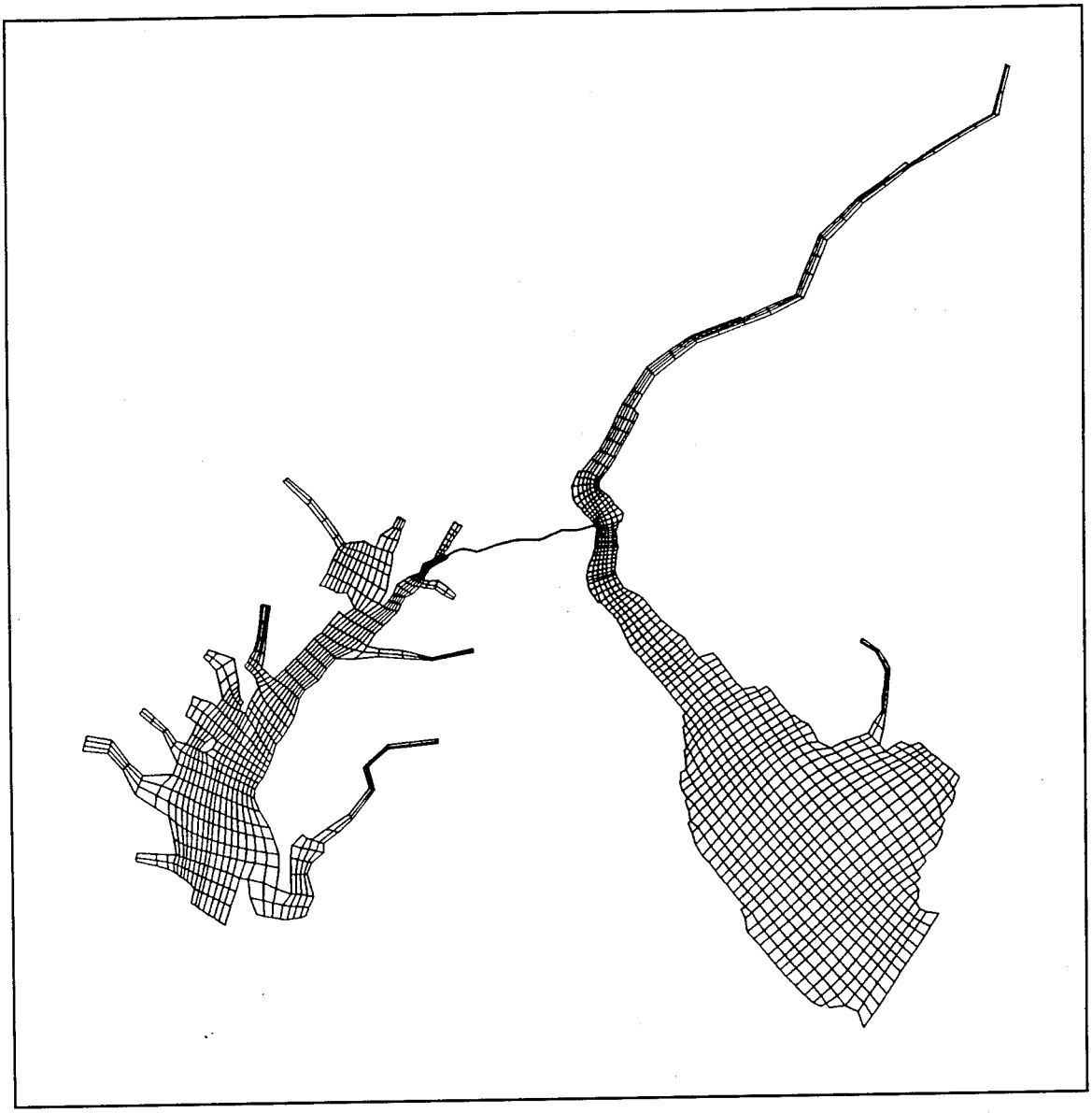

Figure 2. Computational Grid

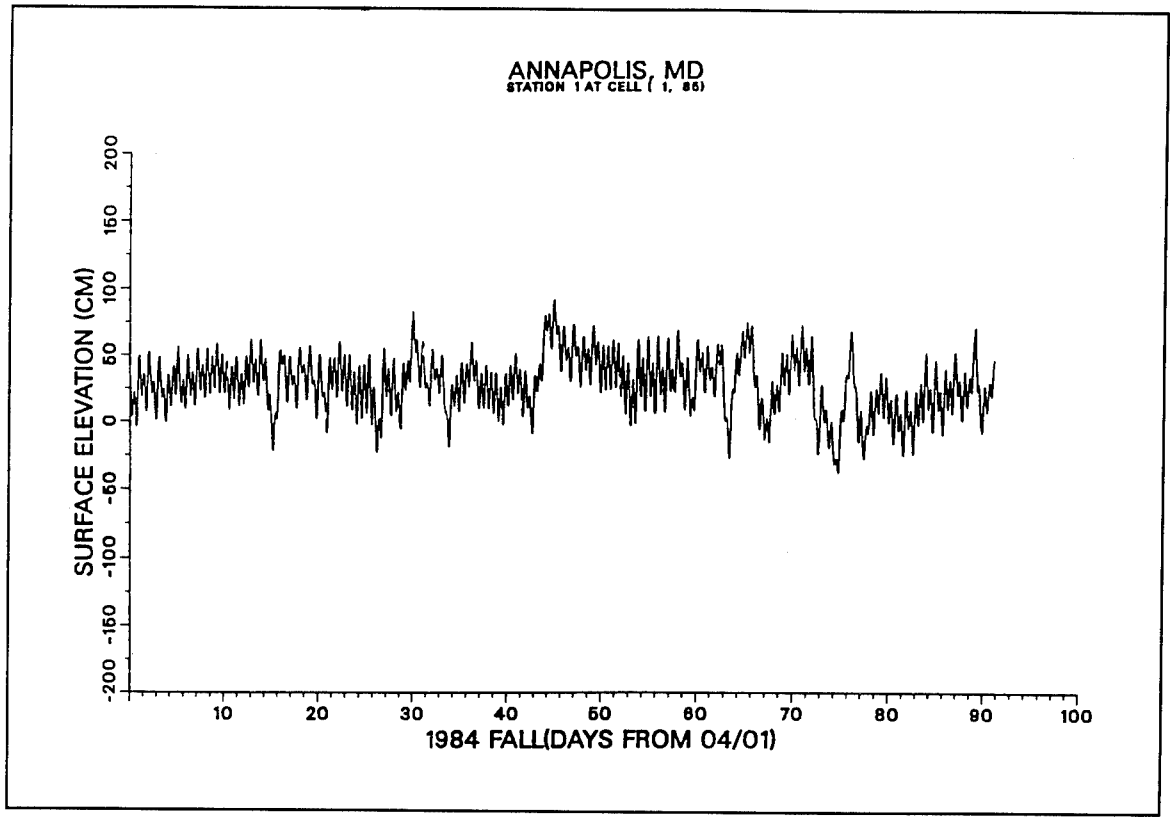

Figure 3a. Recorded tide at Annapolis, MD

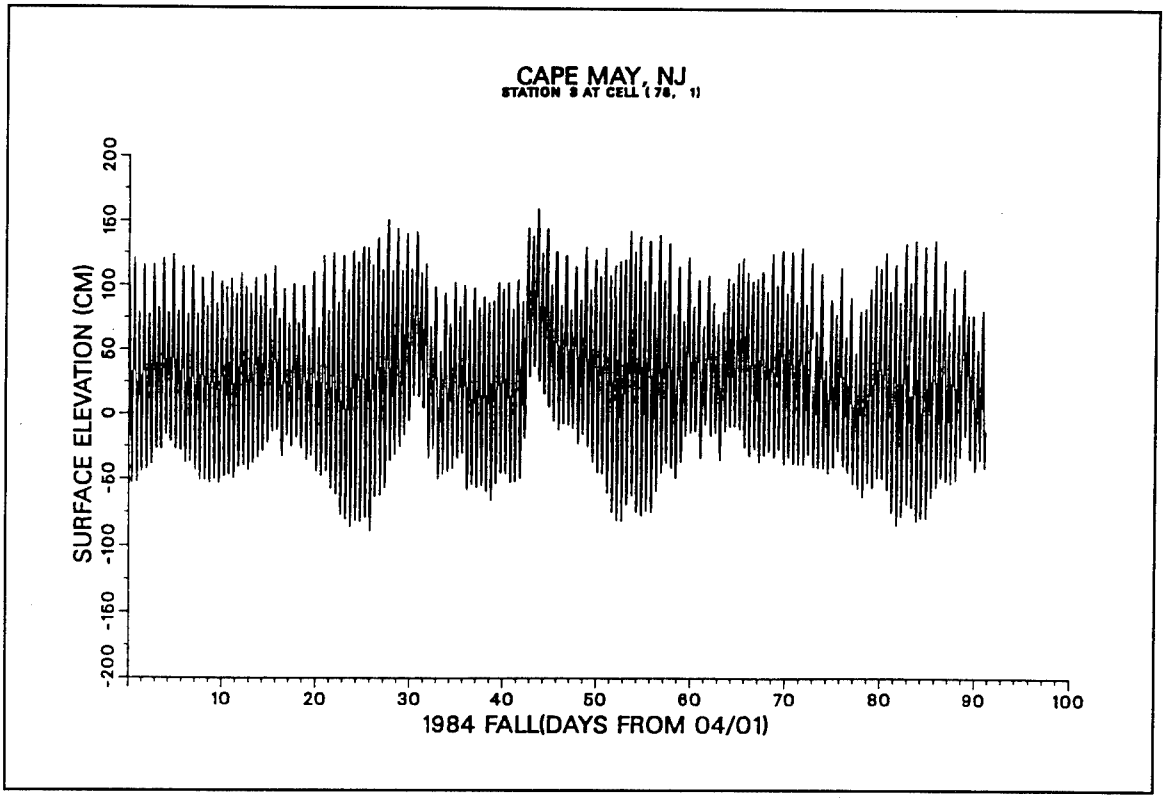

Figure 3b. Recorded tide at Cape May, NJ

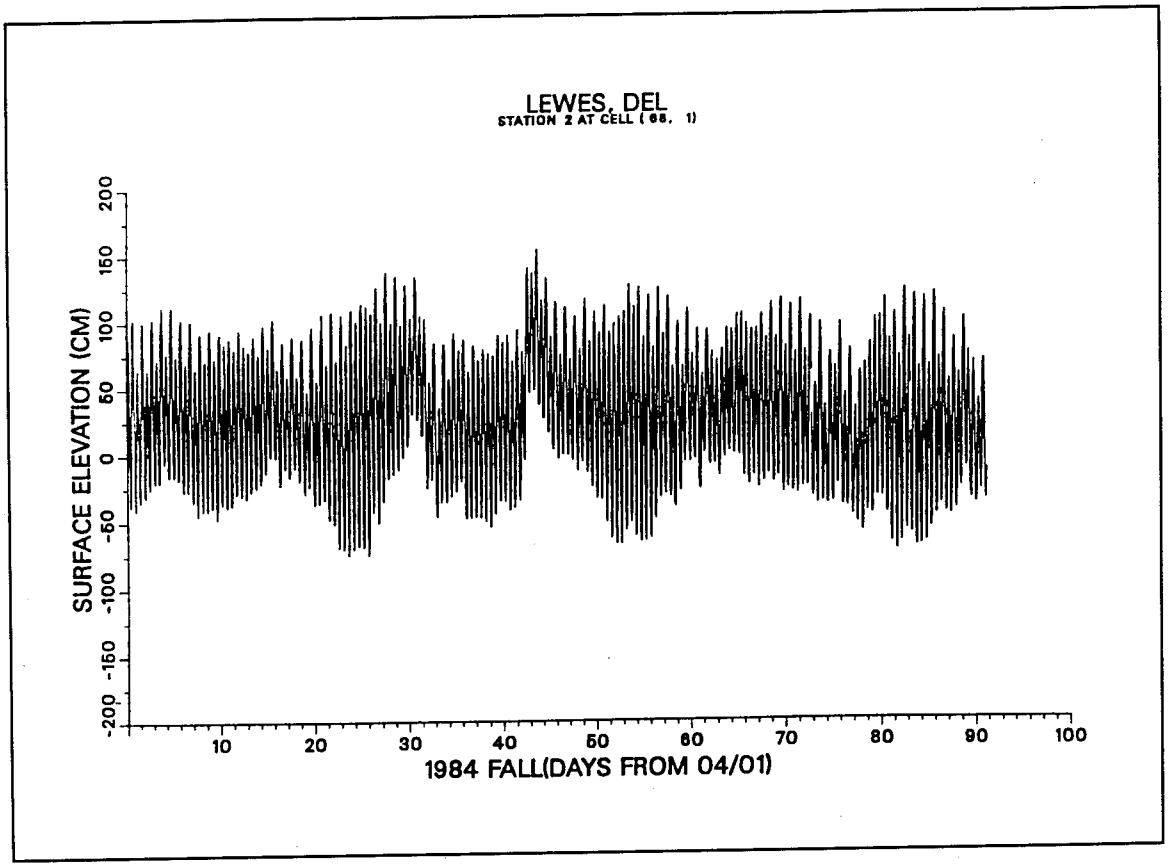

Figure 3c. Recorded tide at Lewes, Del

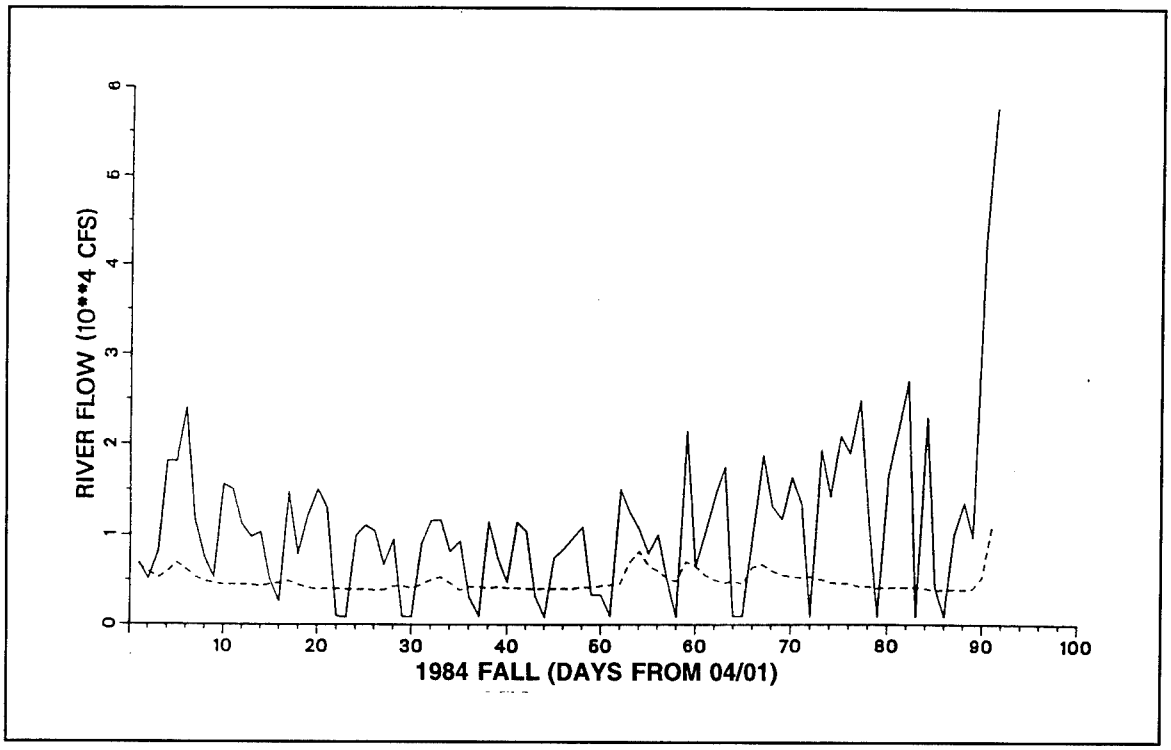

Figure 4. Freshwater Inflow from Susquehanna River (solid line) and Delaware River (dashed line)

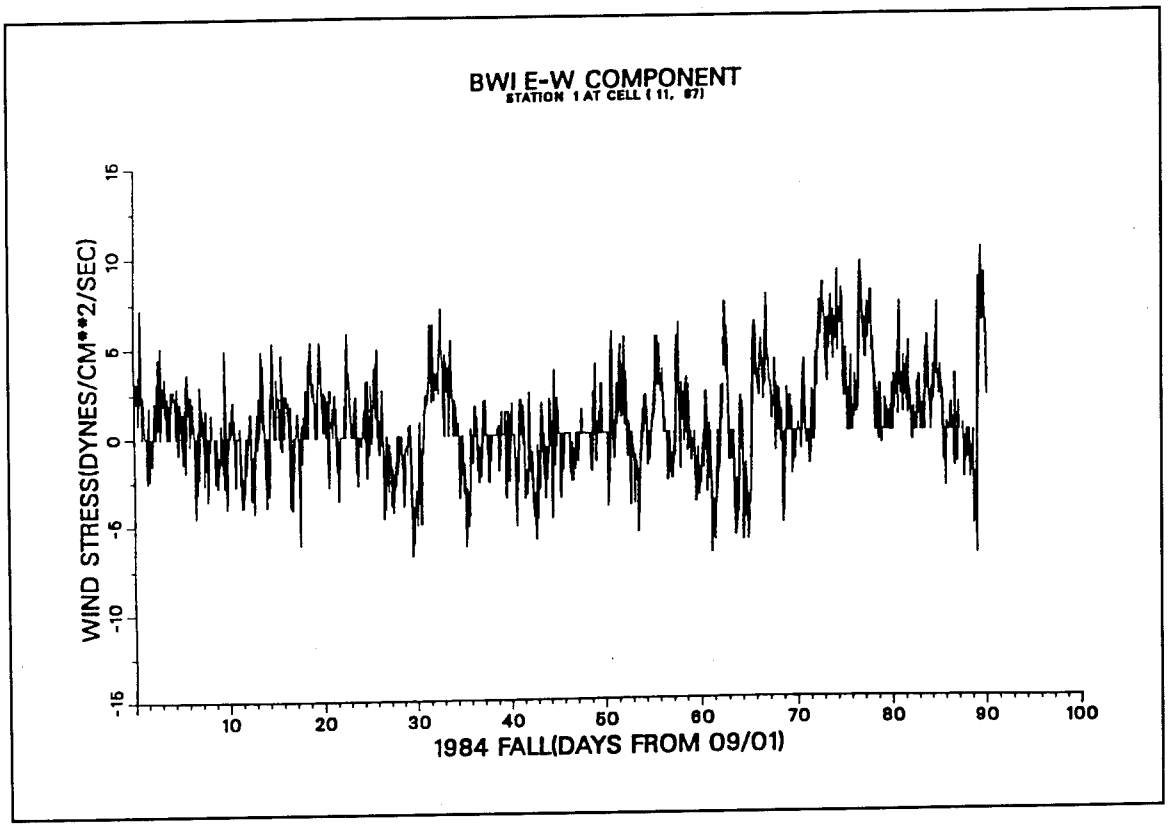

Figure 5a. Wind at BWI (East-West Component)

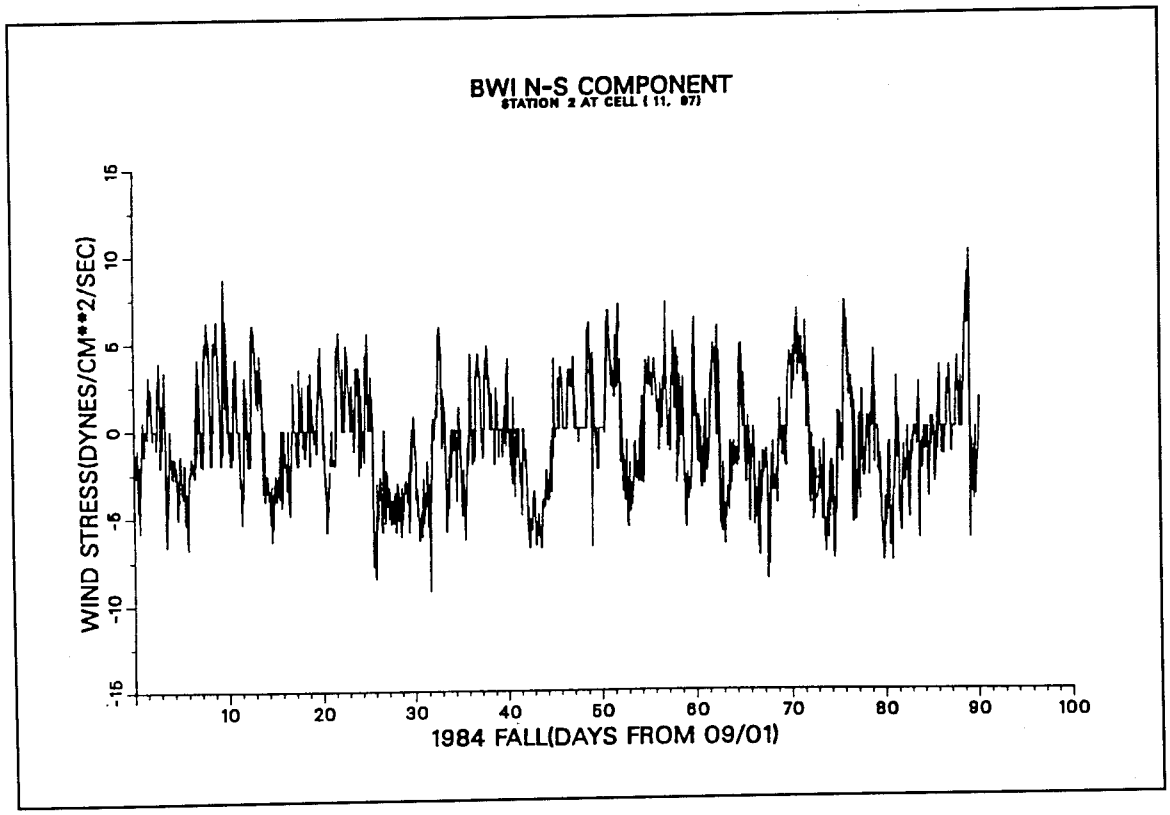

Figure 5b. Wind at BWI (North-South Component)

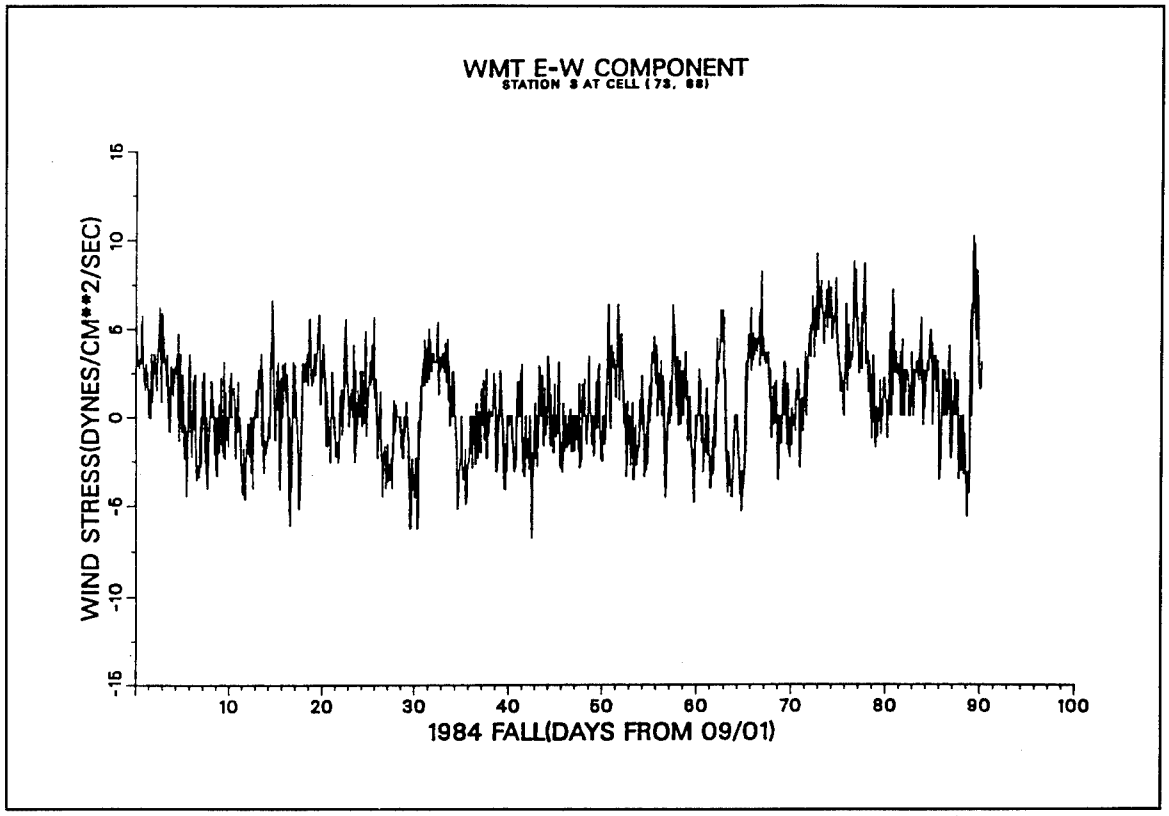

Figure 5c. Wind at Wilmington (East-West Component)

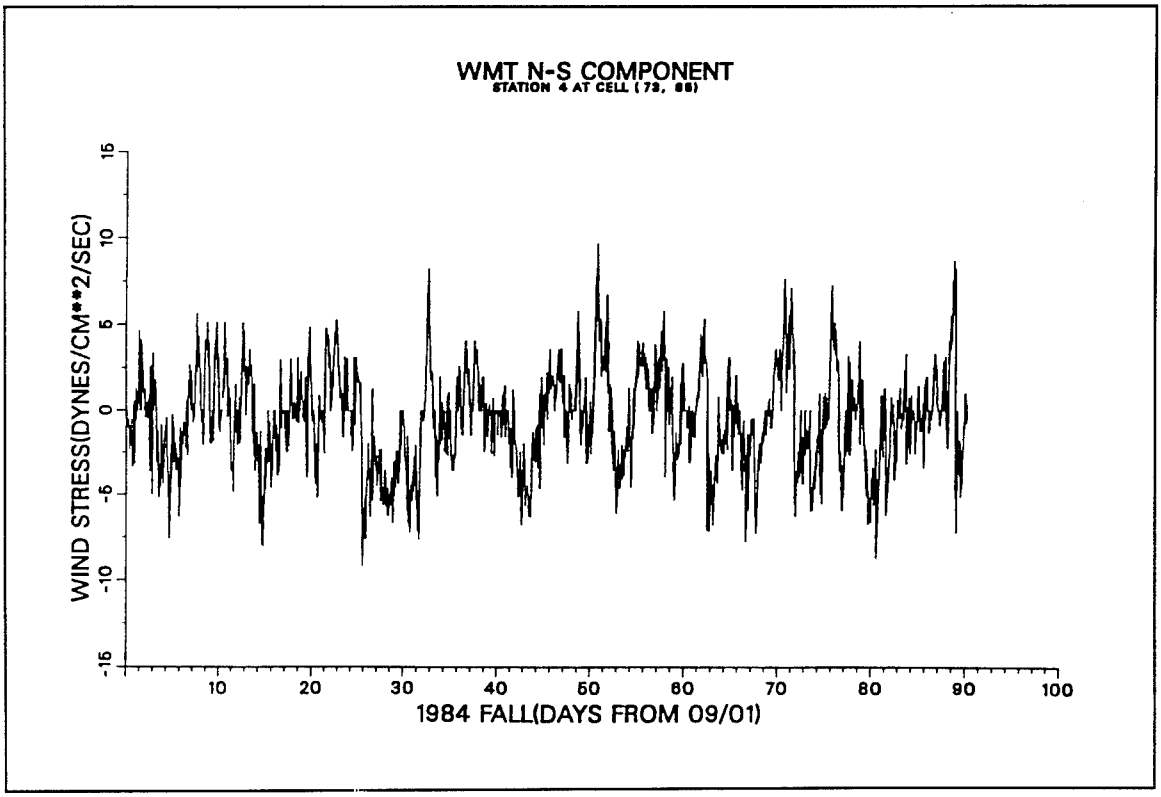

Figure 5d. Wind at Wilmington (North-South Component)

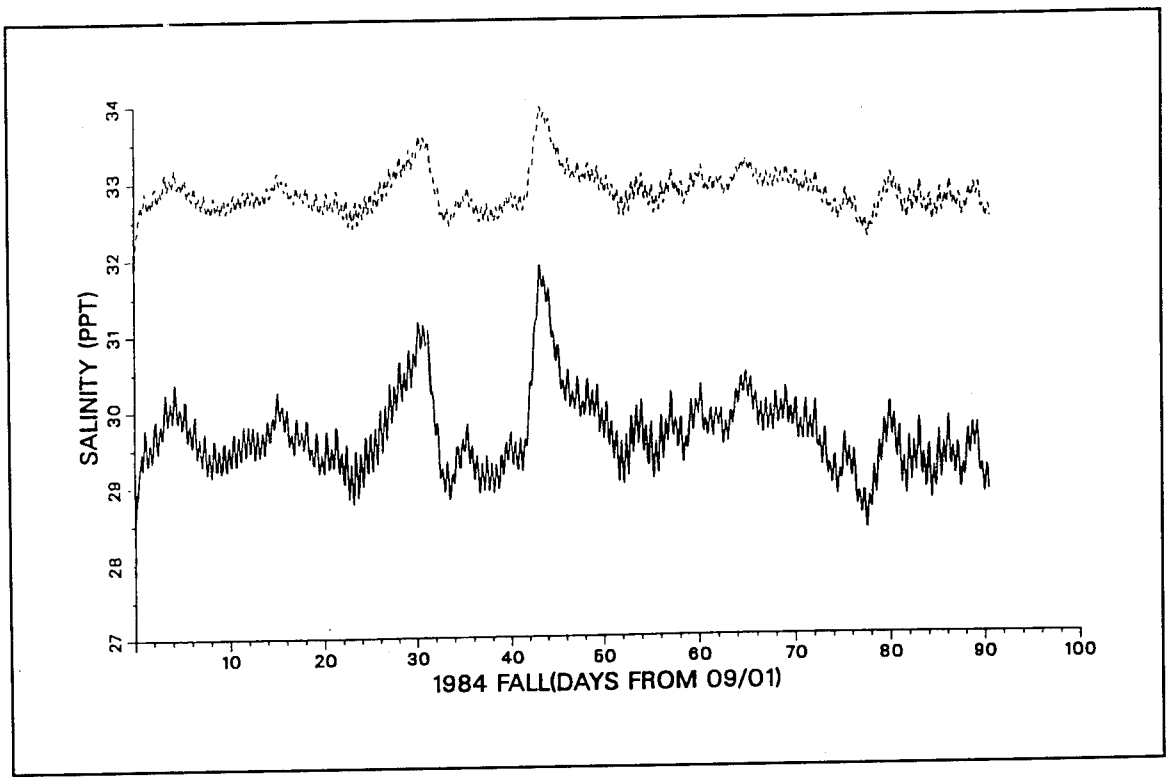

Figure 6a. Synthesized surface (solid line) and bottom (dashed line) salinity boundary at Delaware Bay mouth

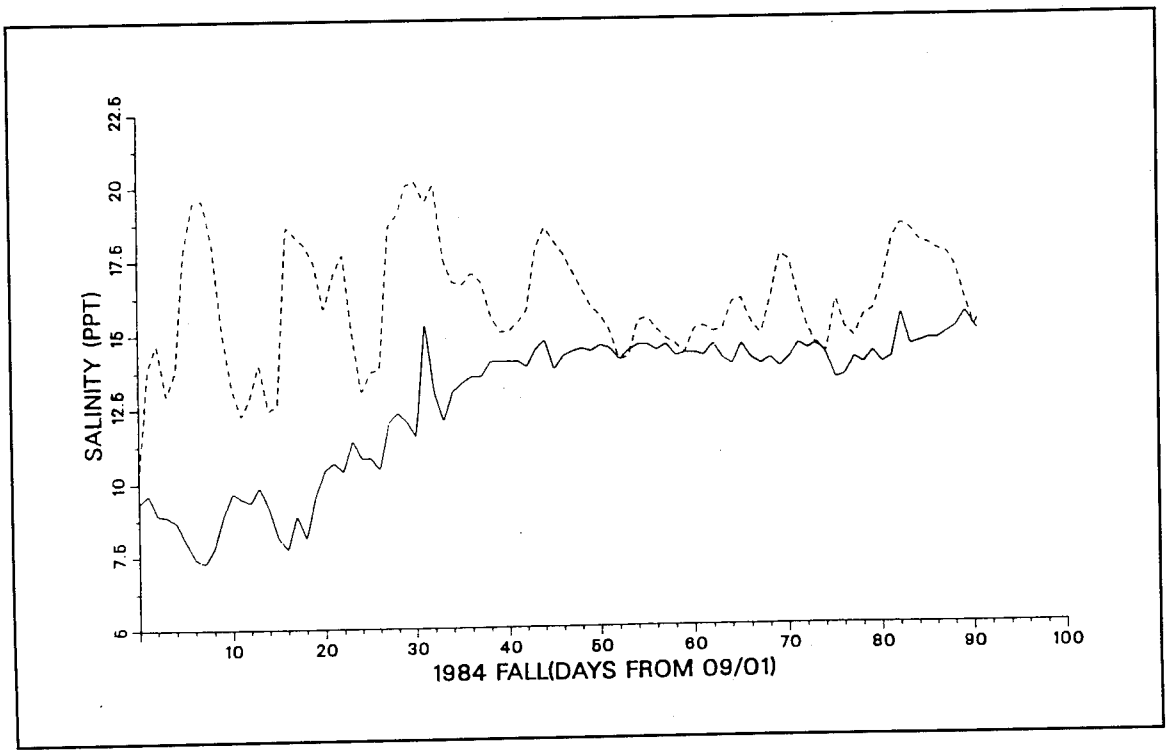

Figure 6b. Synthesized surface (solid line) and bottom (dashed line) salinity boundary at Chesapeake Bay Bridge

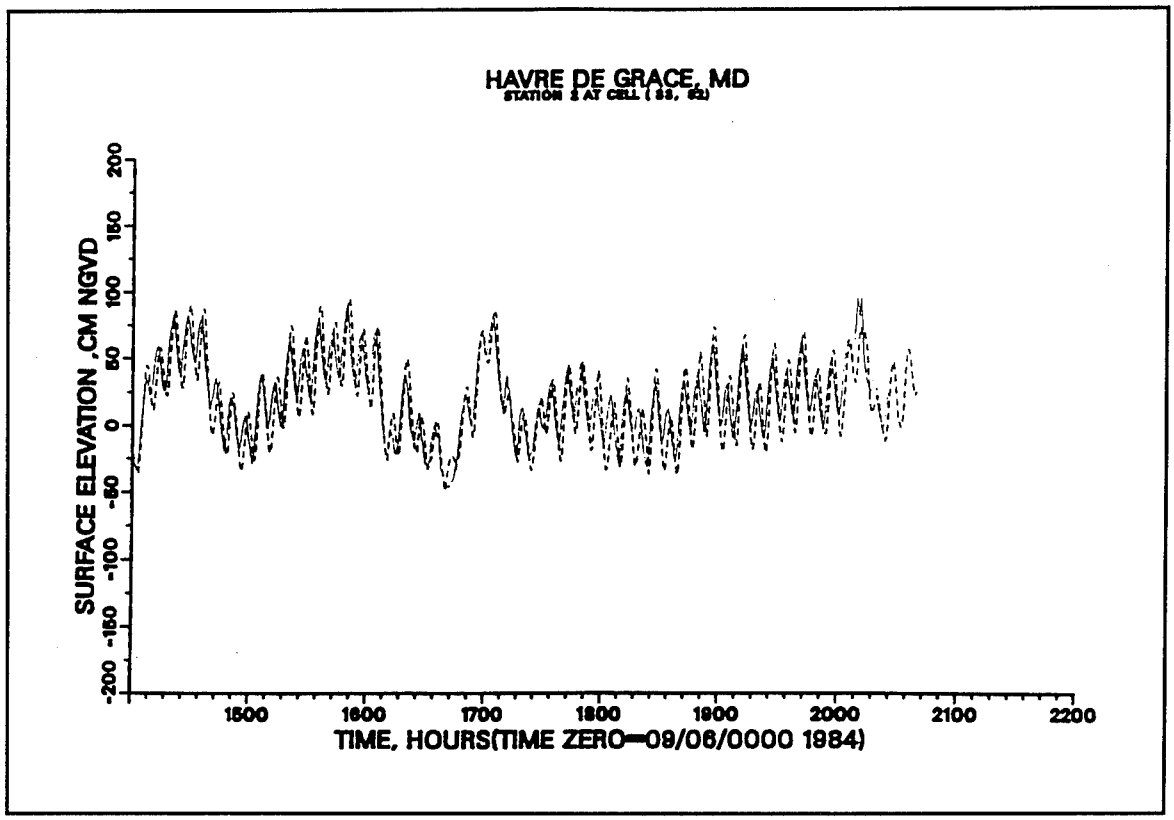

Figure 7a. Computed (____) versus recorded (----) tide at Havre De Grace

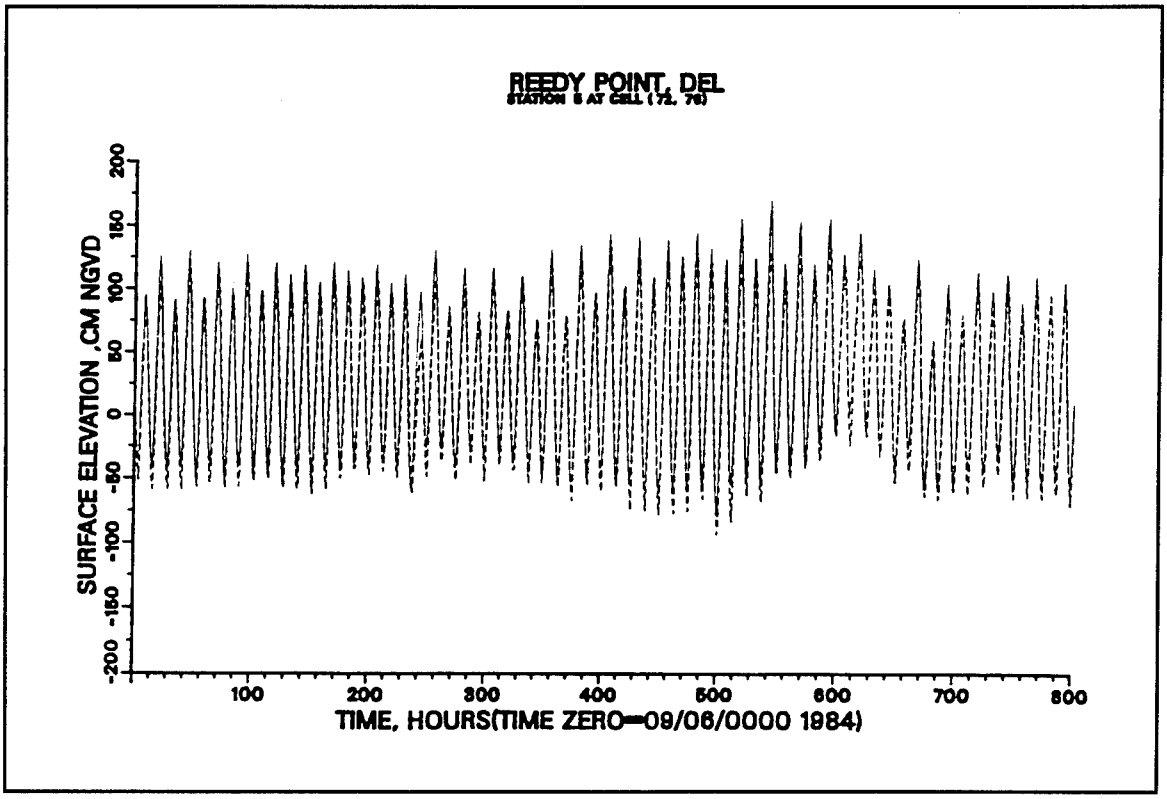

Figure 7b. Computed (____) versus recorded (----) tide at Reedy Point

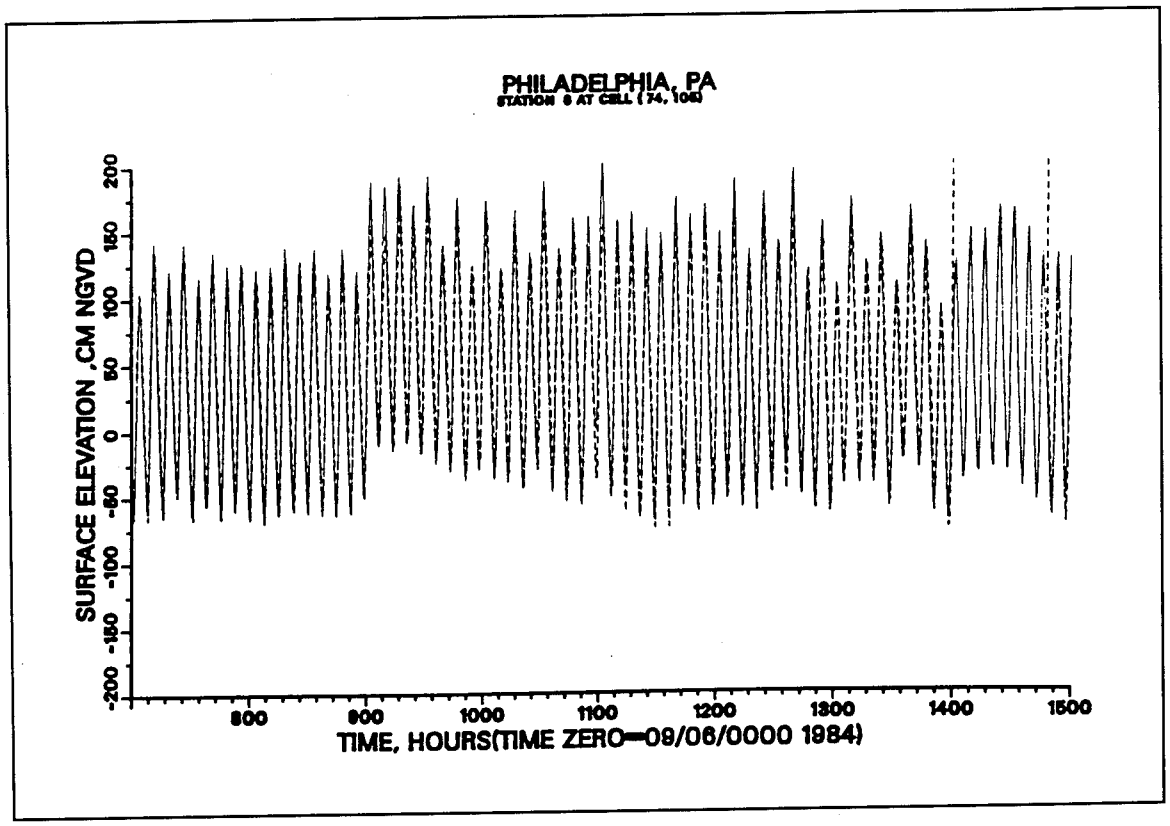

Figure 7c. Computed (____) versus recorded (----) tide at Philadelphia

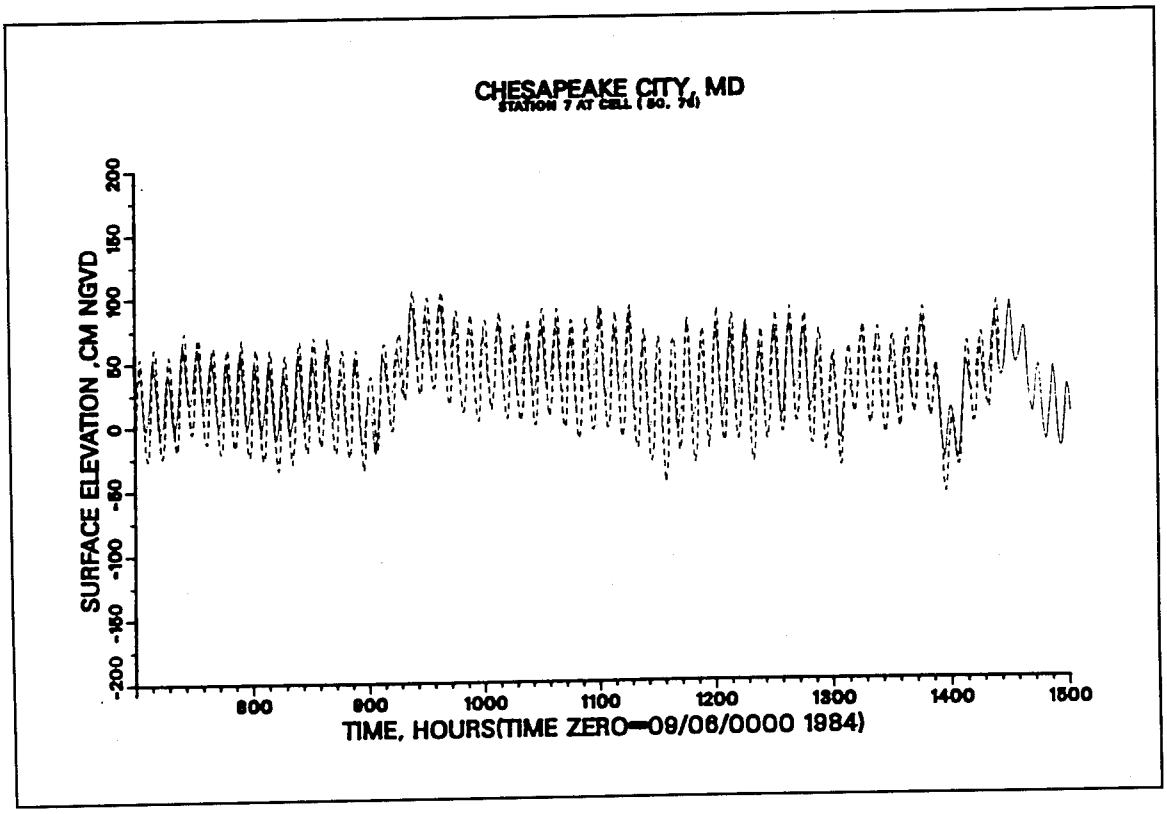

Figure 7d. Computed (____) versus recorded (----) tide at Chesapeake City

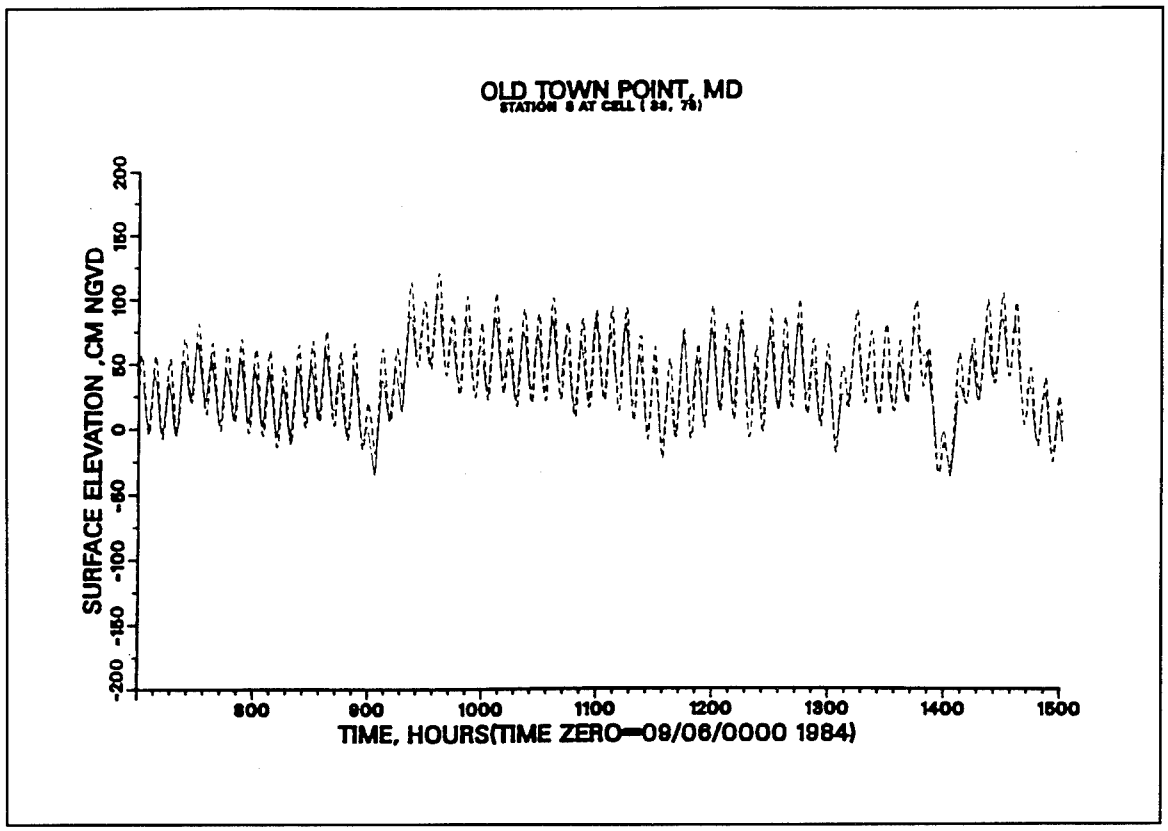

Figure 7e. Computed (____) versus recorded (----) tide at Old Town Point

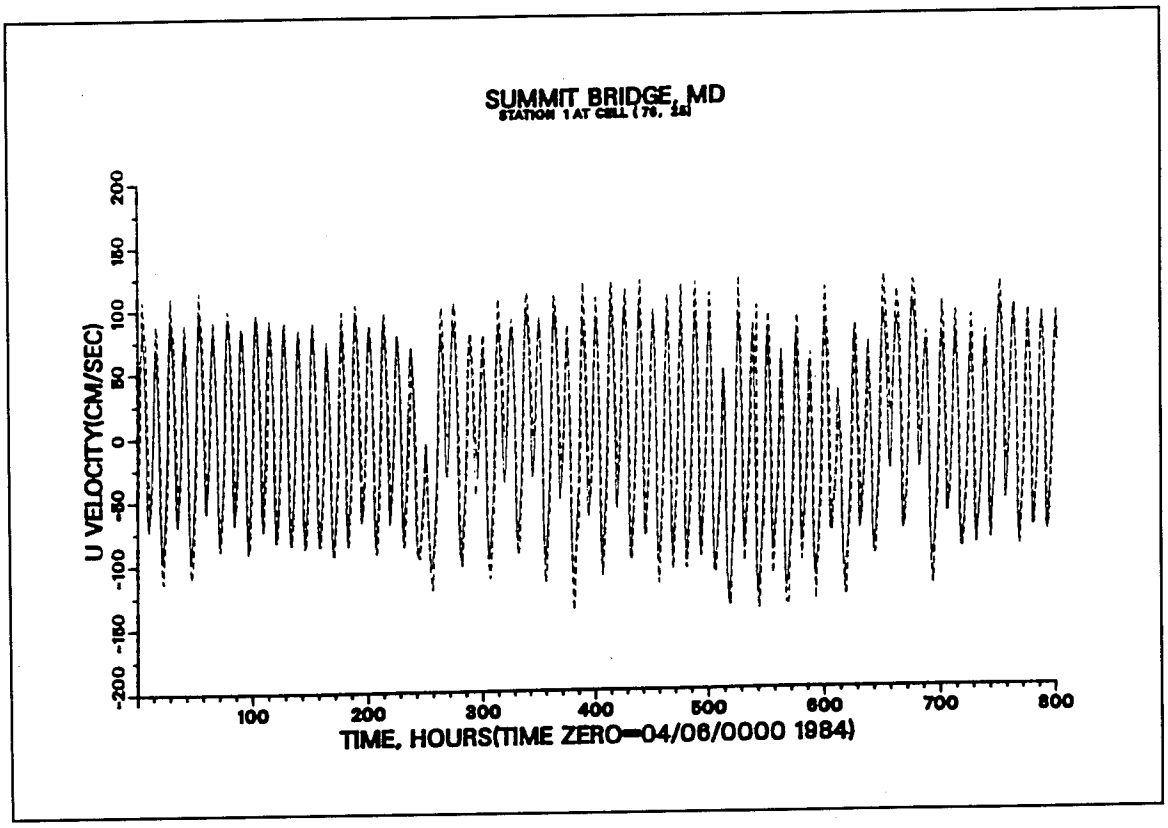

Figure 8a. Computed (____) versus recorded (----) velocity at Summit Bridge (10 m)

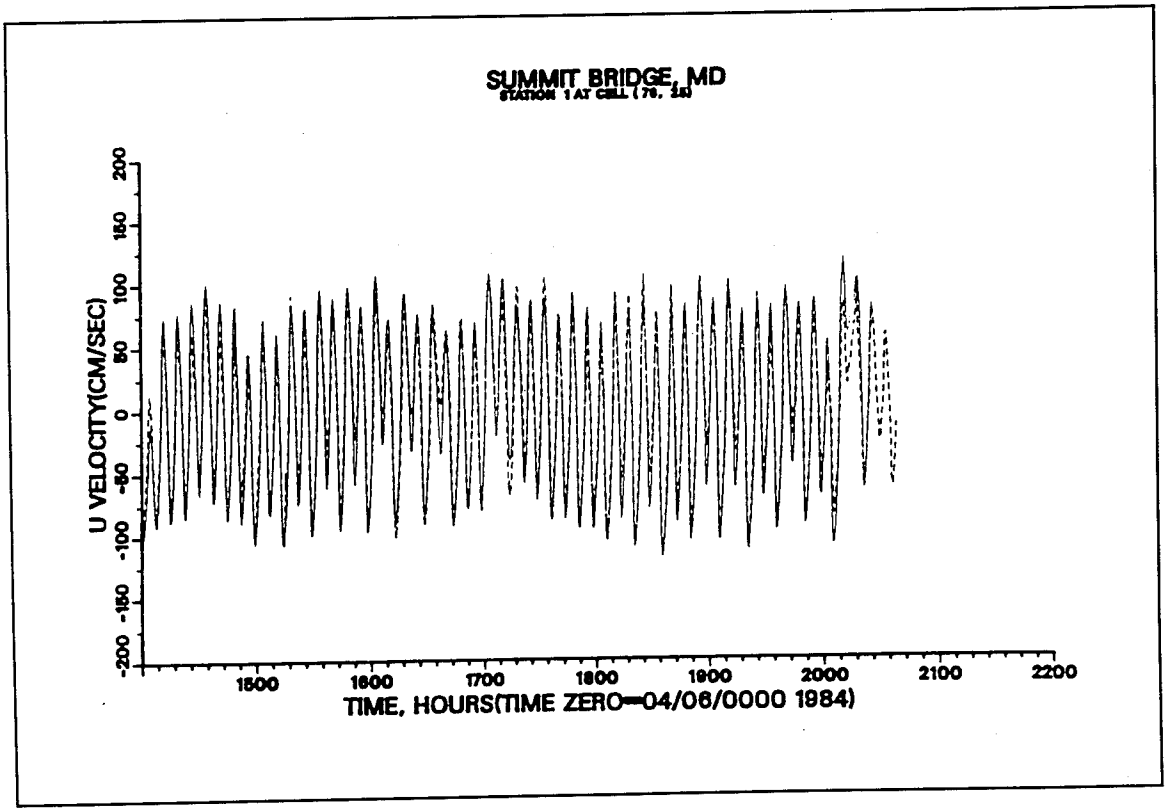

Figure 8b. Computed (____) versus recorded (----) velocity at Summit Bridge (7 m)

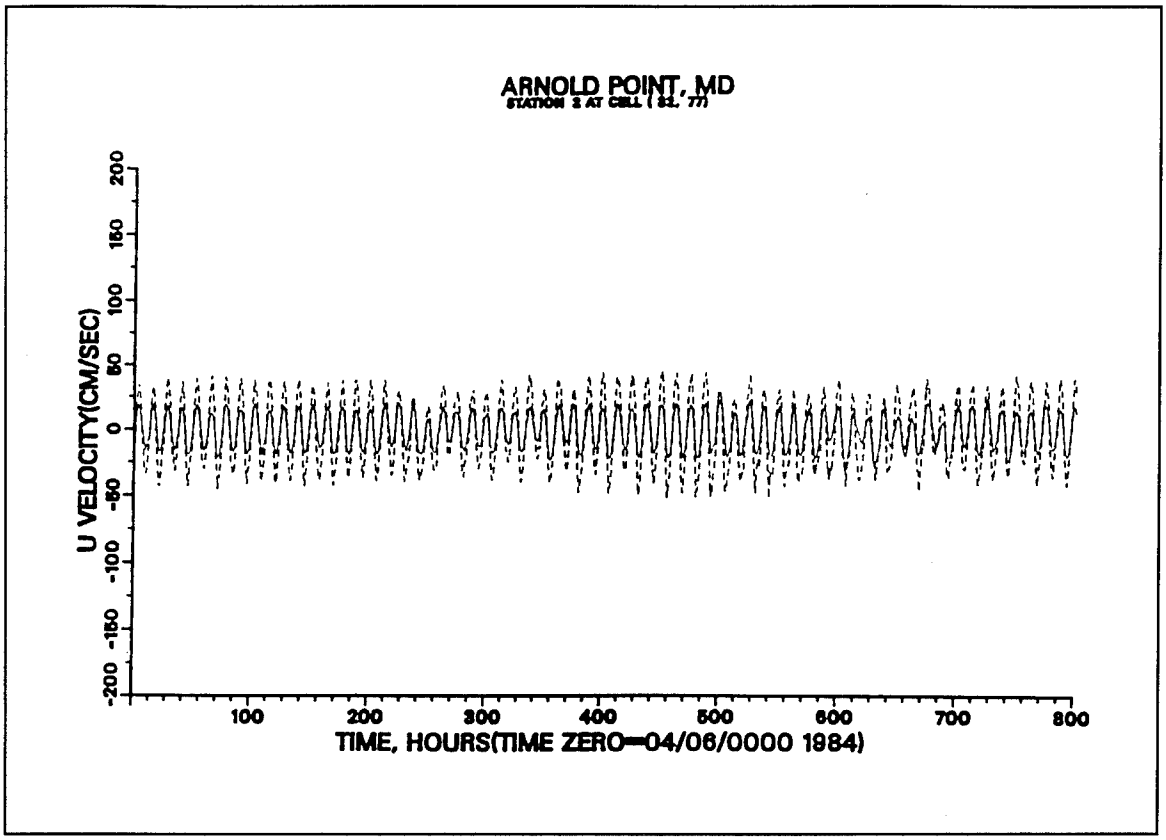

Figure 8c. Computed (____) versus recorded (----) velocity at Arnold Point (4 m)

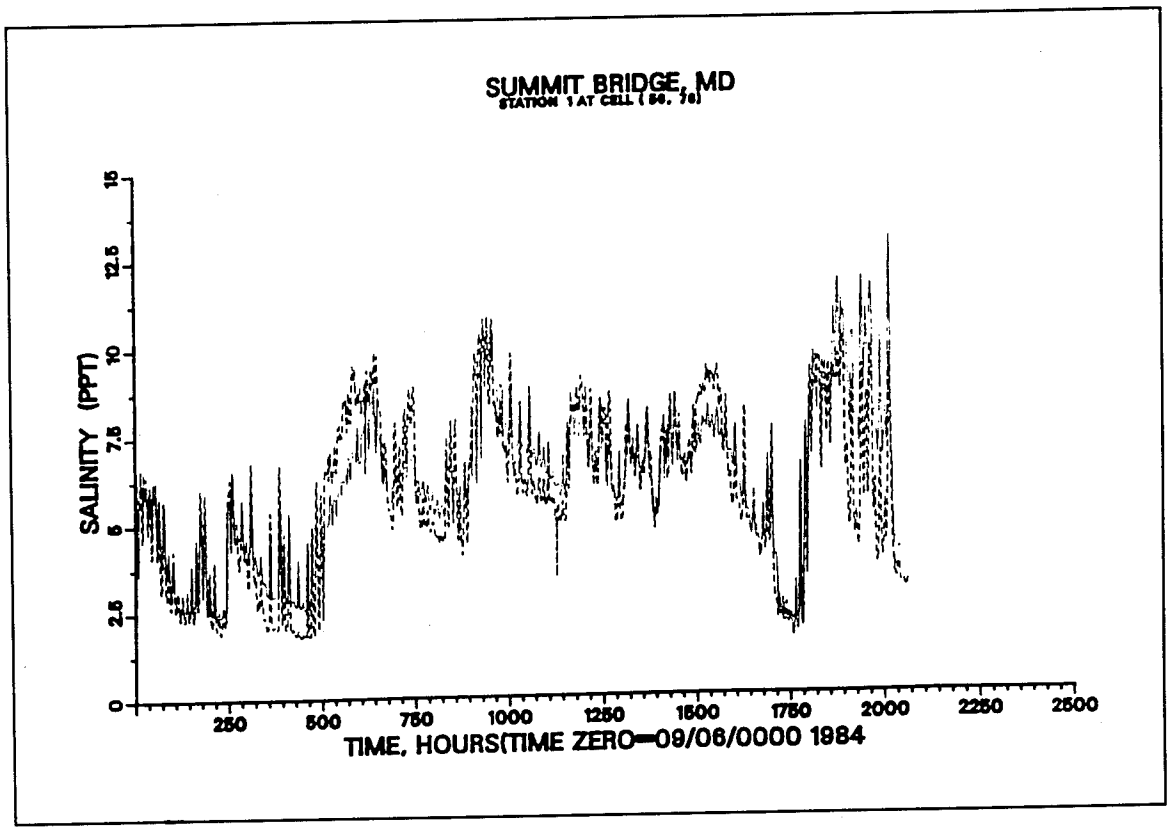

Figure 9a. Computed (____) versus recorded (----) salinity at Summit Bridge (10 m)

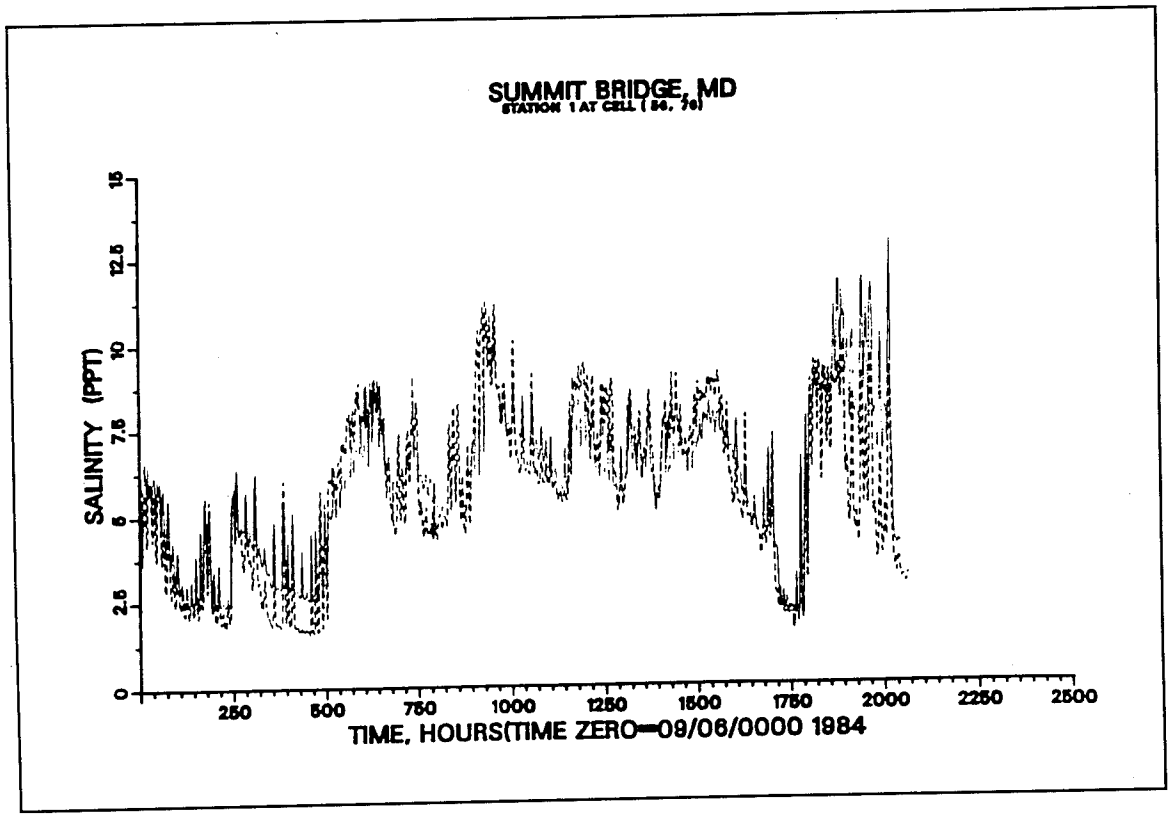

Figure 9b. Computed (____) versus recorded (----) salinity at Summit Bridge (4 m)

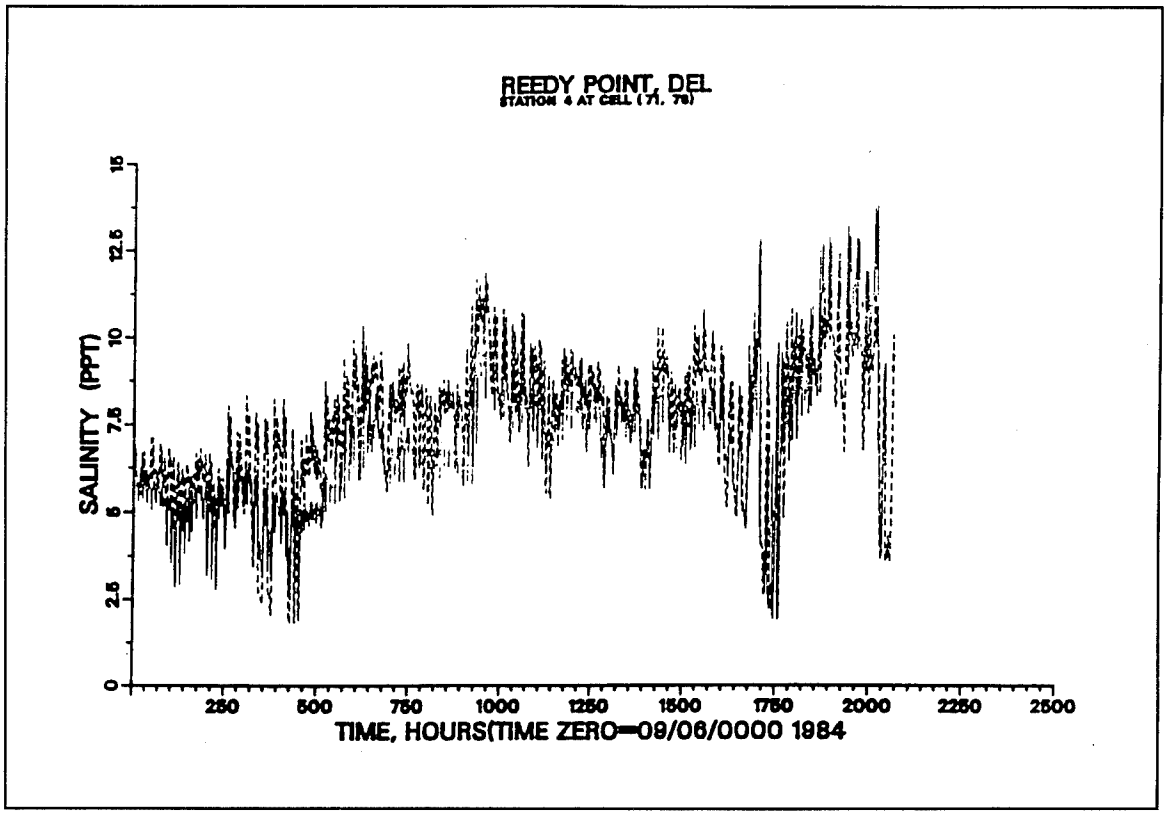

Figure 9c. Computed (____) versus recorded (----) salinity at Reedy Point (2.5 m)

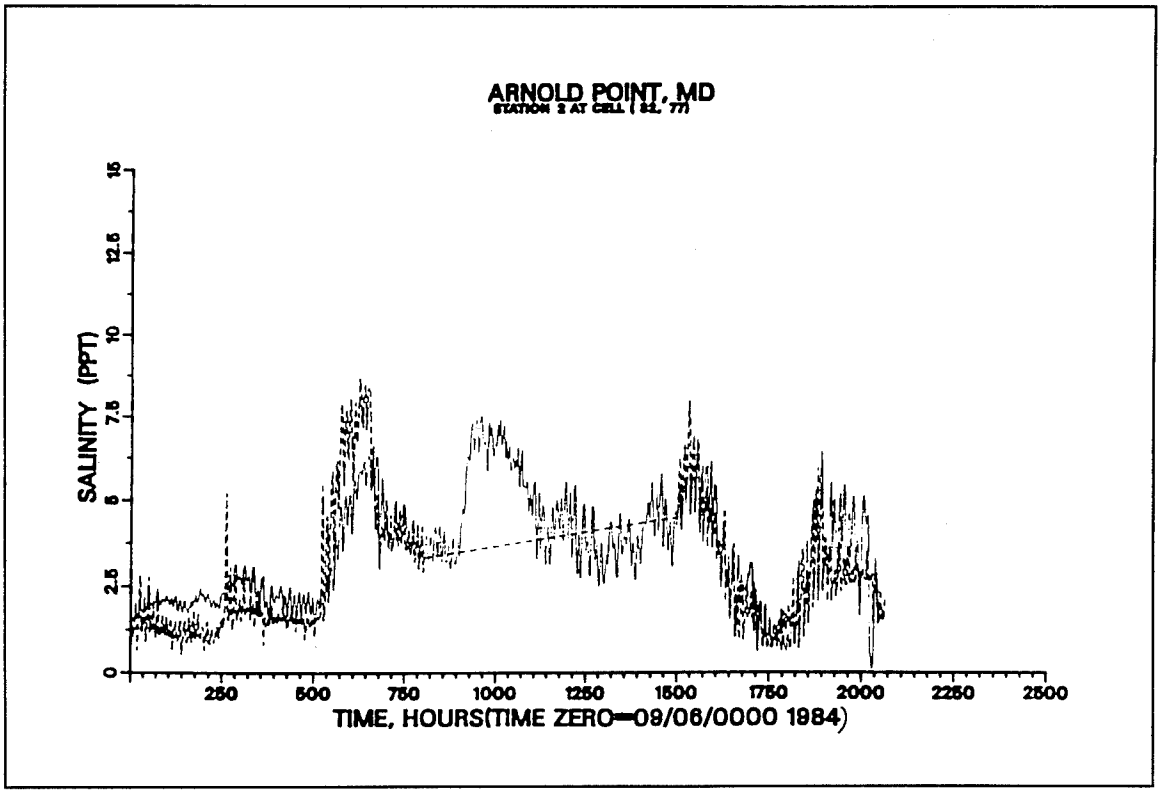

Figure 9d. Computed (____) versus recorded (----) salinity at Arnold Point (4 m)

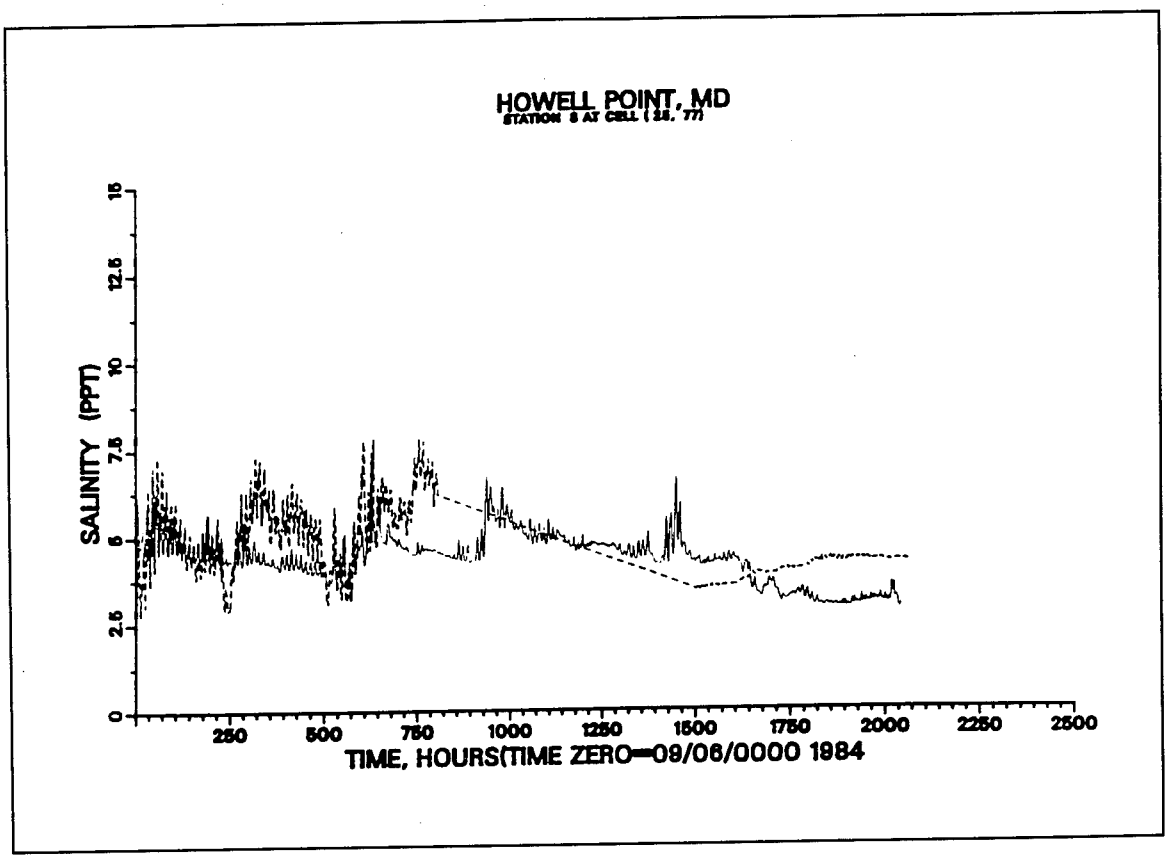

Figure 9e. Computed (____) versus recorded (----) salinity at Howell Point (5.5 m)

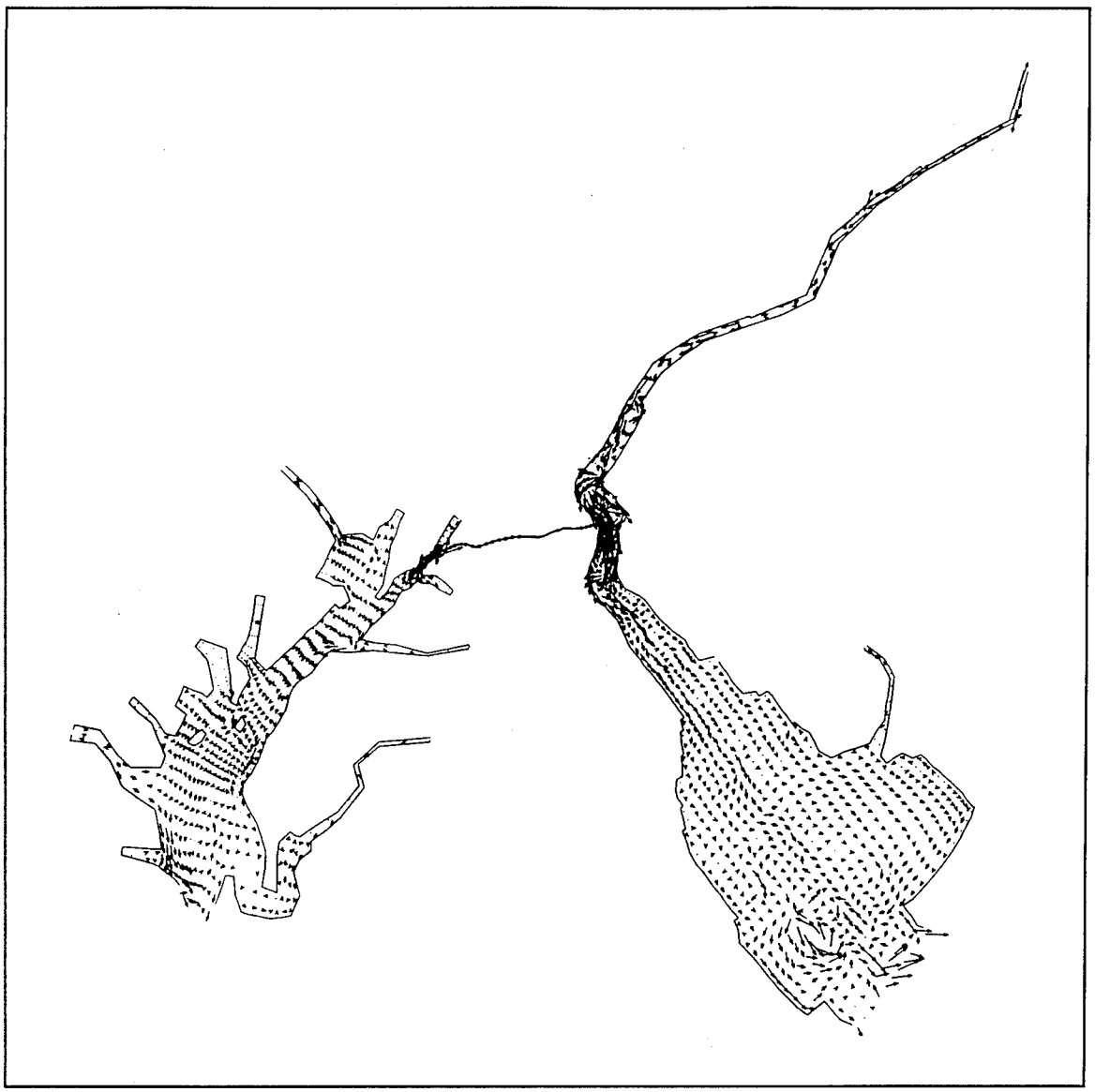

Figure 10a. Seasonal (Fall 1984) averaged current (Layer 16, 0.8 m)

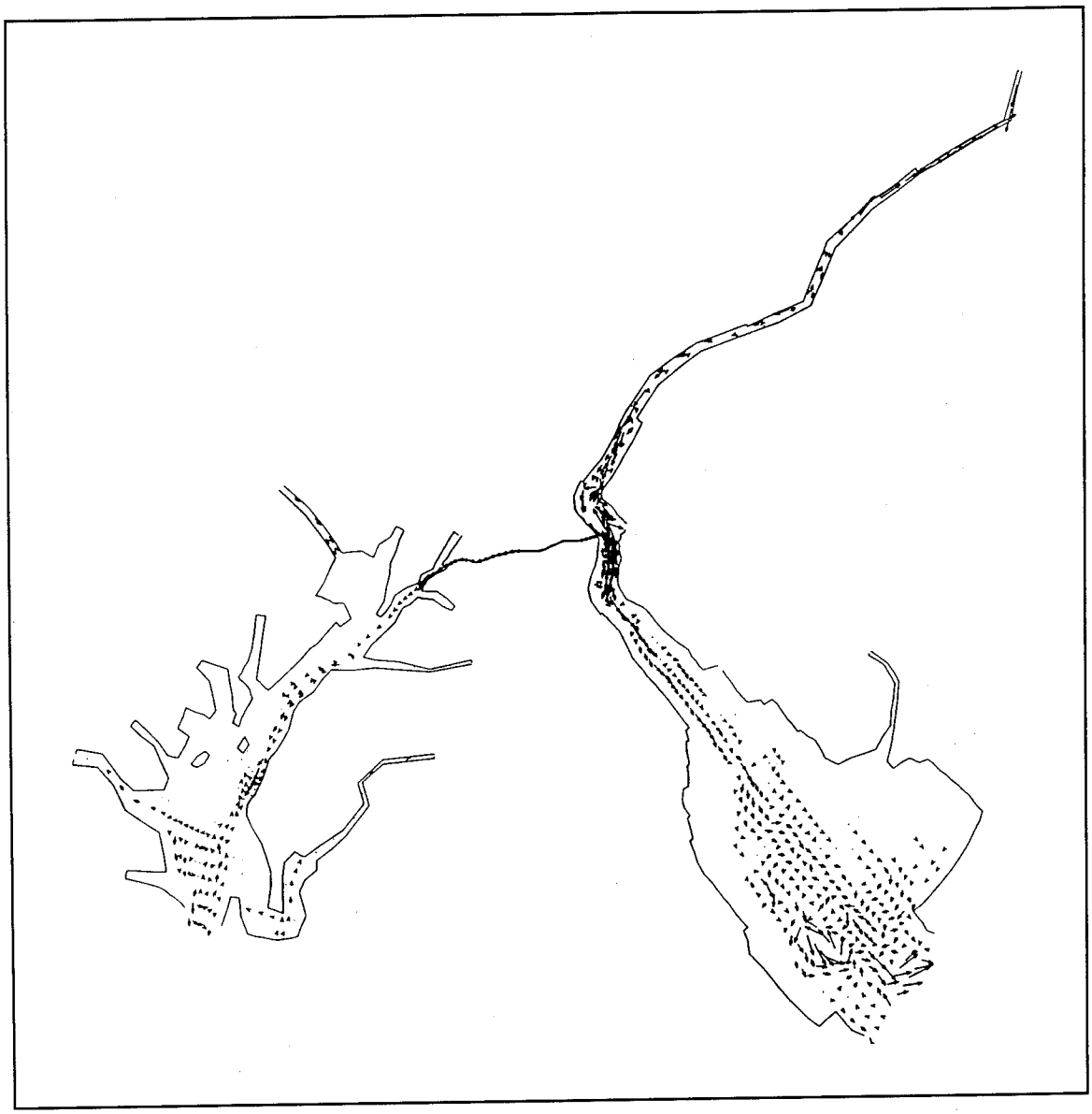

Figure 10b. Seasonal (Fall 1984) averaged current (Layer 13, 5.3 m)

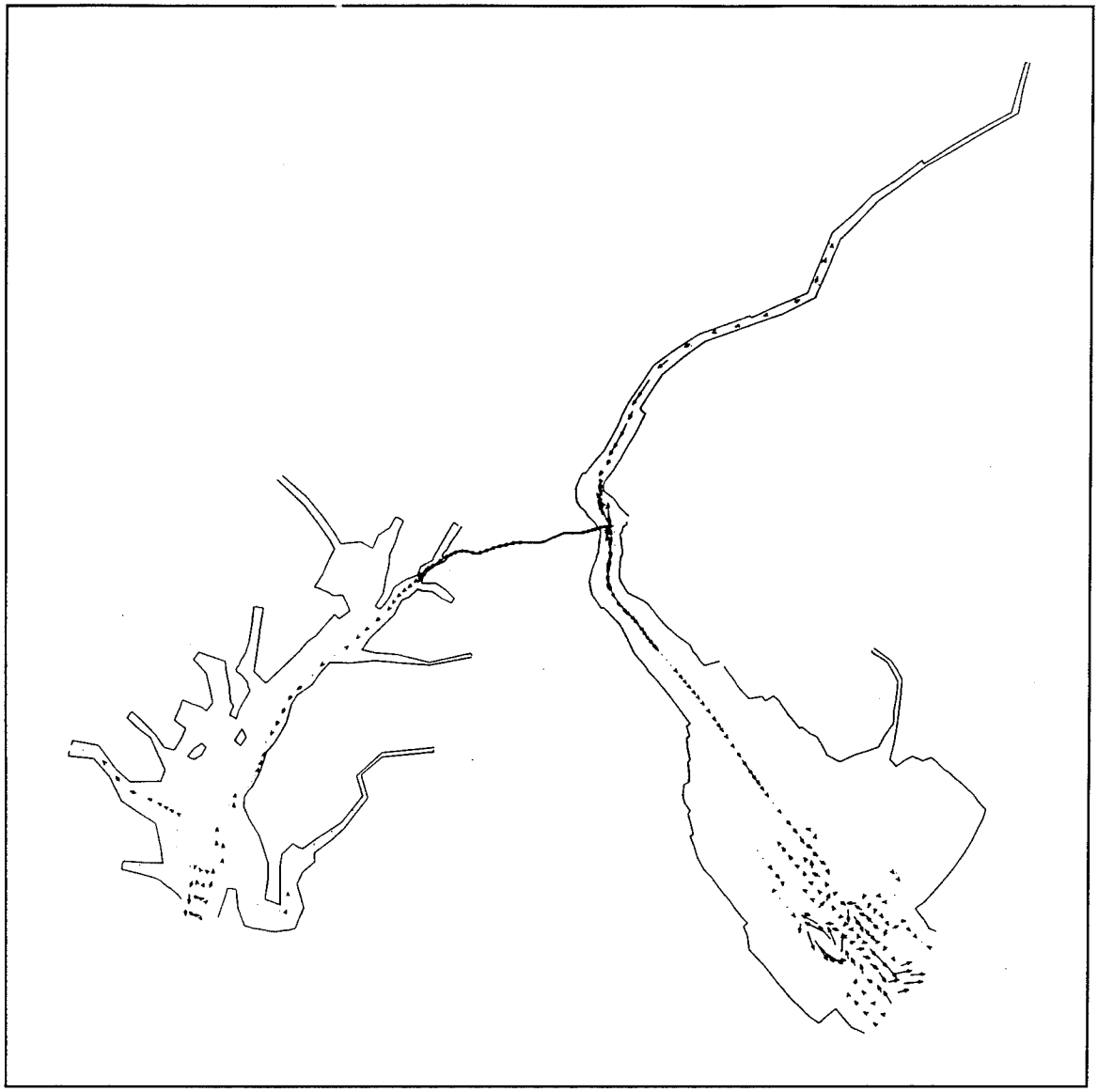

Figure 10c. Seasonal (Fall 1984) averaged current (Layer 10, 9.8 m)

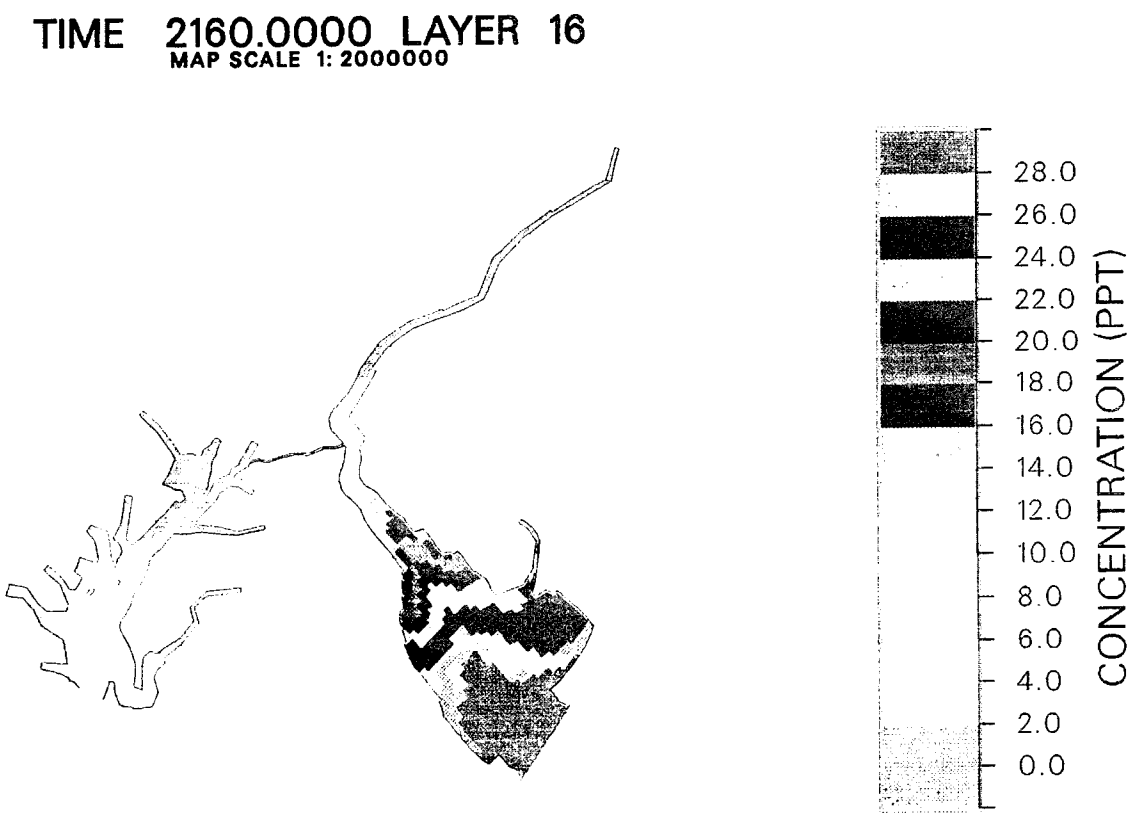

Figure 11a. Seasonal (Fall 1984) averaged salinity (Layer 16, 0.8 m)

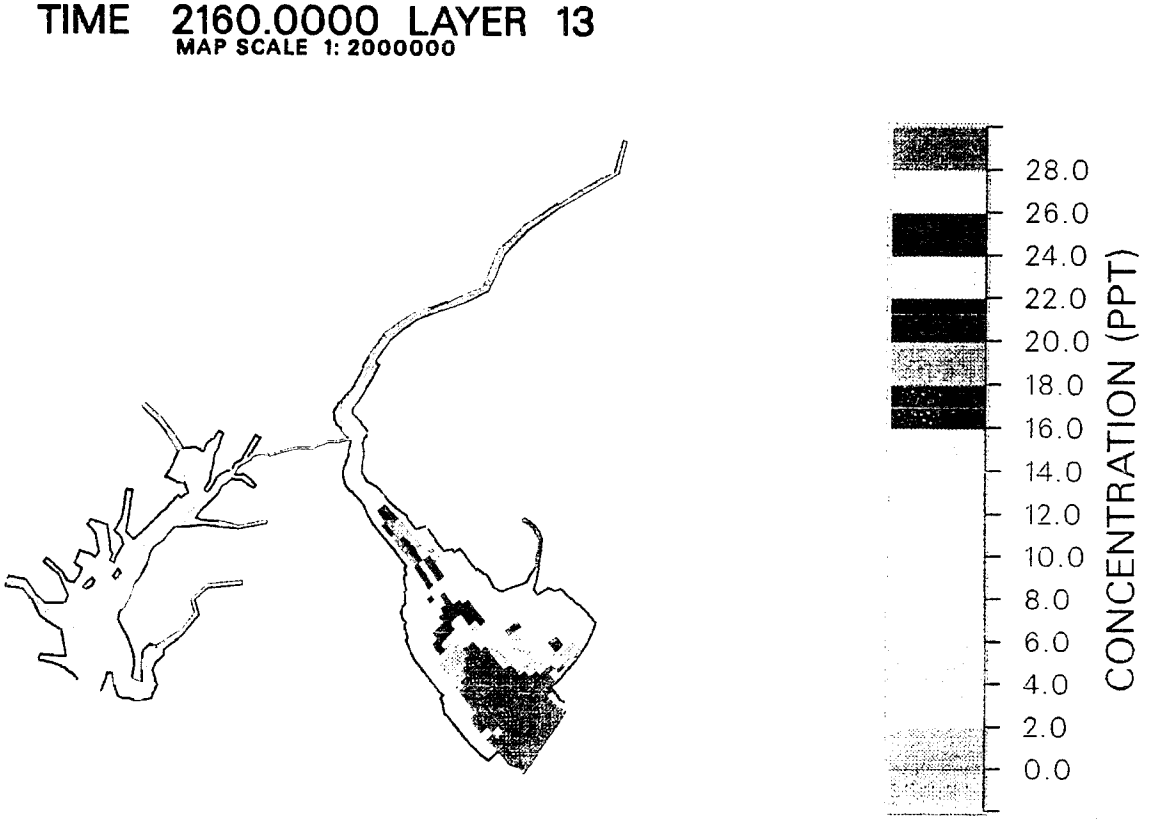

Figure 11b. Seasonal (Fall 1984) averaged salinity (Layer 13, 5.3 m)

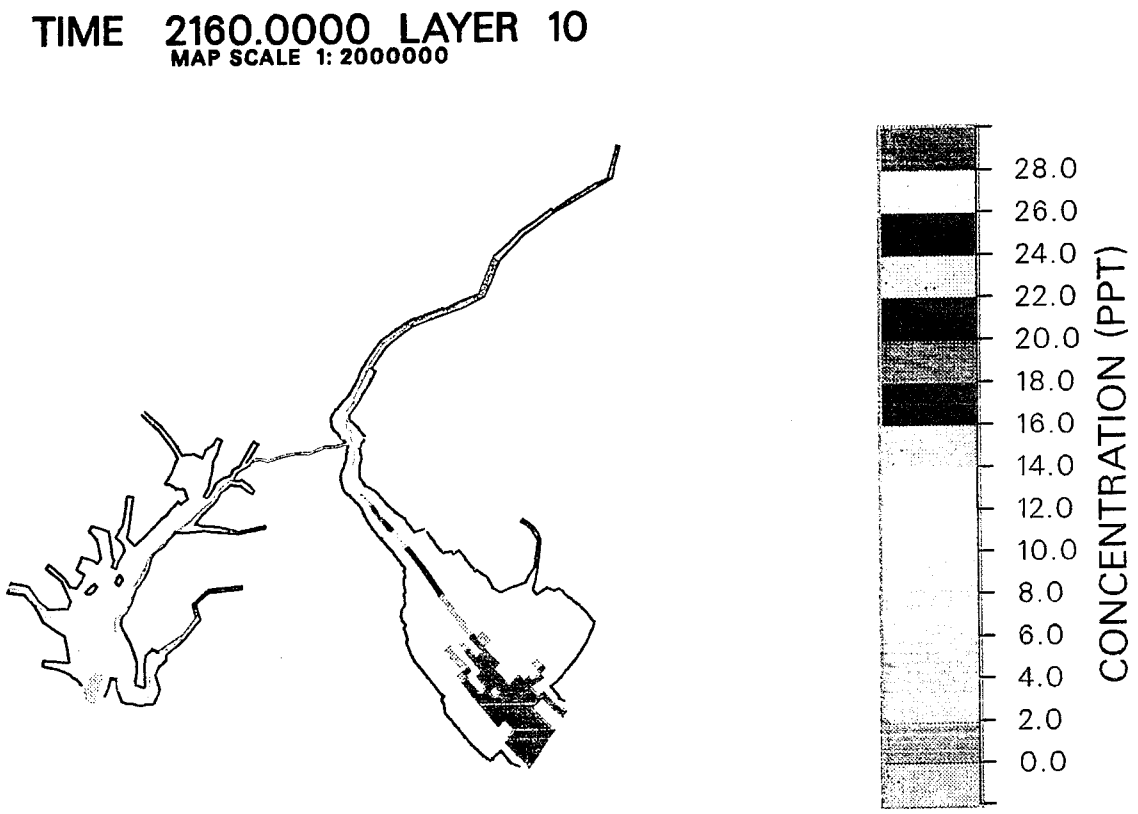

Figure 11c. Seasonal (Fall 1984) averaged salinity (Layer 10, 9.8 m)

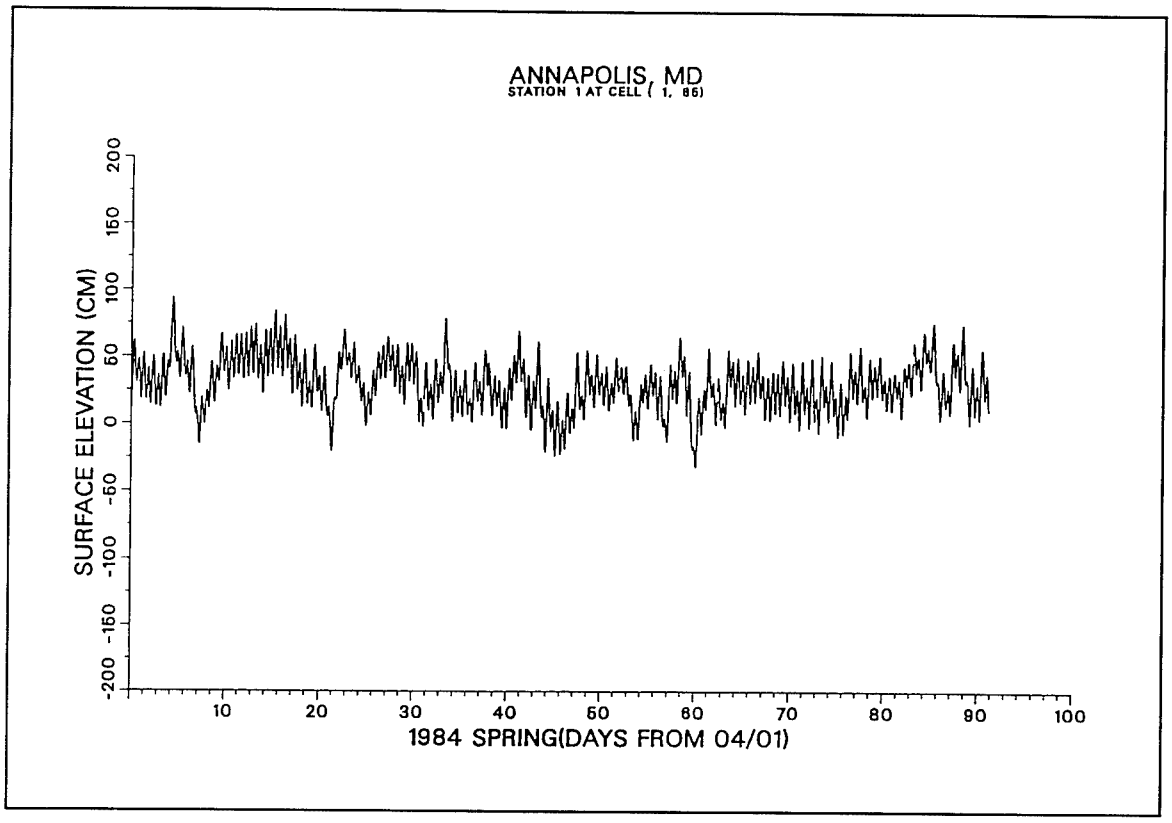

Figure 12a. Recorded tide at Annapolis

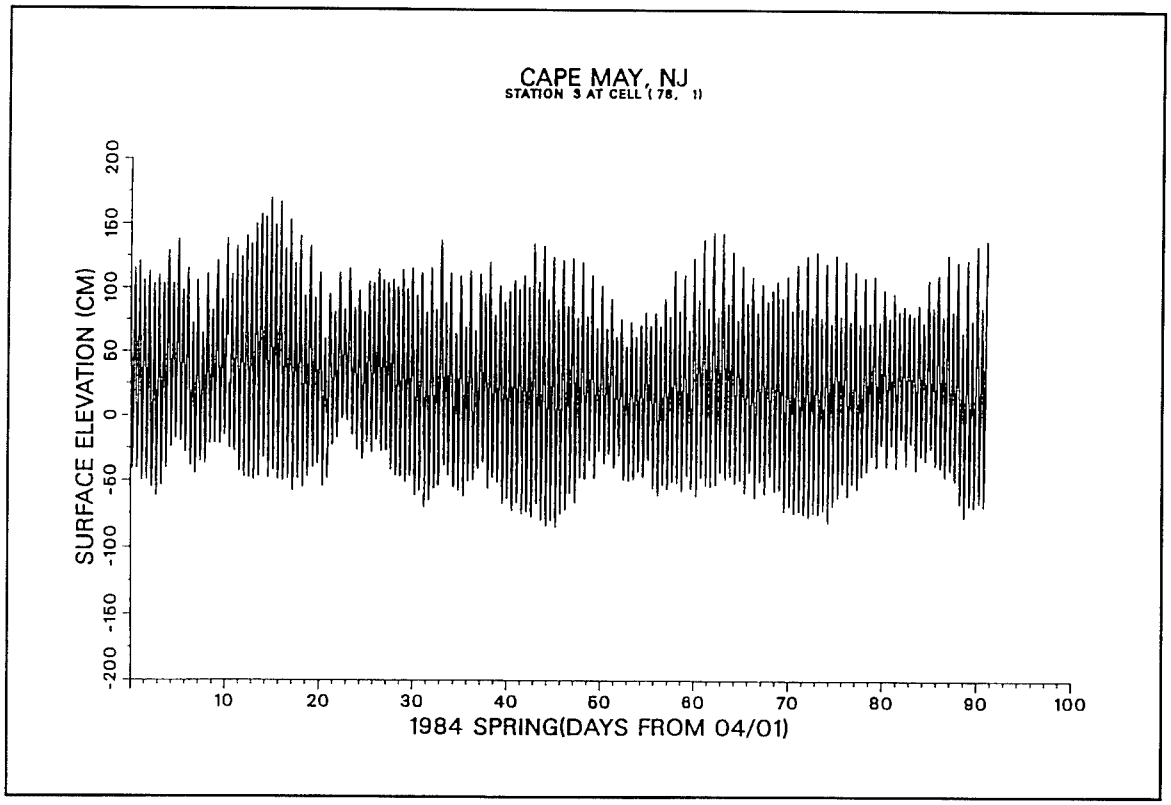

Figure 12b. Recorded tide at Cape May

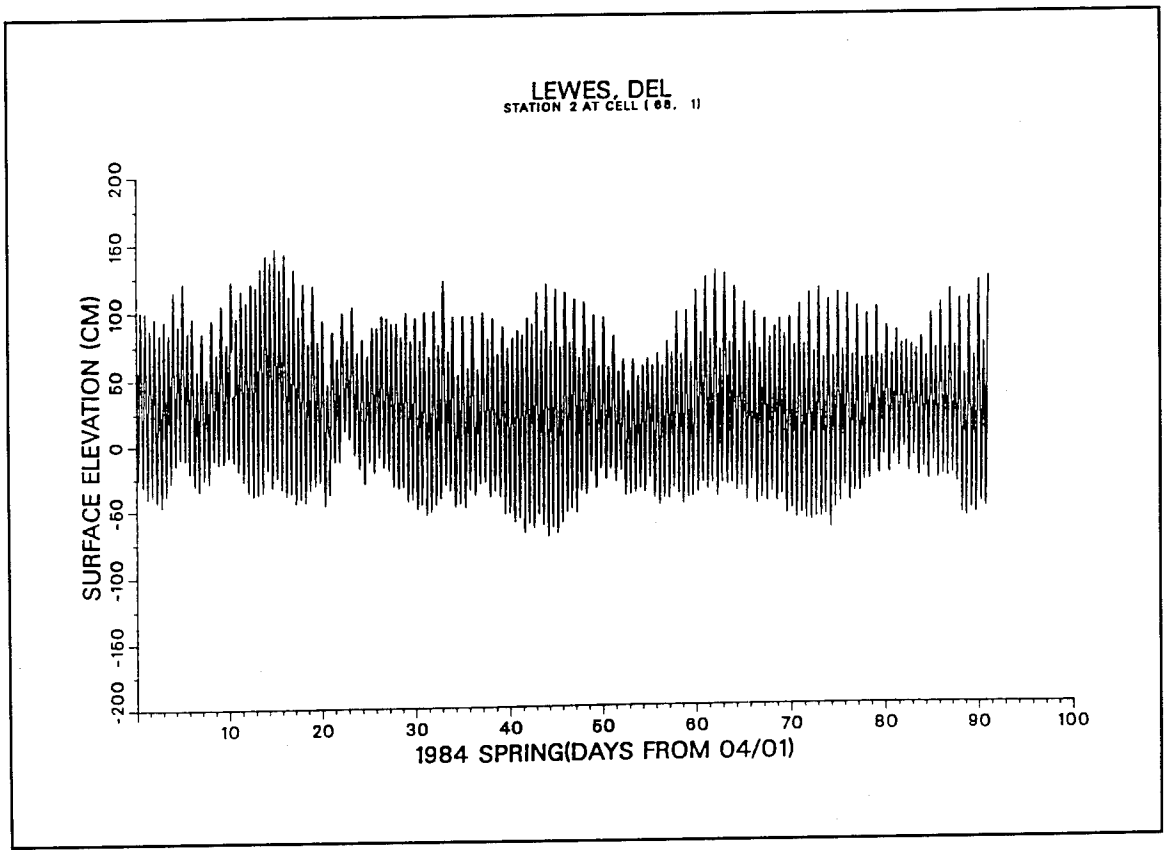

Figure 12c. Recorded tide at Lewes

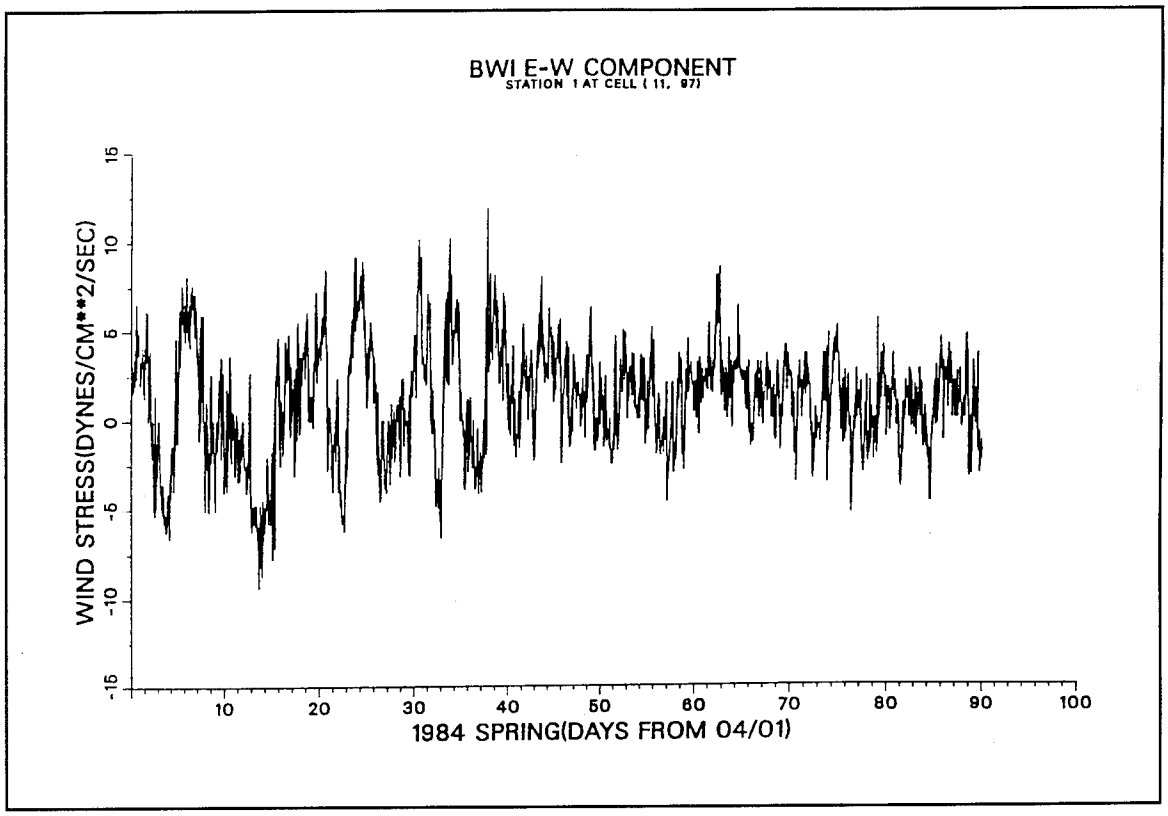

Figure 14a. Wind at BWI (East-West Component)

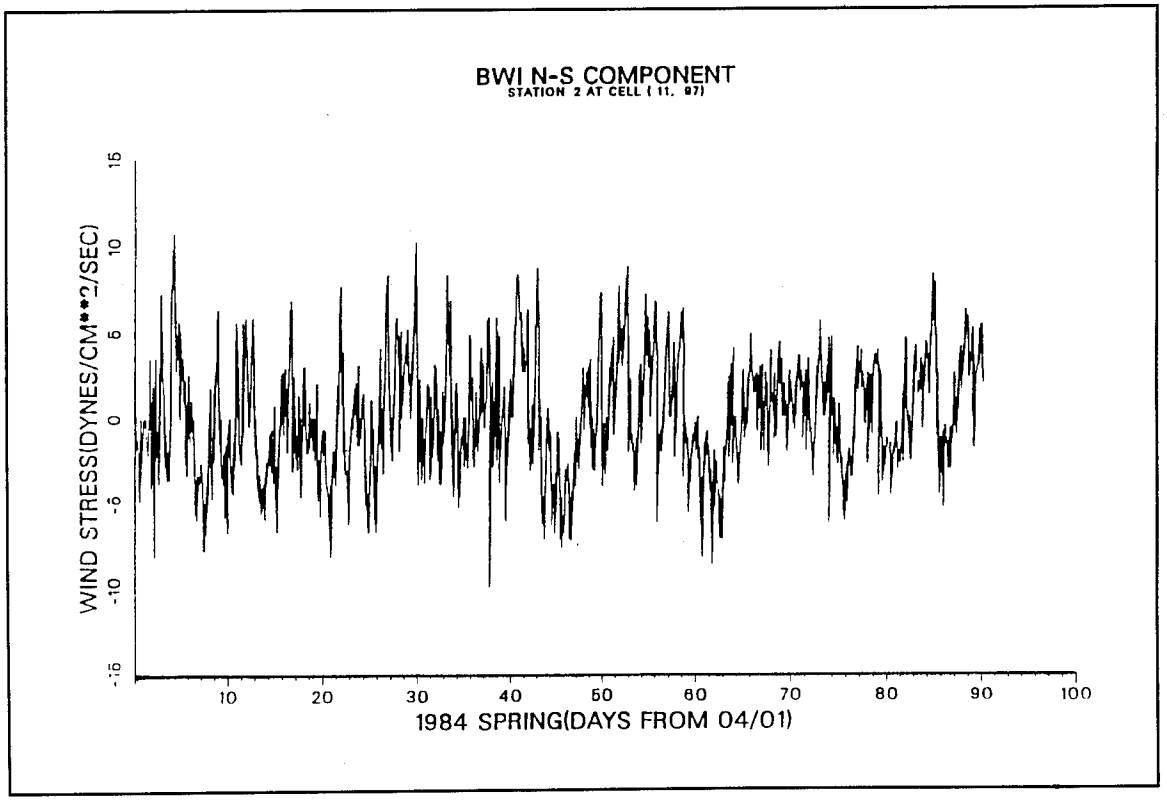

Figure 14b. Wind at BWI (North-South Component)

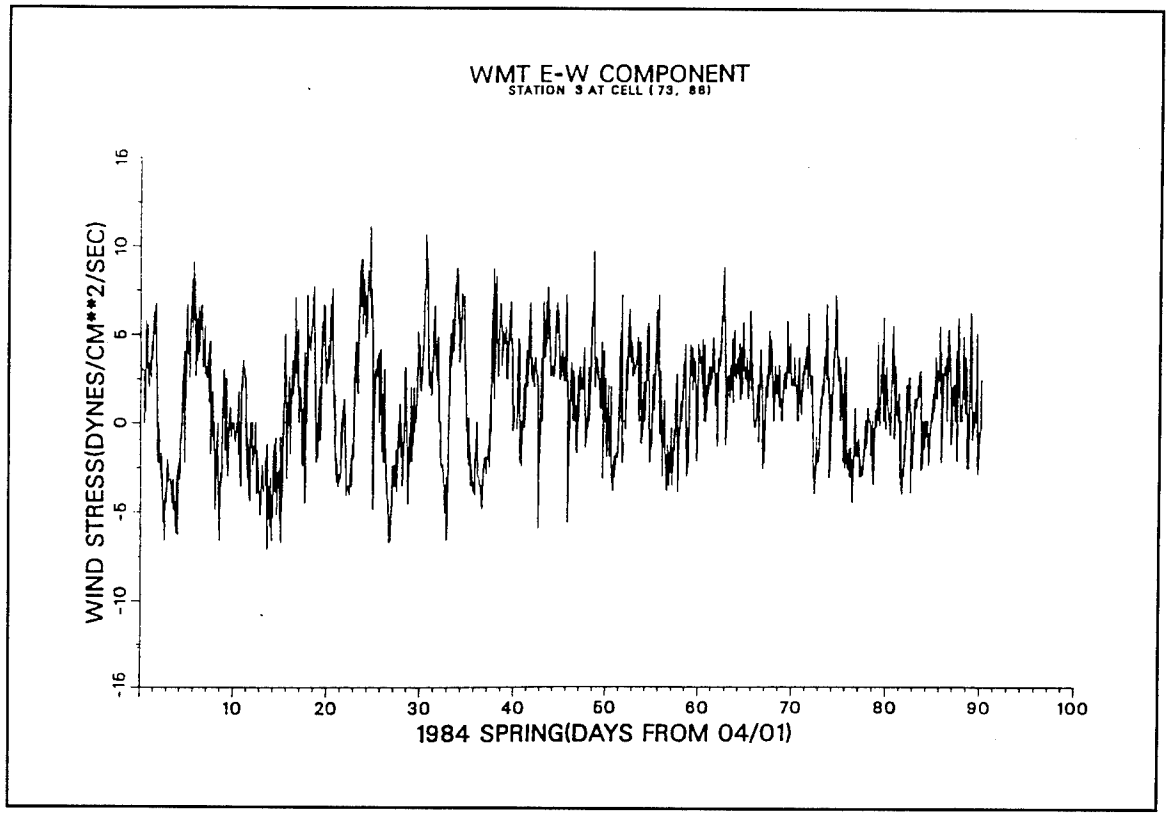

Figure 14c. Wind at Wilmington (East-West Component)

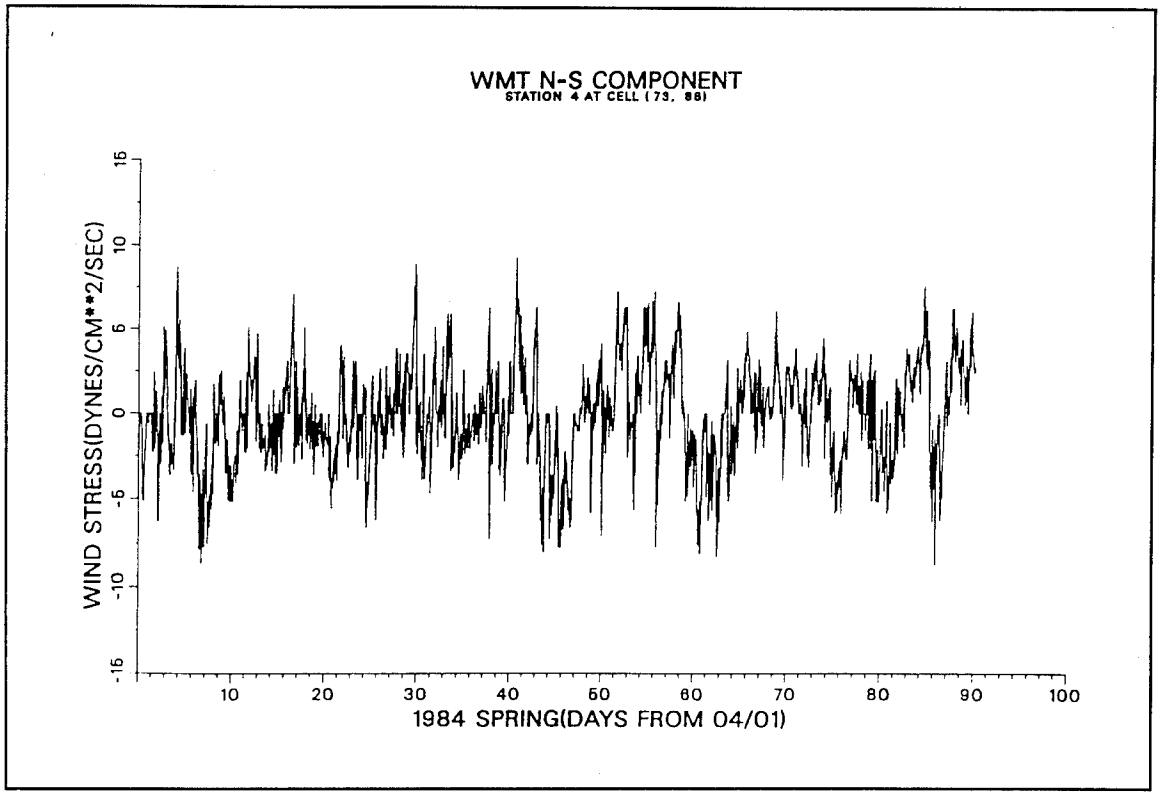

Figure 14d. Wind at Wilmington (North-South Component)

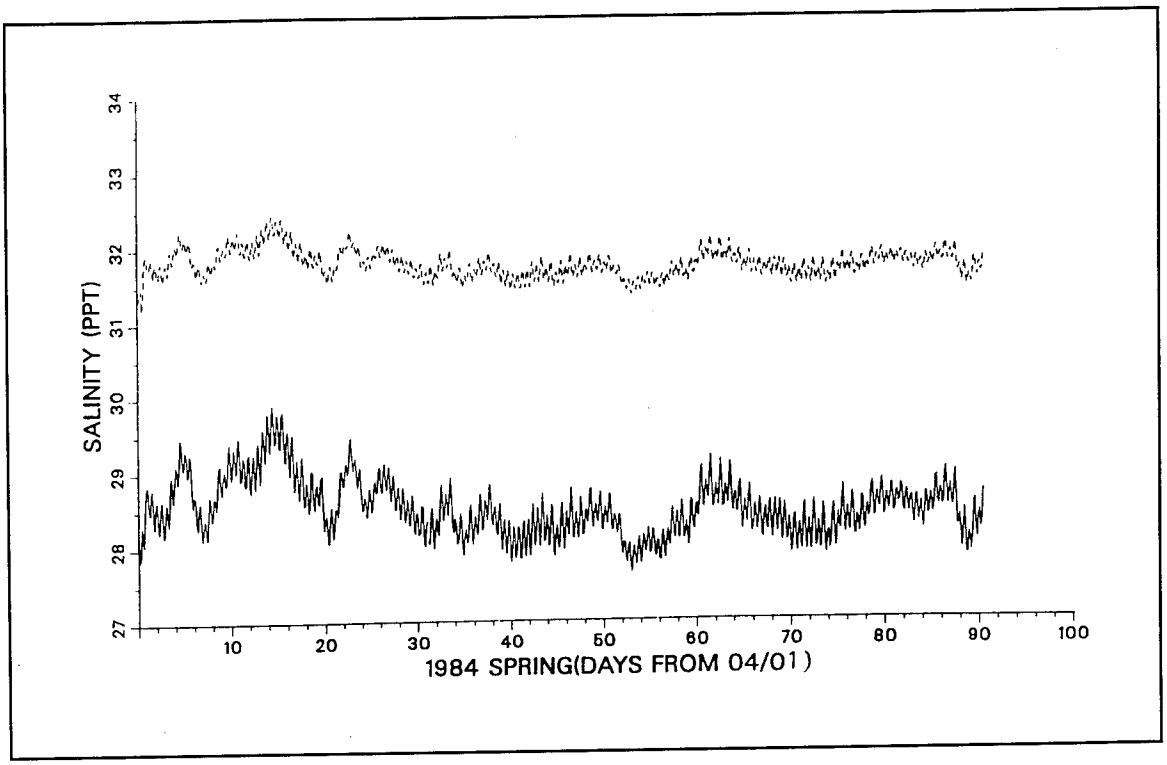

Figure 15a. Synthesized surface (solid line) and bottom (dashed line) salinity boundary at Delaware Bay mouth

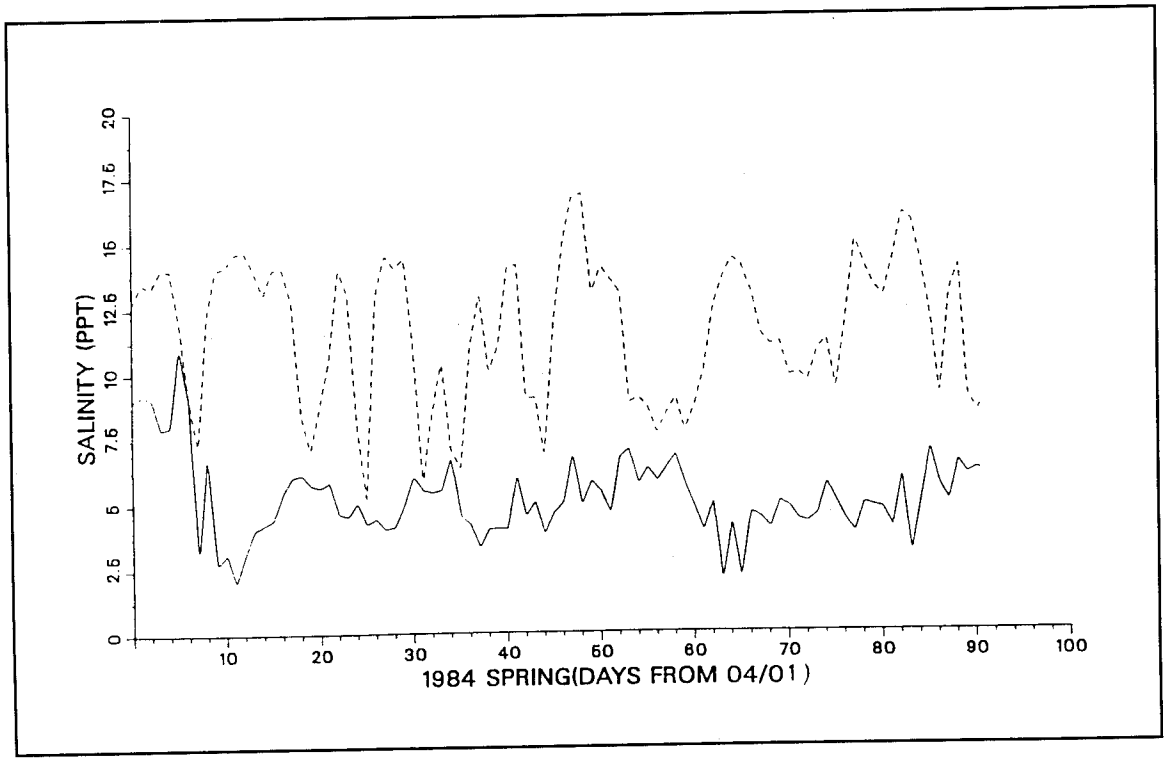

Figure 15b. Synthesized surface (solid line) and bottom (dashed line) salinity boundary at Chesapeake Bay Bridge

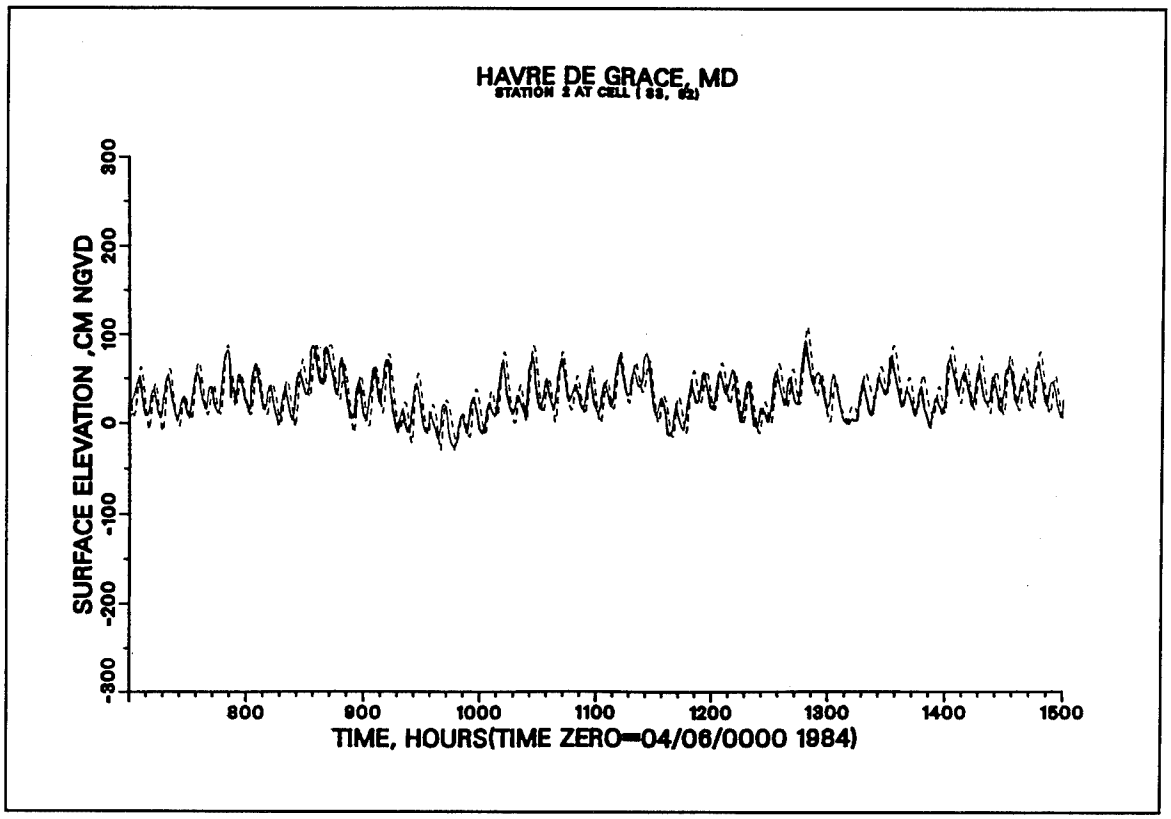

Figure 16a. Computed (__) versus recorded (---) tide at Havre de Grace

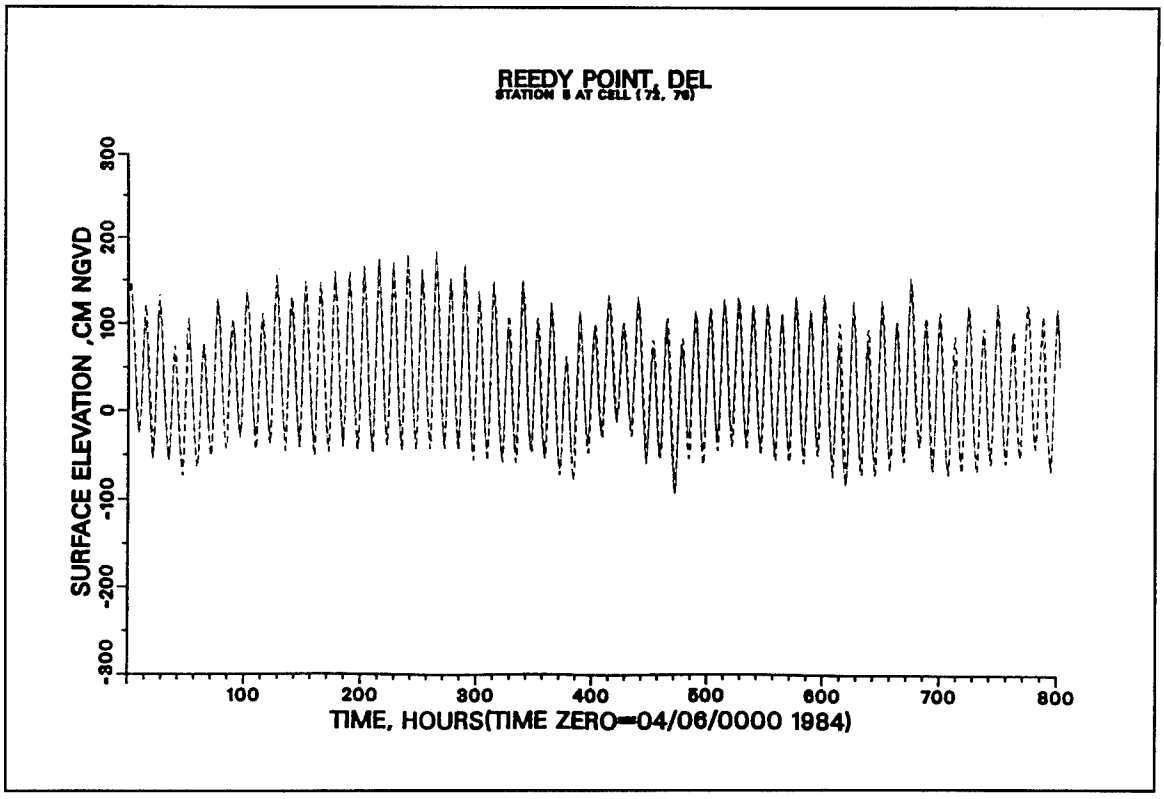

Figure 16b. Computed (__) versus recorded (---) tide at Reedy Point

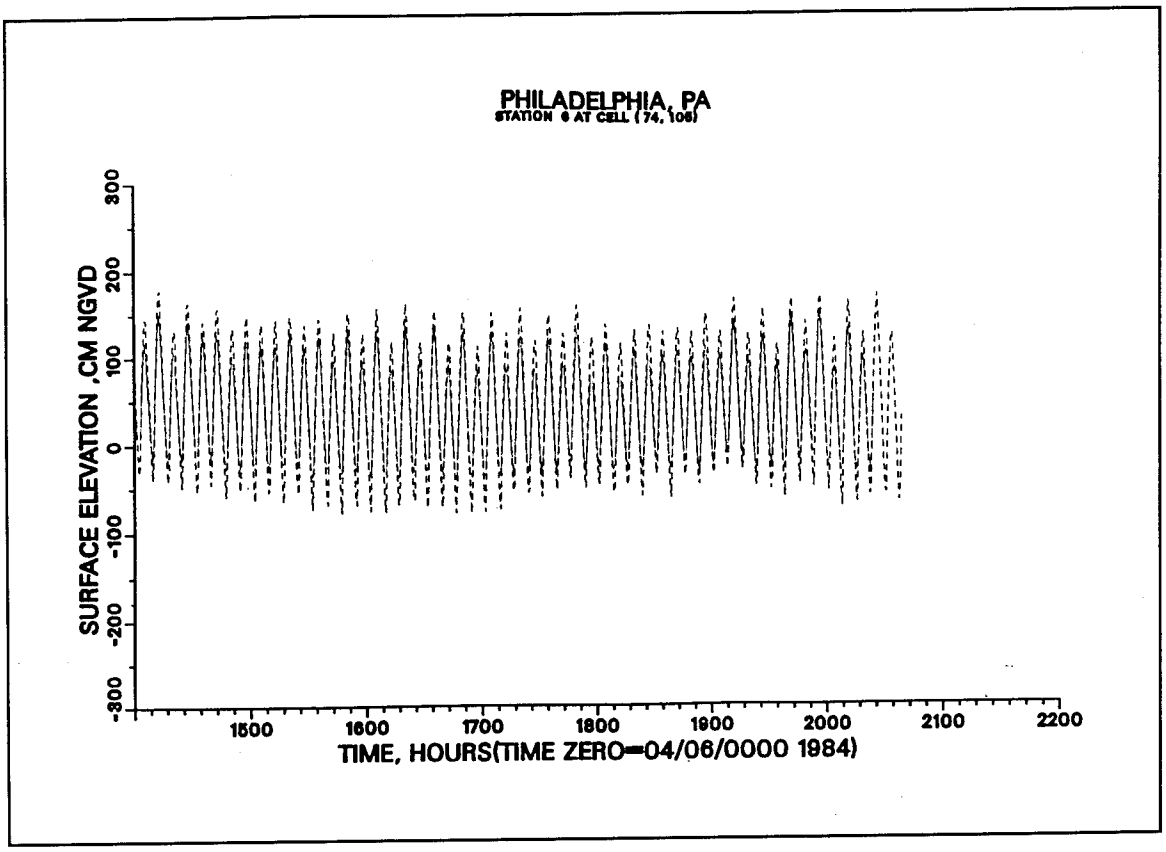

Figure 16c. Computed (__) versus recorded (---) tide at Philadelphia

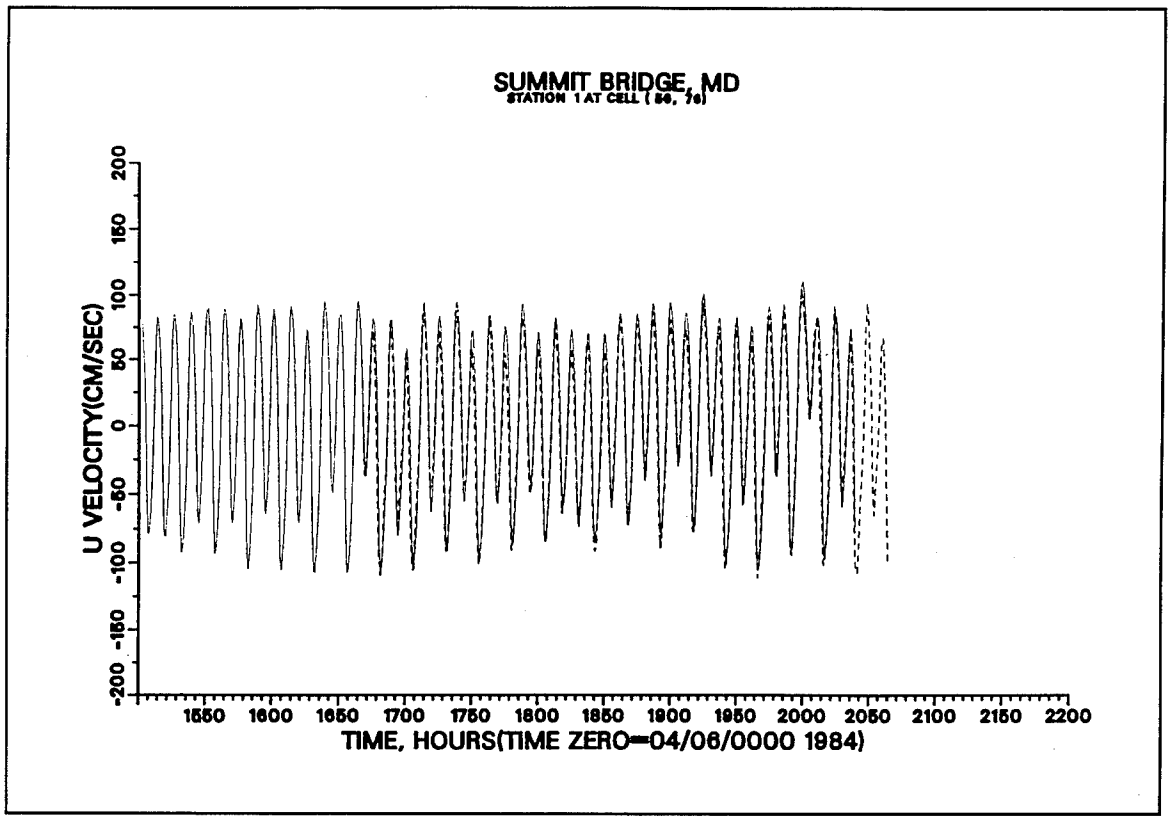

Figure 17a. Computed (___) versus recorded (---) velocity at Summit Bridge (10 m)

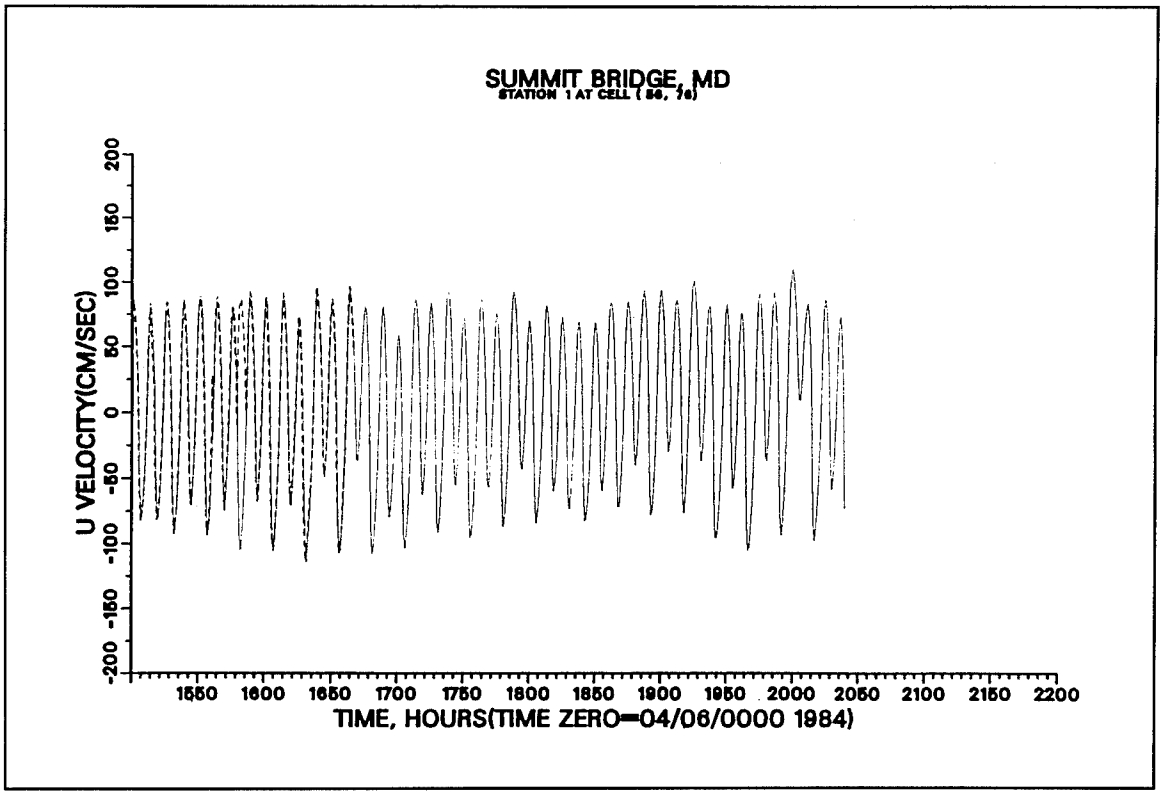

Figure 17b. Computed (___) versus recorded (---) velocity at Summit Bridge (7m)

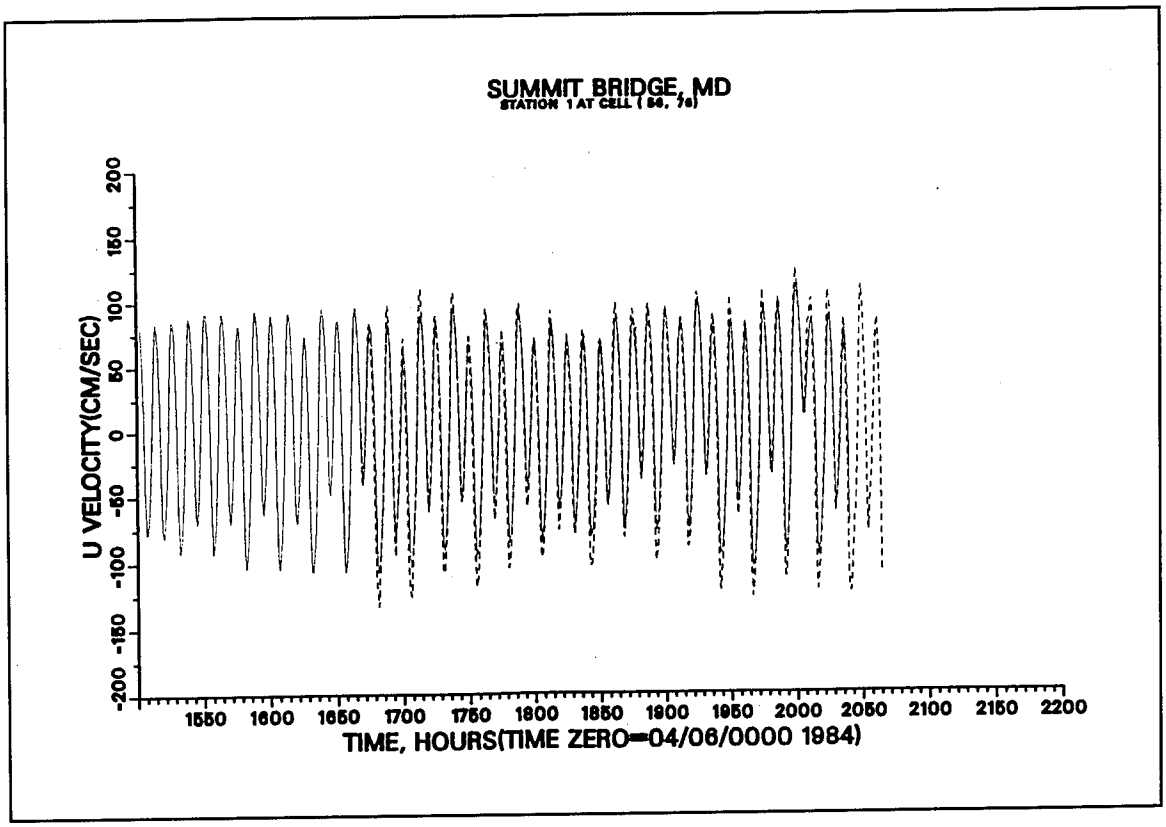

Figure 17c. Computed (___) versus recorded (---) velocity at Summit Bridge (4m)

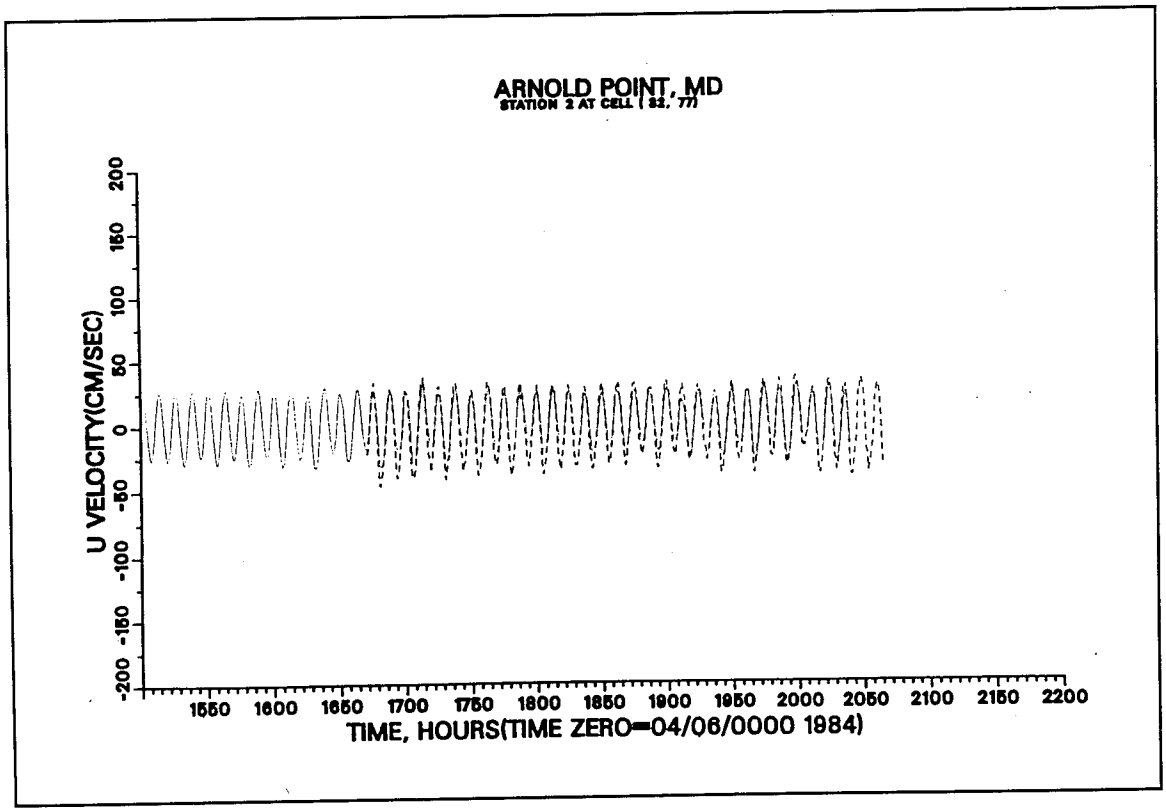

Figure 17d. Computed (___) versus recorded (---) velocity at Arnold Point (4m)

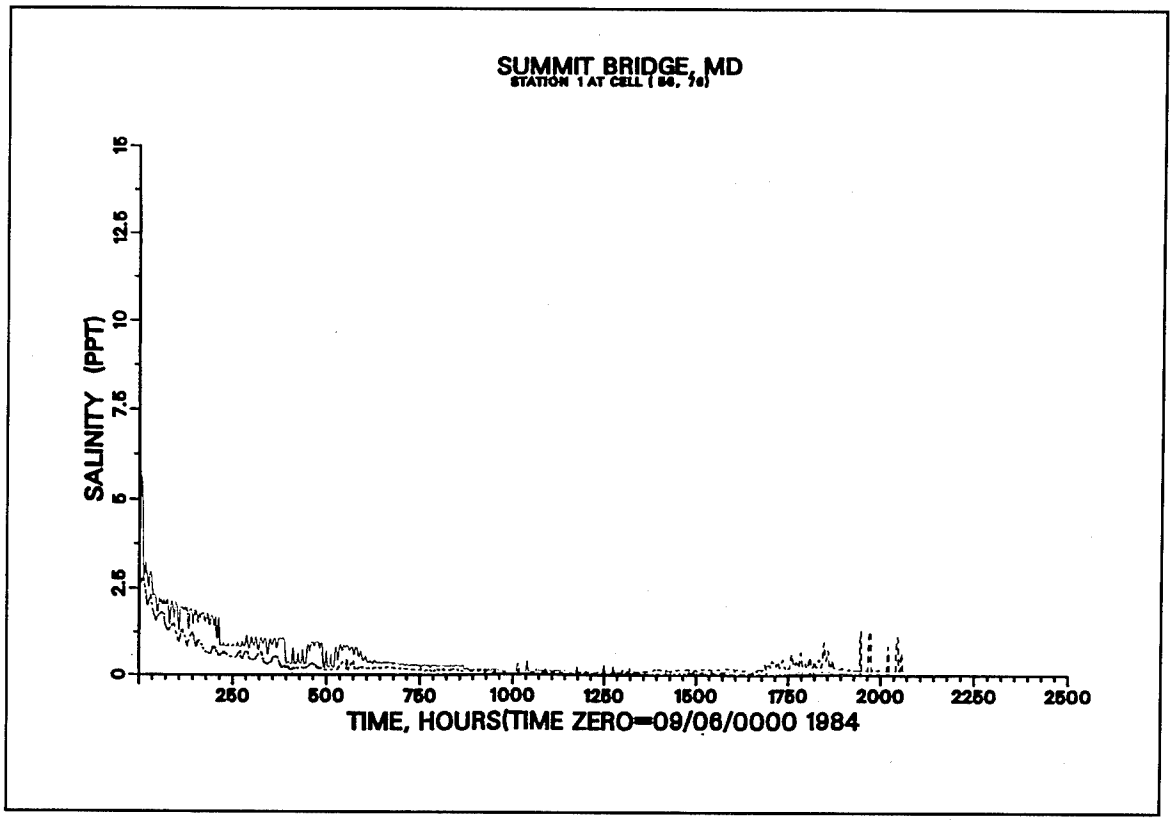

Figure 18a. Computed (___) versus recorded (---) salinity at Summit Bridge (10m)

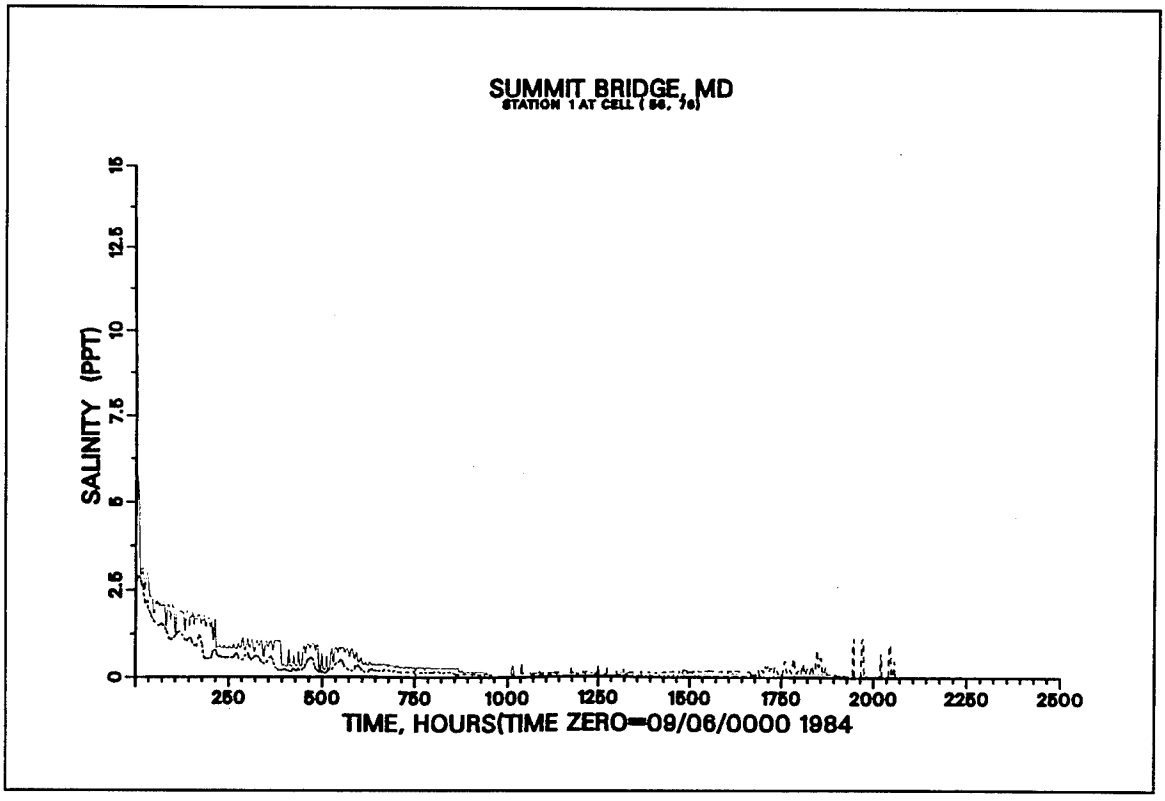

Figure 18b. Computed (___) versus recorded (---) salinity at Summit Bridge (4m)

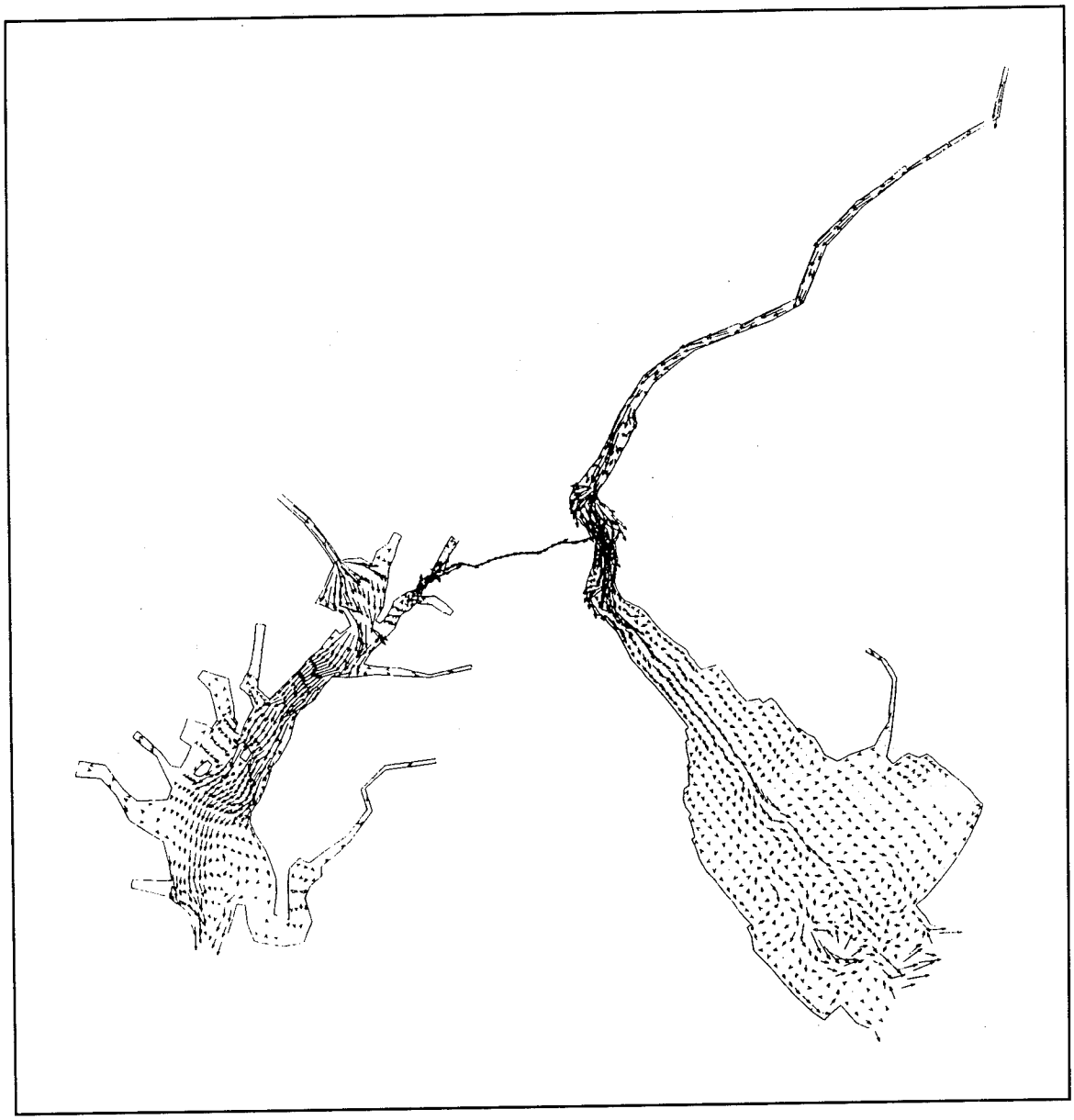

Figure 19a. Seasonal (Spring 1984) averaged current (Layer 16, 0.8 m)

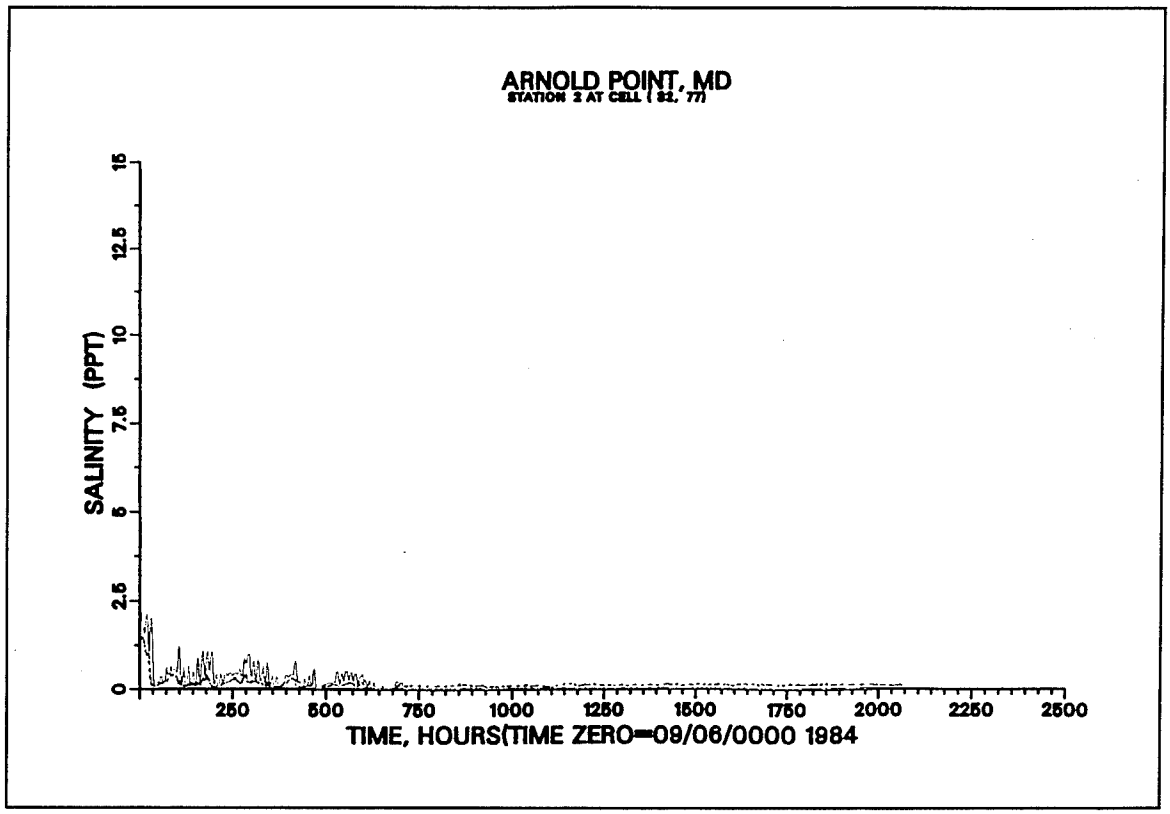

Figure 18c. Computed (___) versus recorded (---) salinity at Arnold Point (4m)

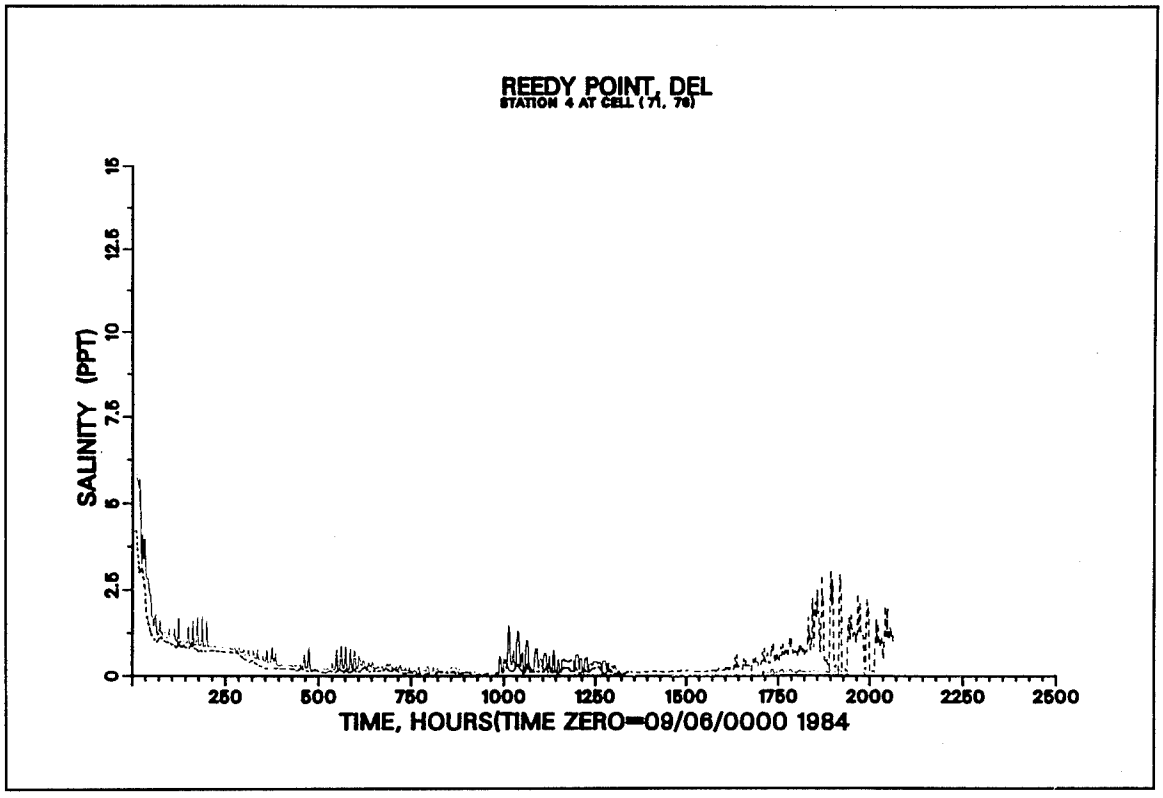

Figure 18d. Computed (___) versus recorded (---) salinity at Reedy Point (2.5 m)

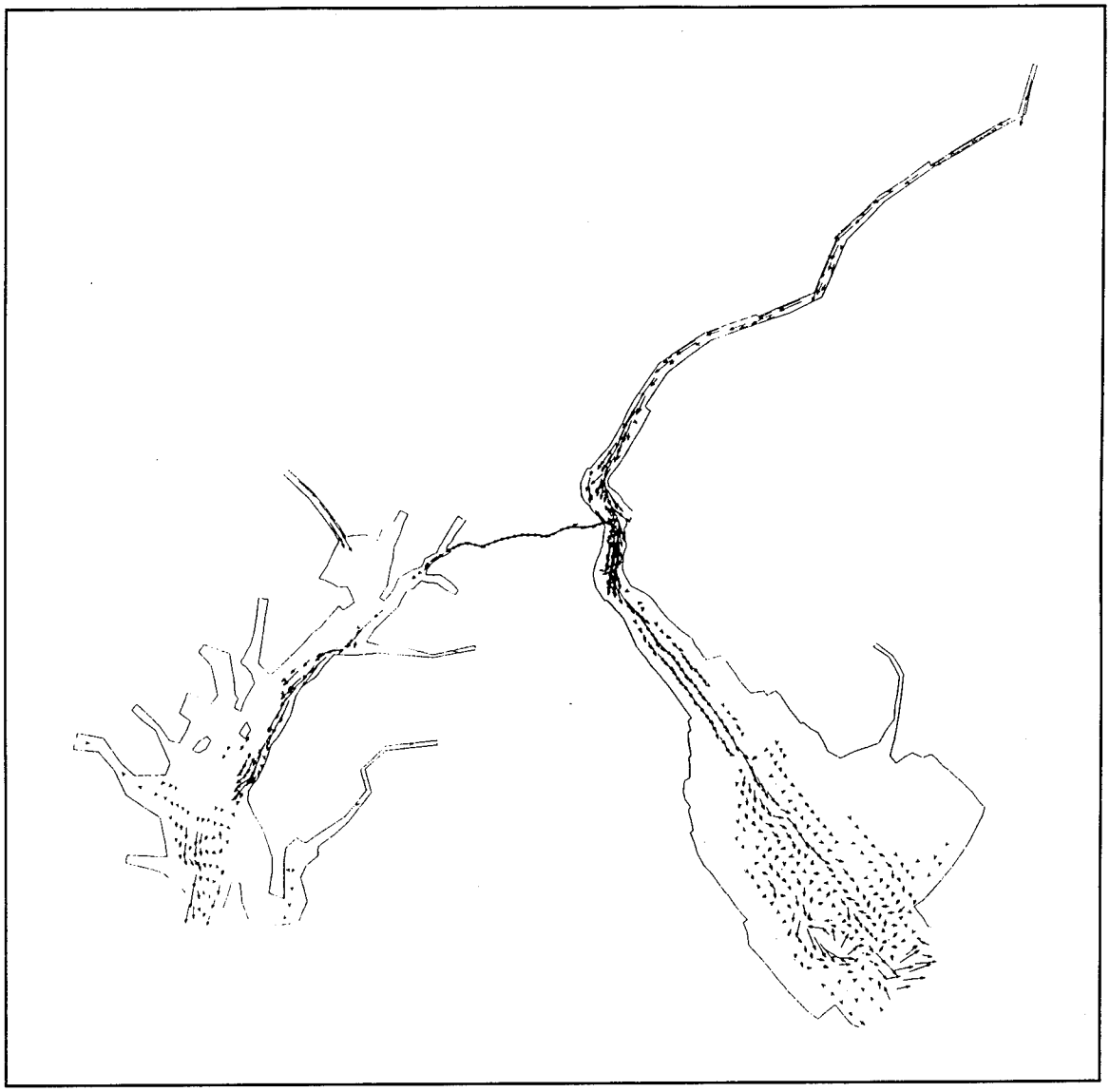

Figure 19b. Seasonal (Spring 1984) averaged current (Layer 13, 5.3 m)

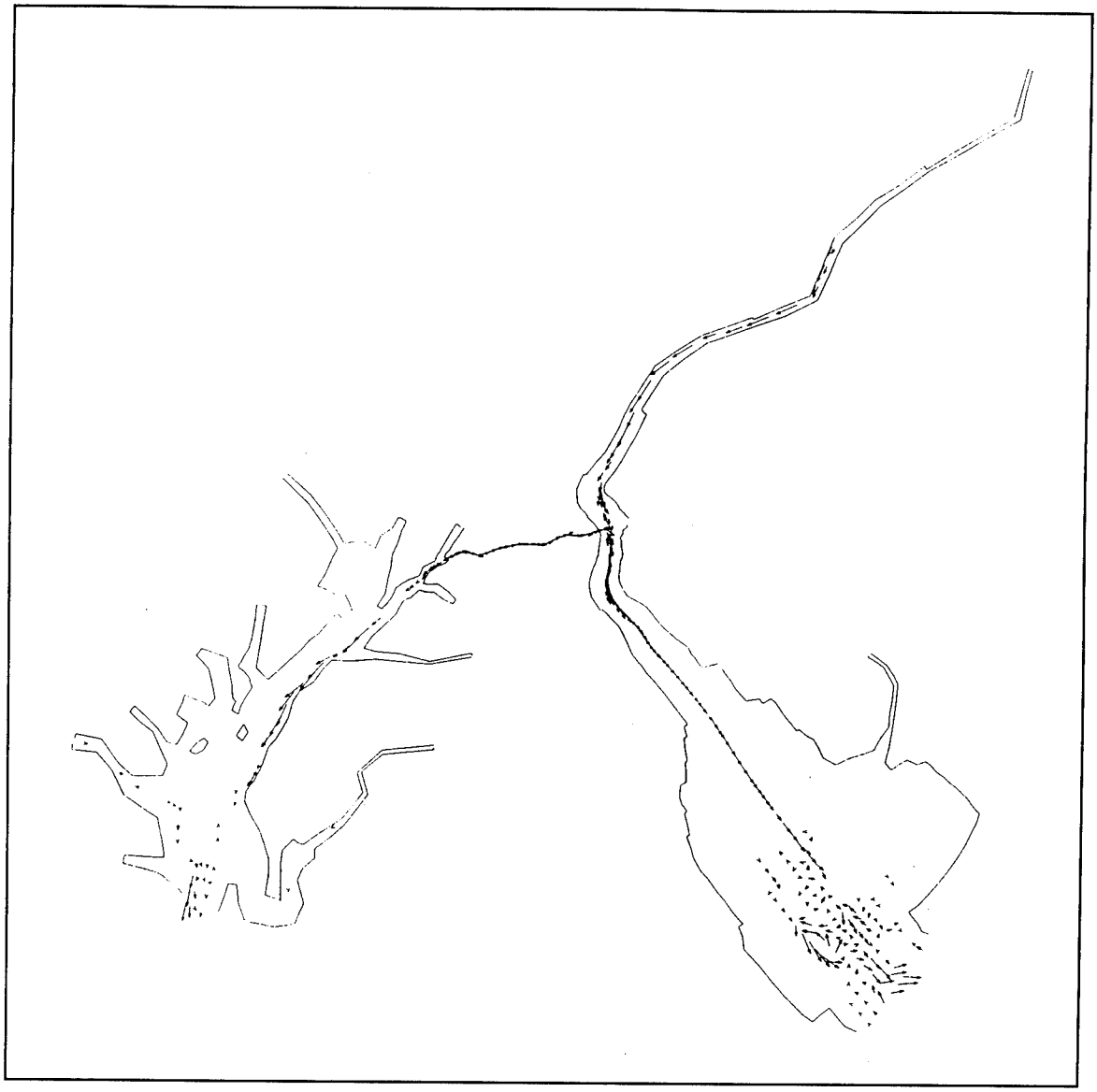

Figure 19c. Seasonal (Spring 1984) averaged current (Layer 10, 9.8 m)

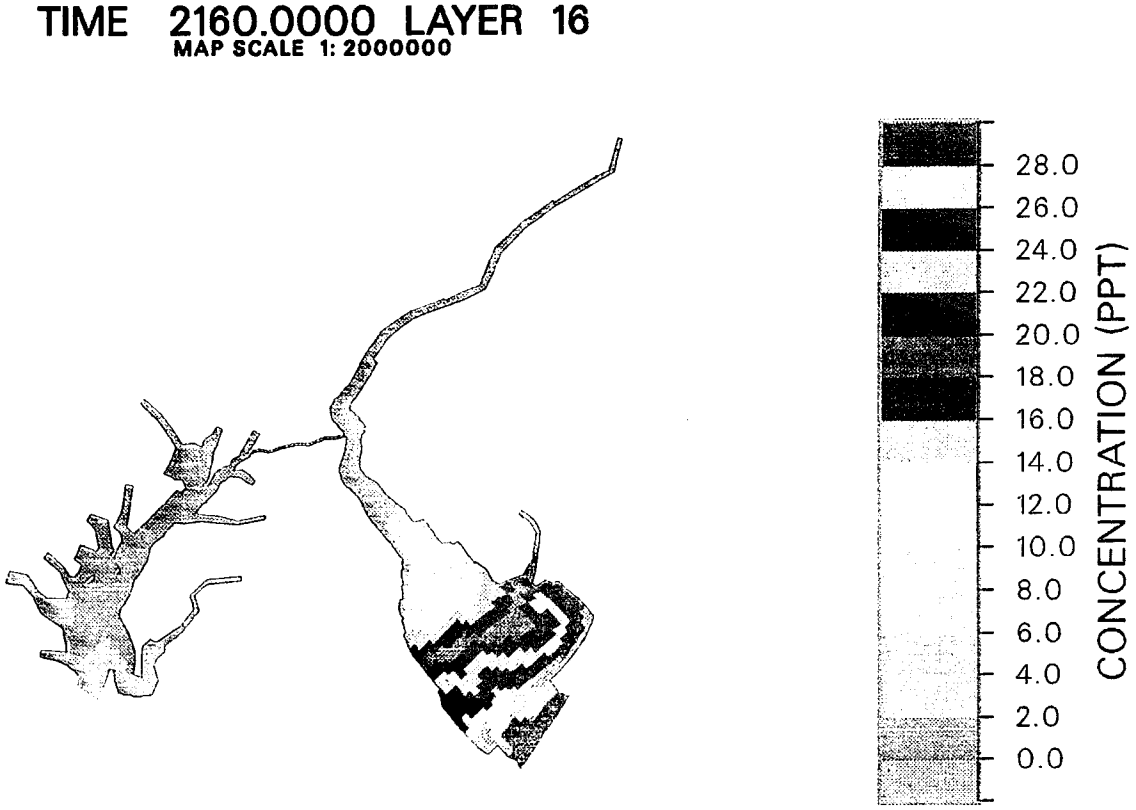

Figure 20a. Seasonal (Spring 1984) averaged salinity (Layer 16, 0.8 m)

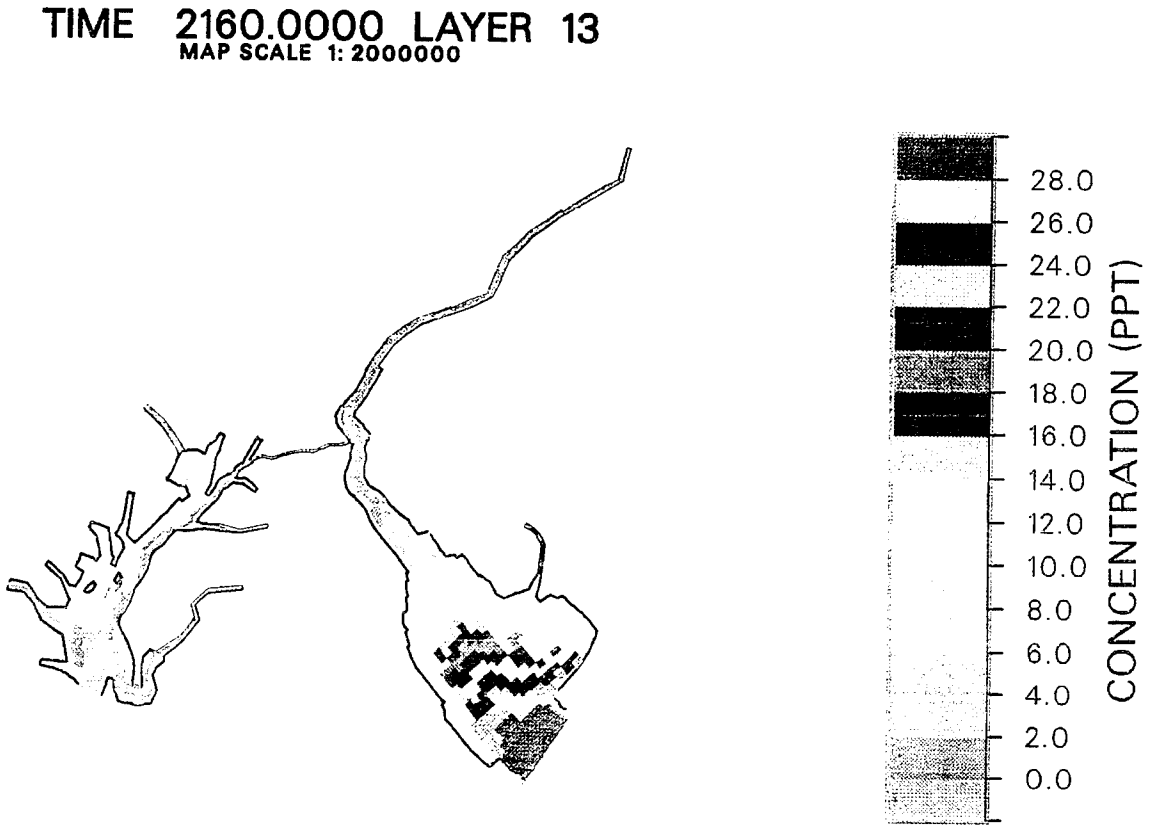

Figure 20b. Seasonal (Spring 1984) averaged salinity (Layer 13, 5.3 m)

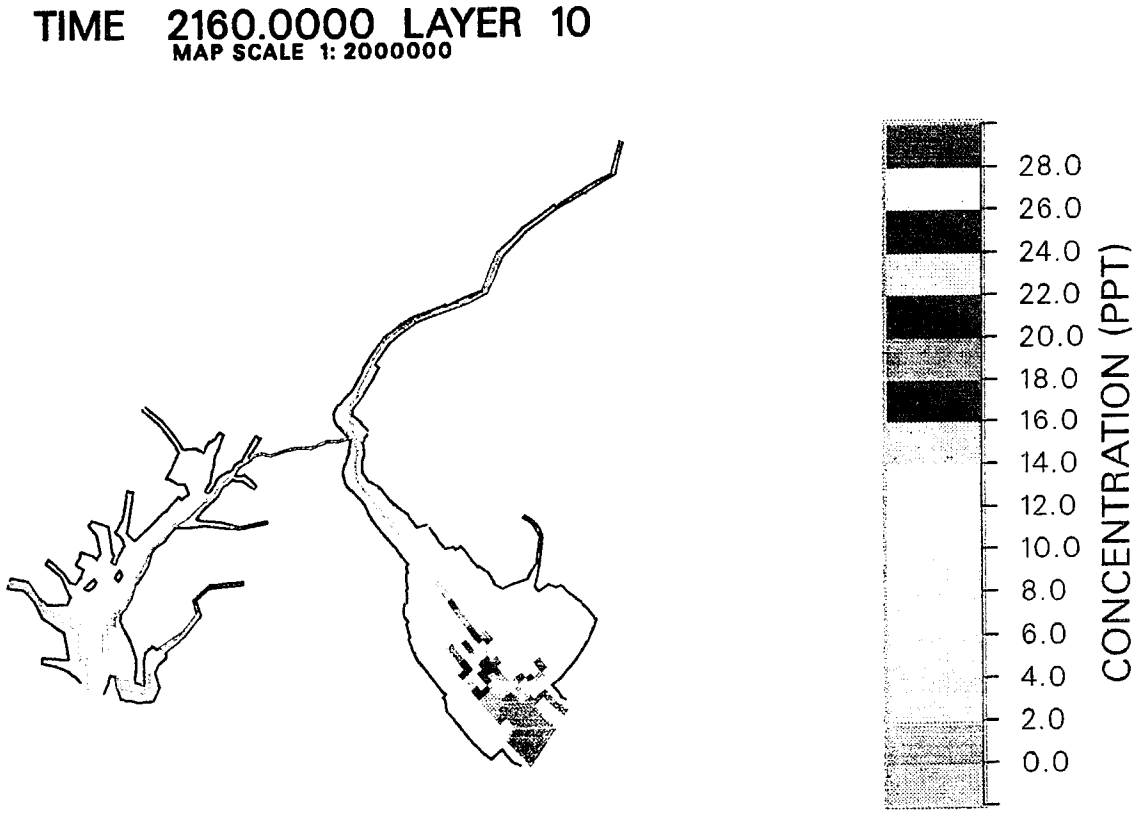

Figure 20c. Seasonal (Spring 1984) averaged salinity (Layer 10, 9.8 m)

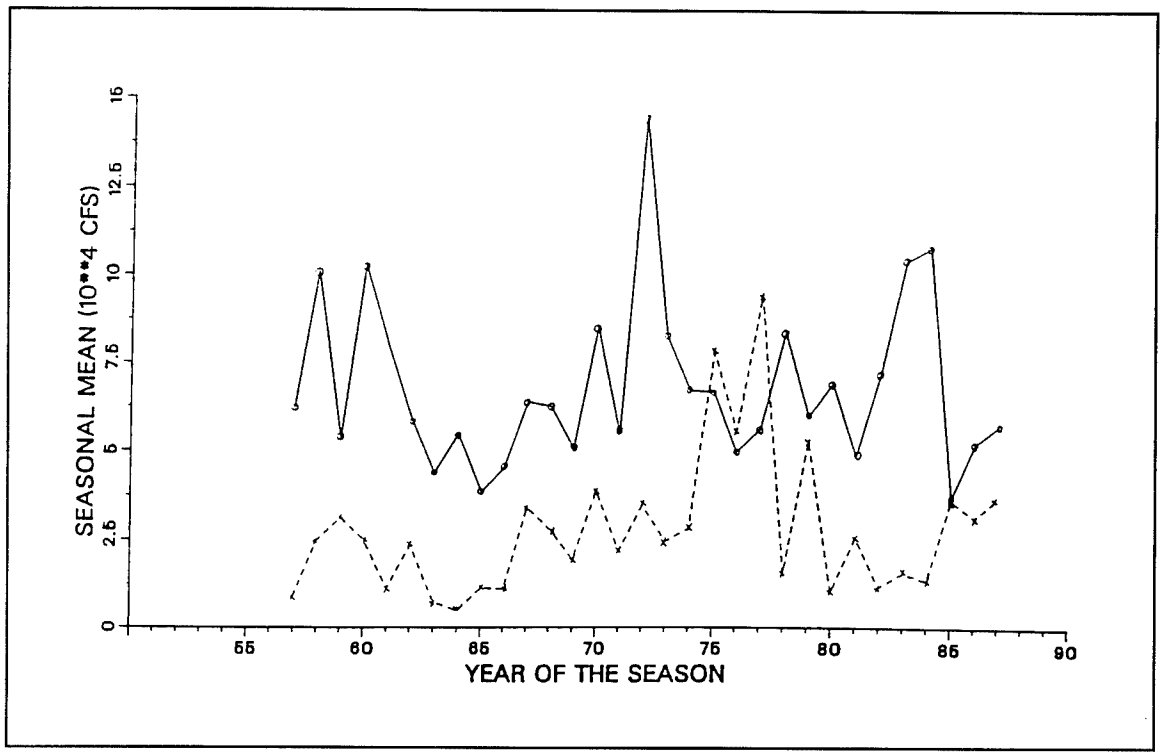

Figure 21a. High-flow (__) and low-flow (---) periods of seasonal mean inflow total for Susquehanna River and Delaware River

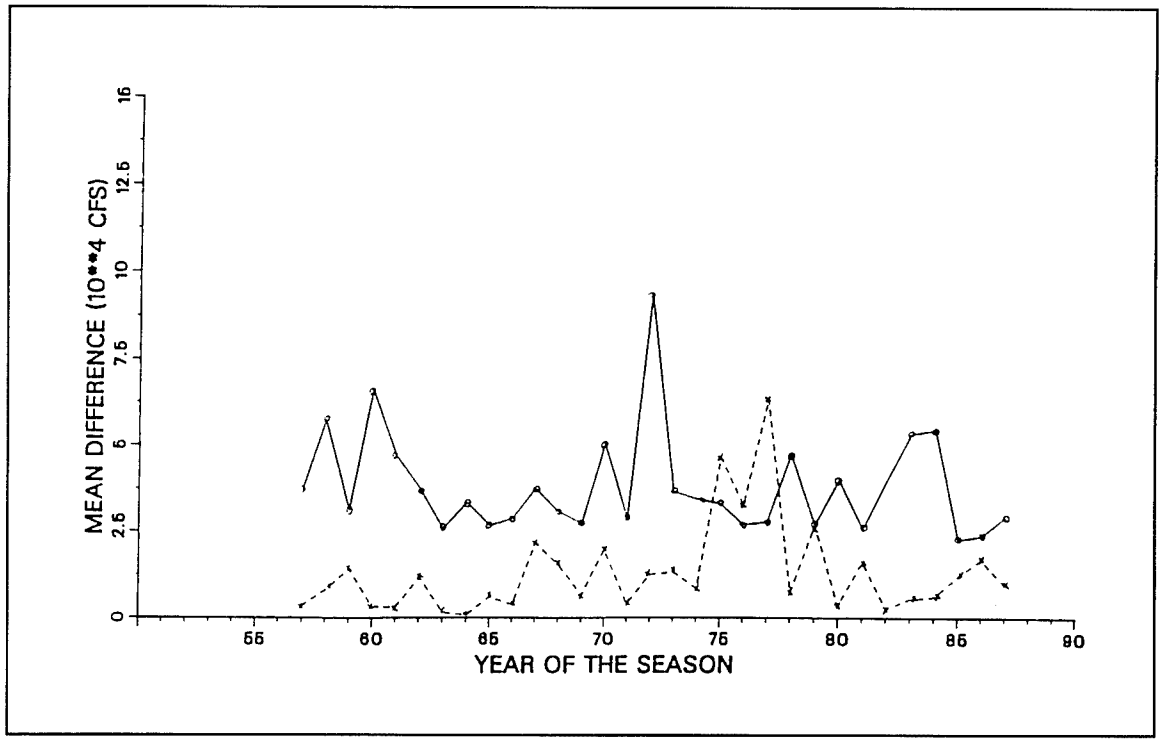

Figure 21b. High-flow (__) and low-flow (---) periods of seasonal mean inflow difference for Susquehanna River and Delaware River

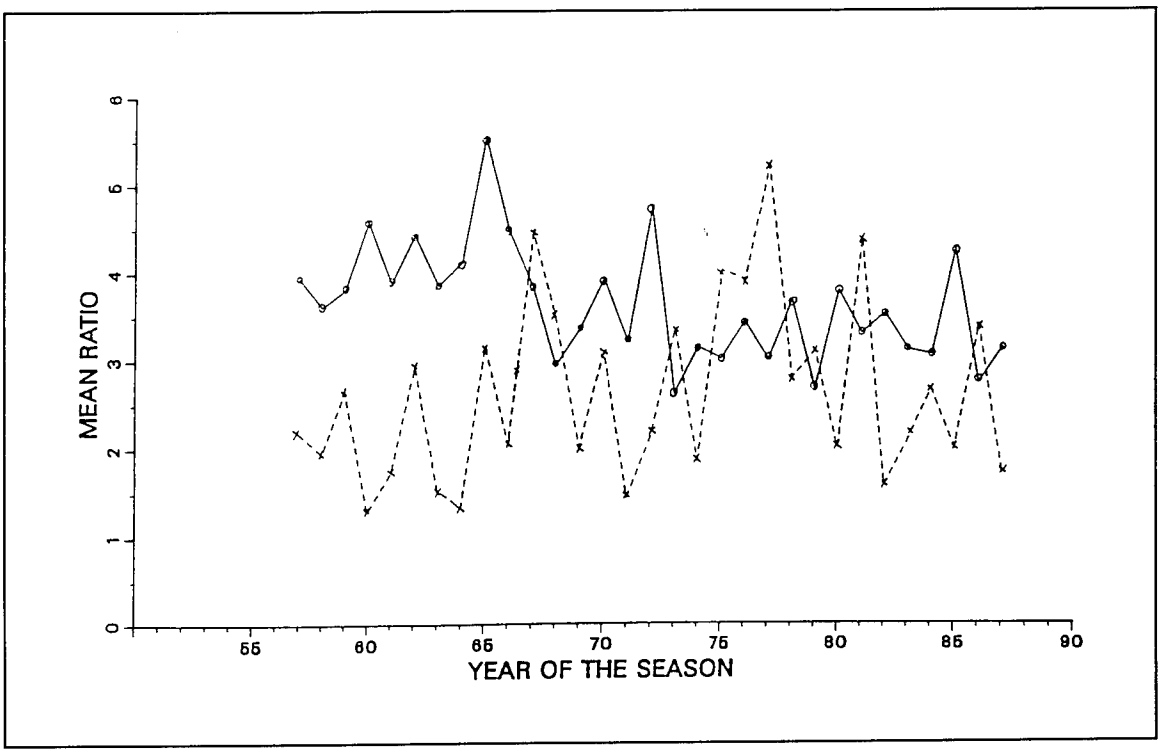

Figure 21c. High-flow (__) and low-flow (---) periods of seasonal mean ratio for Susquehanna River and Delaware River

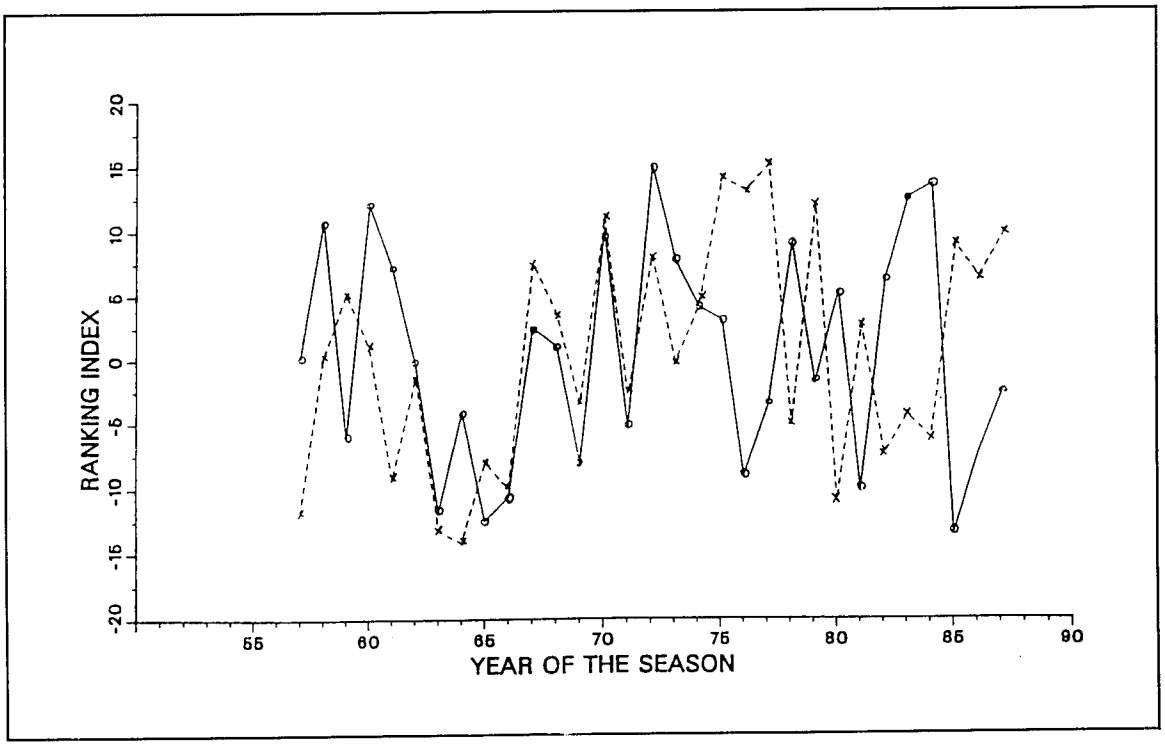

Figure 21d. High-flow (__) and low-flow (---) periods of seasonal mean inflow ranking indexes

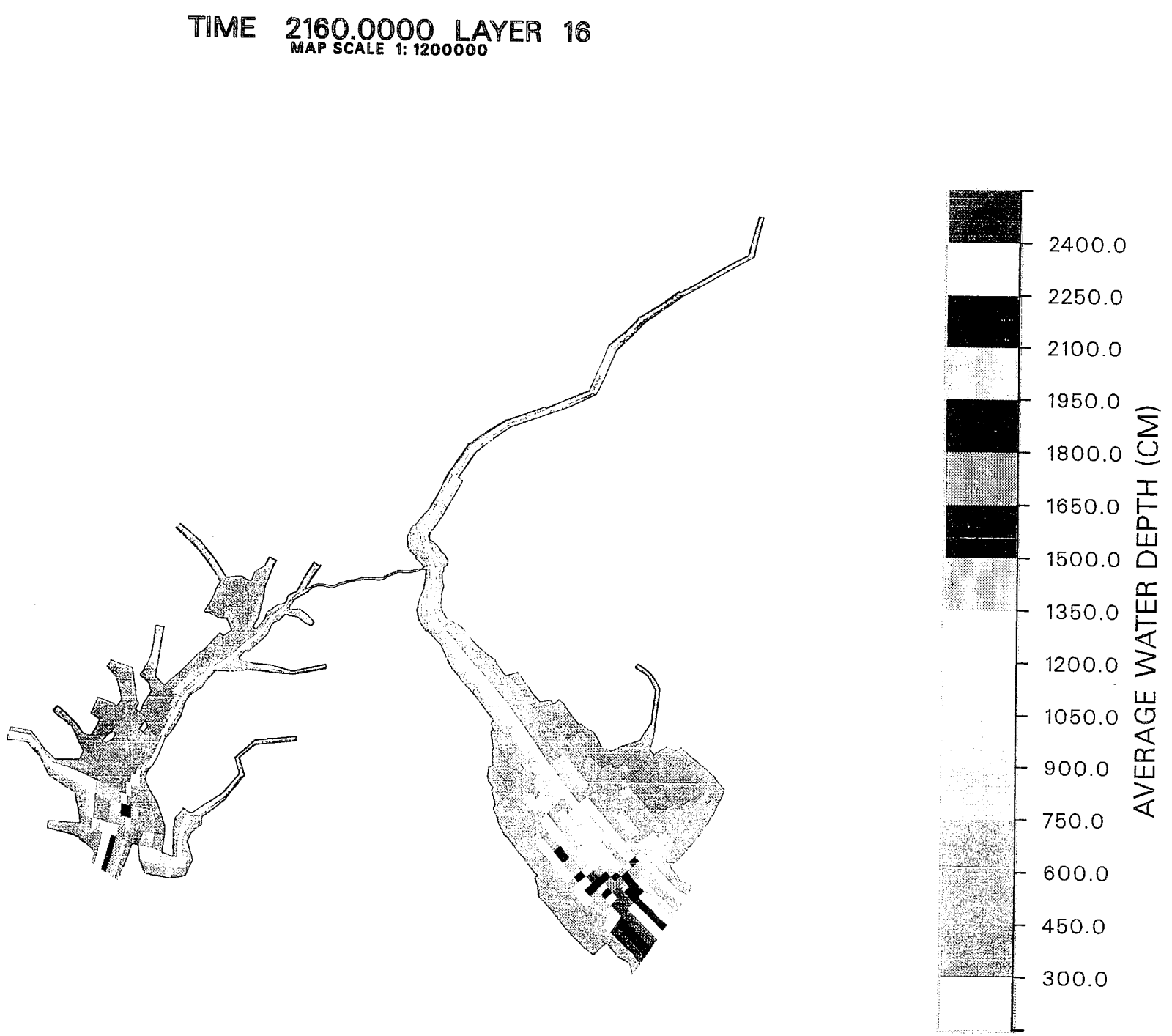

Figure 22. Averaged water depth with 5-ft increment for existing condition

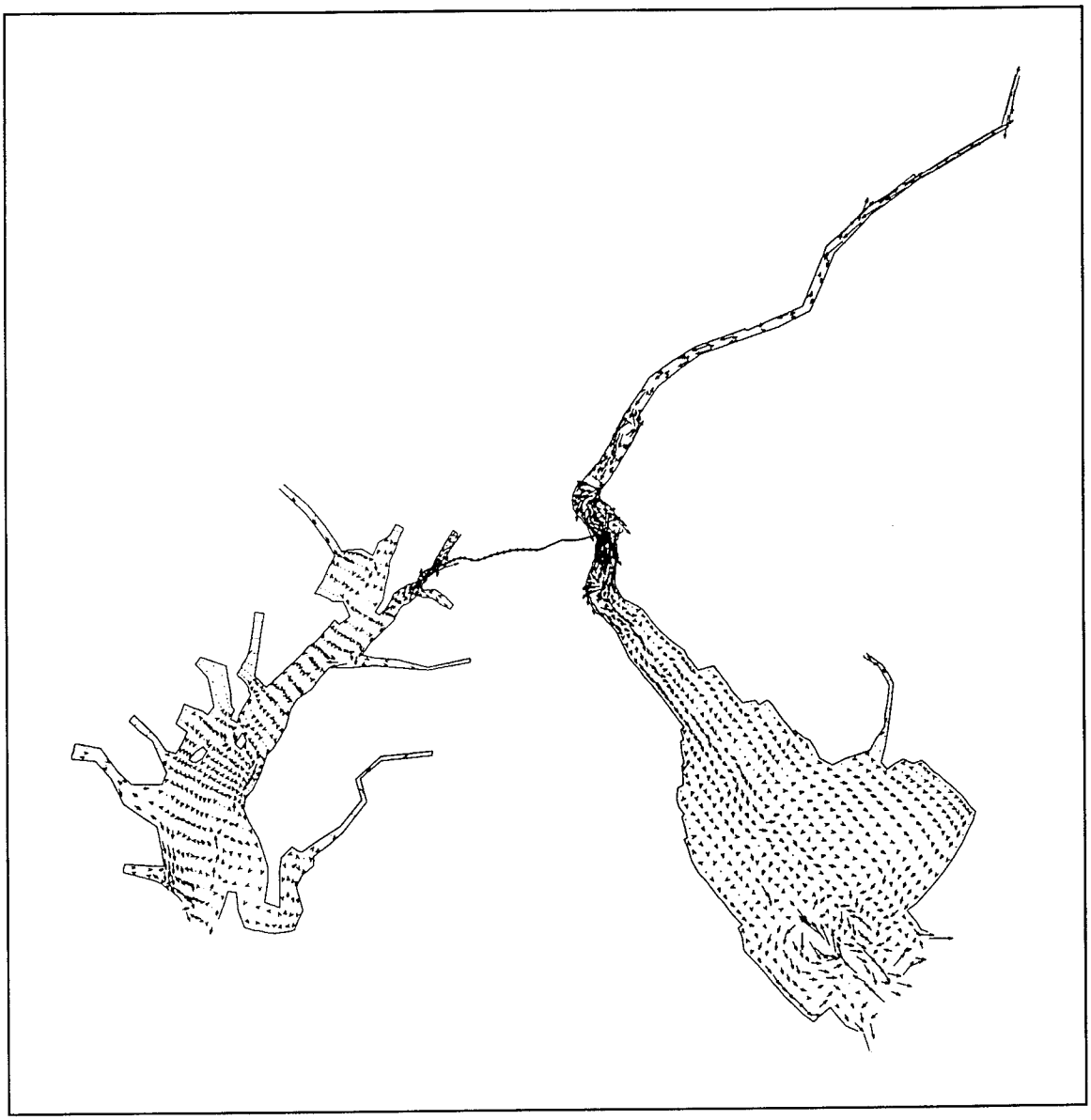

Figure 23a. Seasonal averaged flow (lowest-low flow, 1964) in layer 16 (0.8 m)

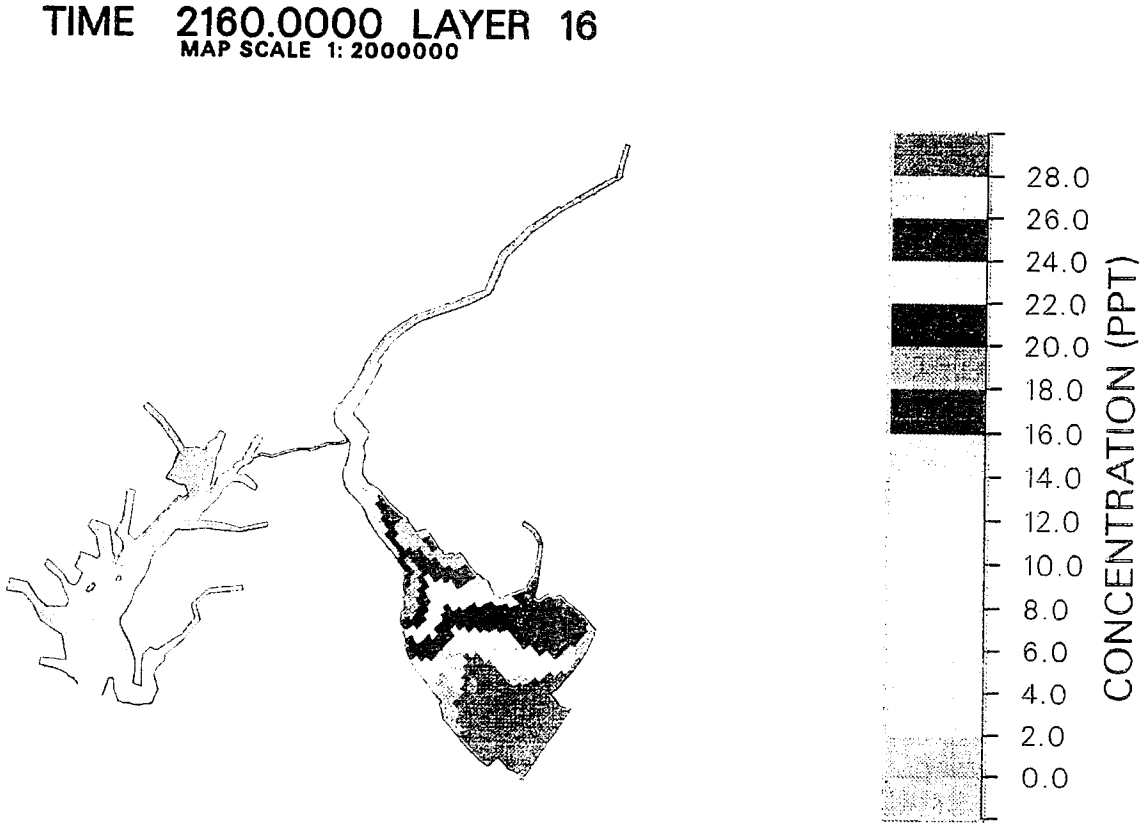

Figure 23b. Seasonal averaged salinity (lowest-low flow, 1964) in layer 16 (0.8 m)

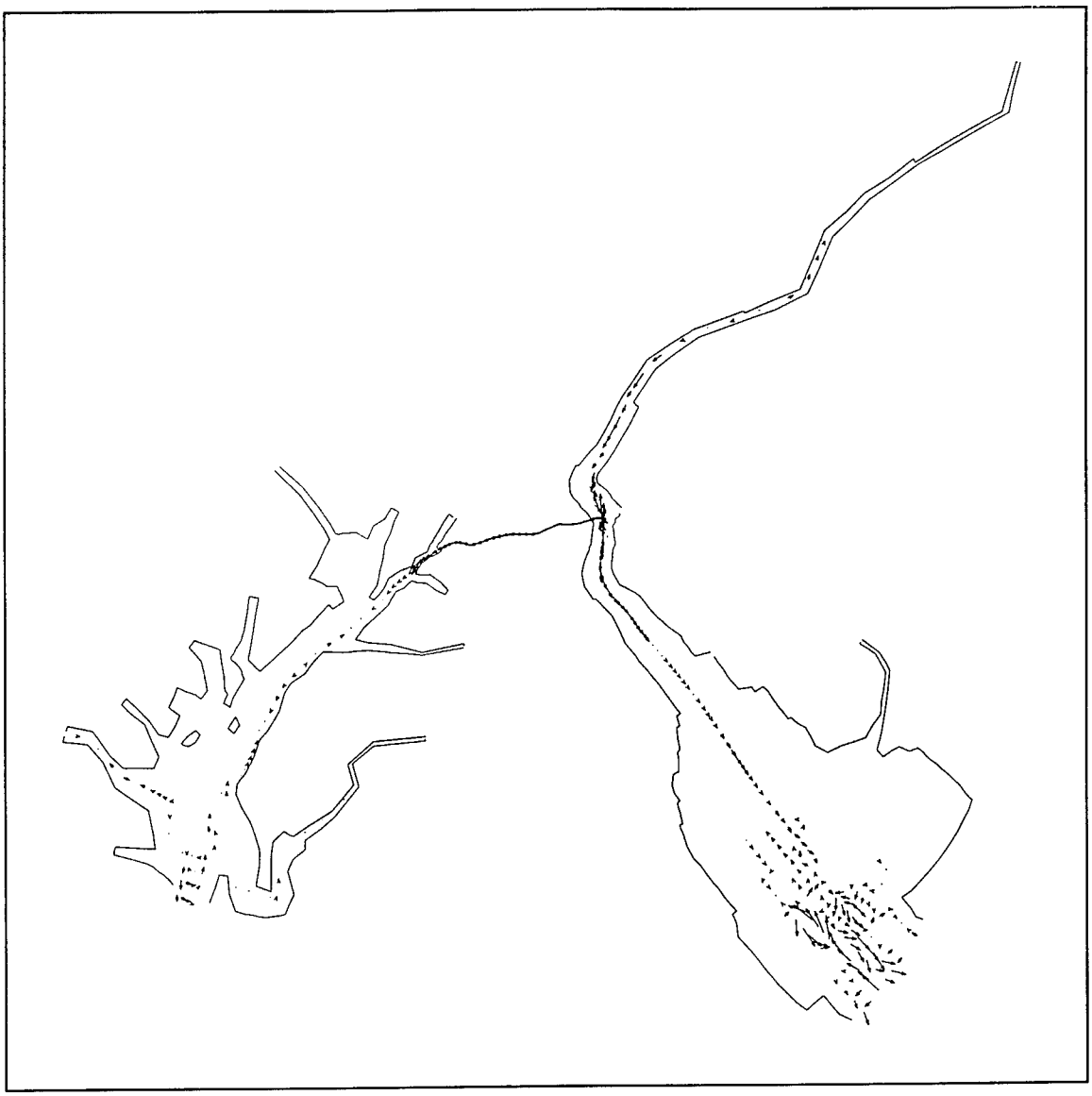

Figure 23c. Seasonal averaged flow (lowest-low flow, 1964) in layer 10 (9.8 m)

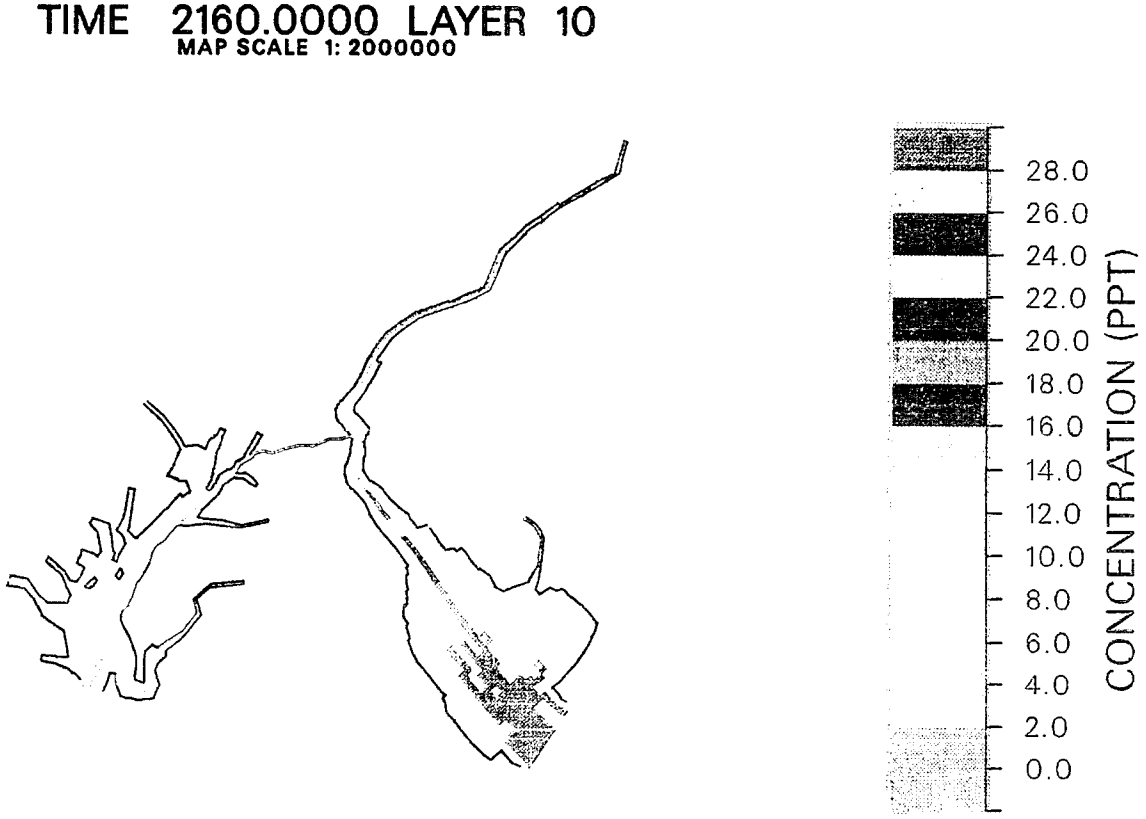

Figure 23d. Seasonal averaged salinity (lowest-low flow, 1964) in layer 10 (9.8 m)

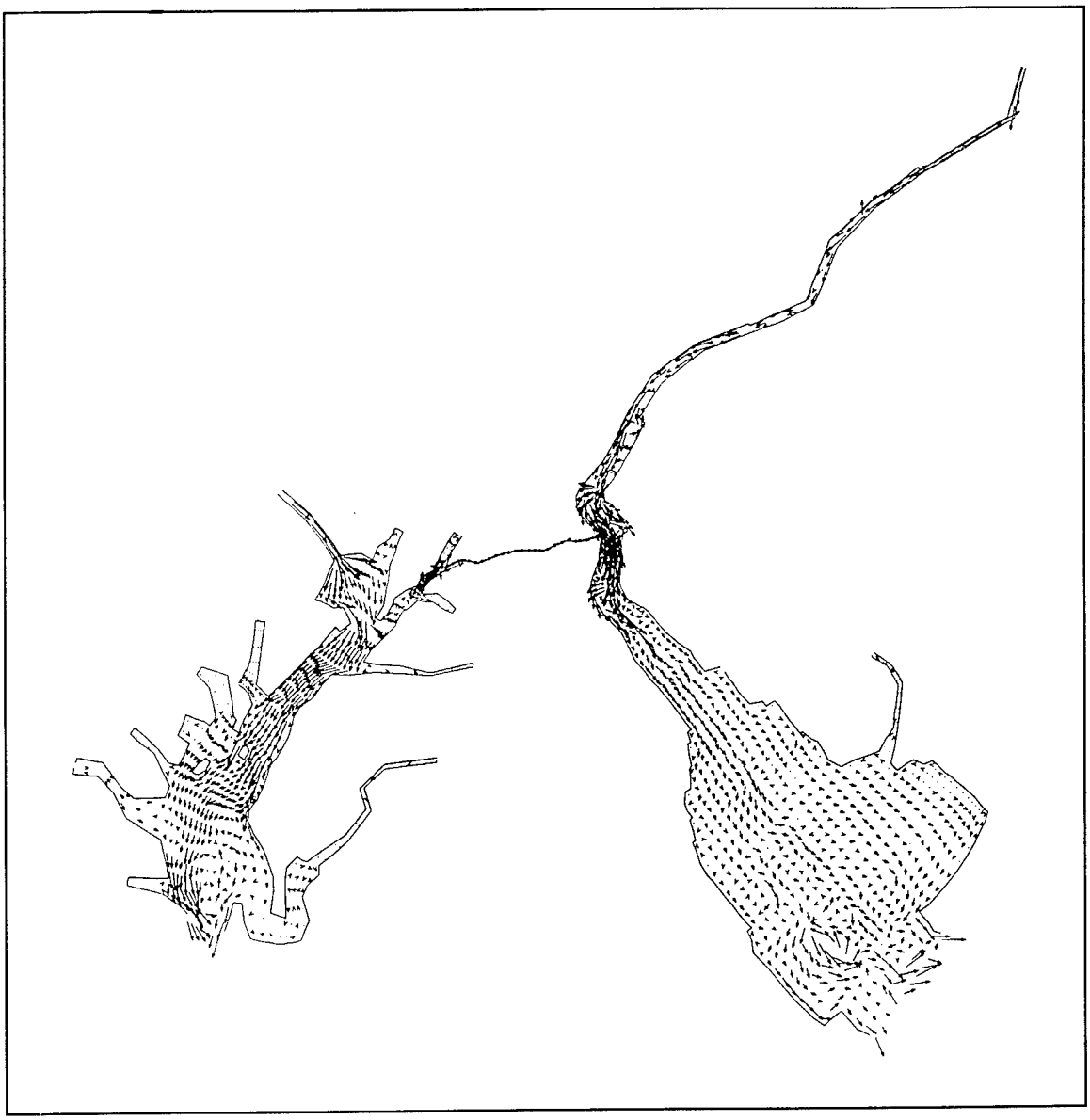

Figure 24a. Seasonal averaged flow (highest-low flow, 1977) in layer 16 (0.8 m)

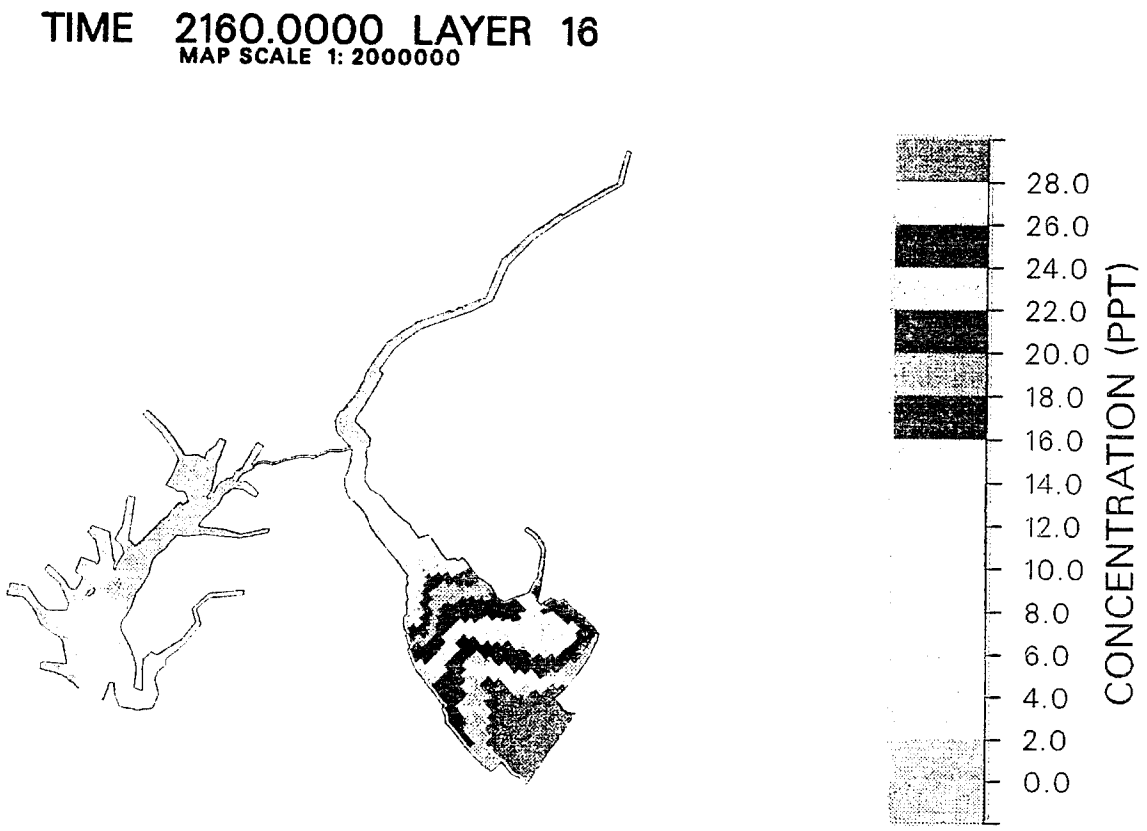

Figure 24b. Seasonal averaged salinity (highest-low flow, 1977) in layer 16 (0.8 m)

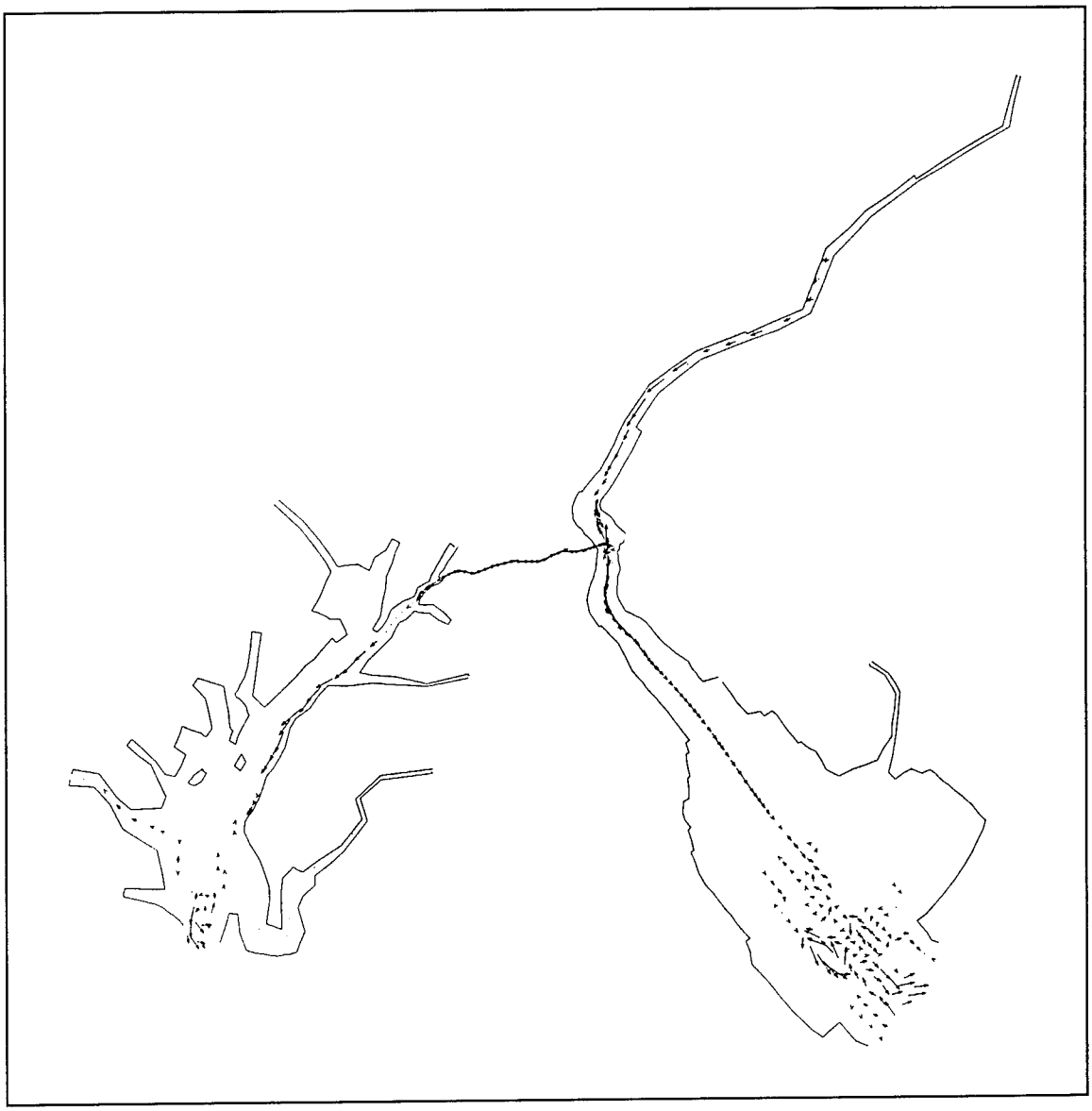

Figure 24c. Seasonal averaged flow (highest-low flow, 1977) in layer 10 (9.8 m)

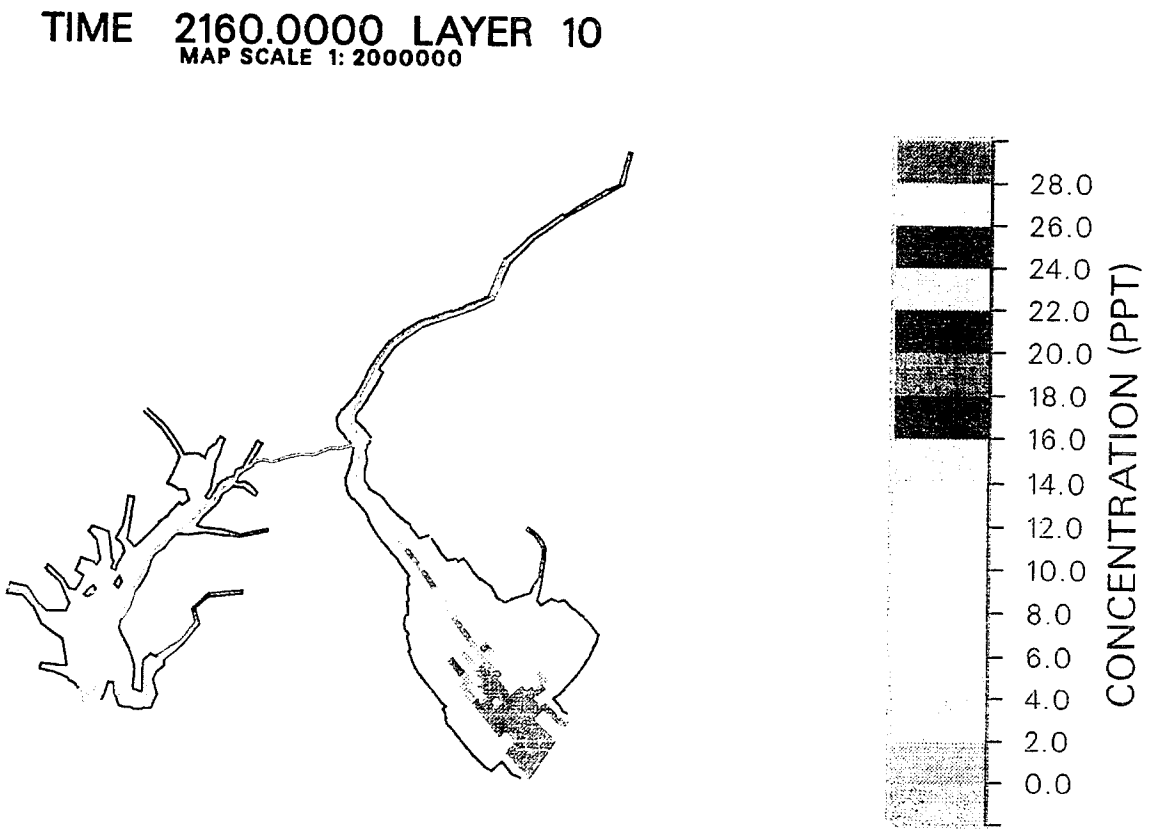

Figure 24d. Seasonal averaged salinity (highest-low flow, 1977) in layer 10 (9.8 m)

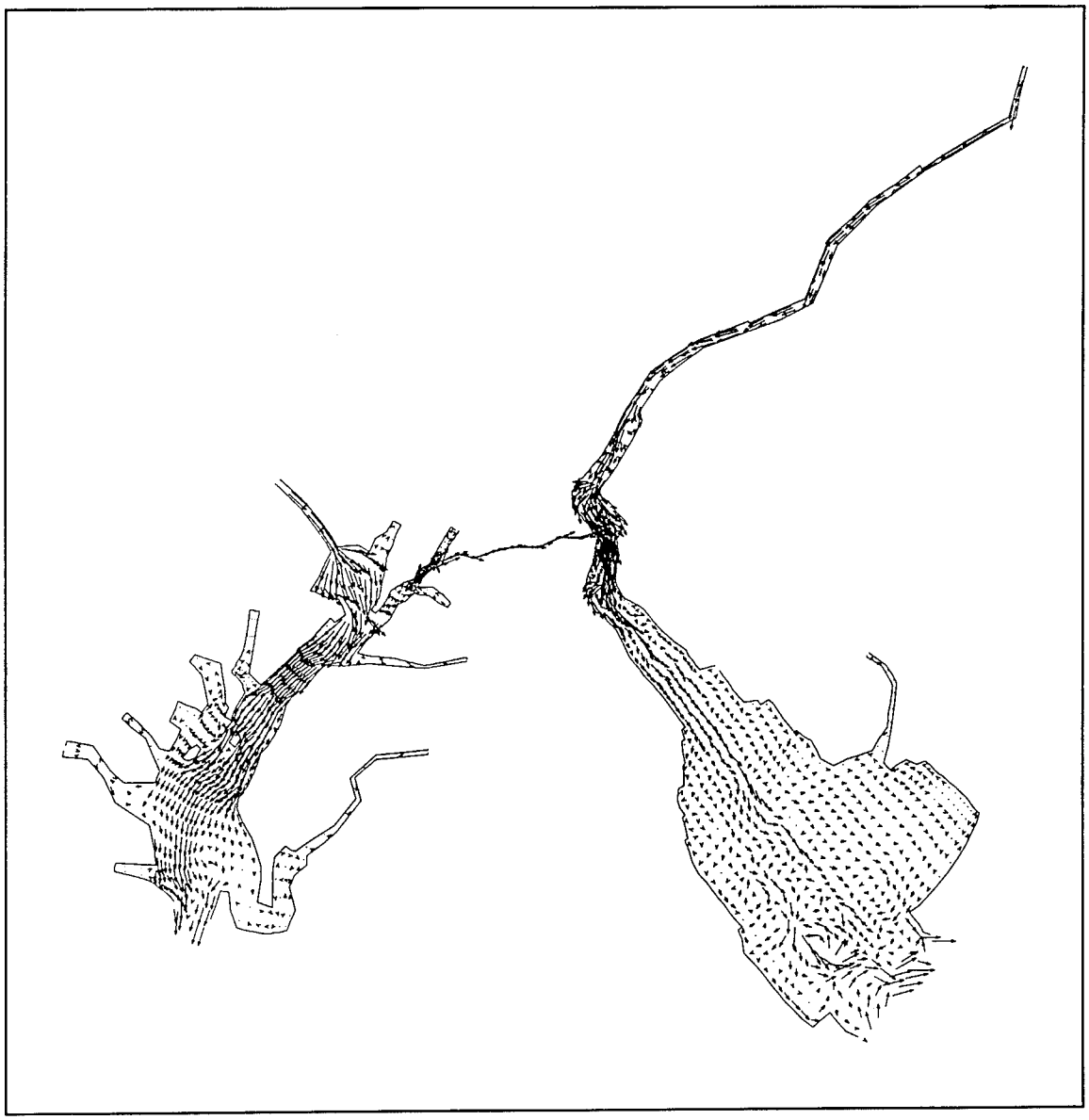

Figure 25a. Seasonal averaged flow (highest-low flow, 1972) in layer 16 (0.8 m)

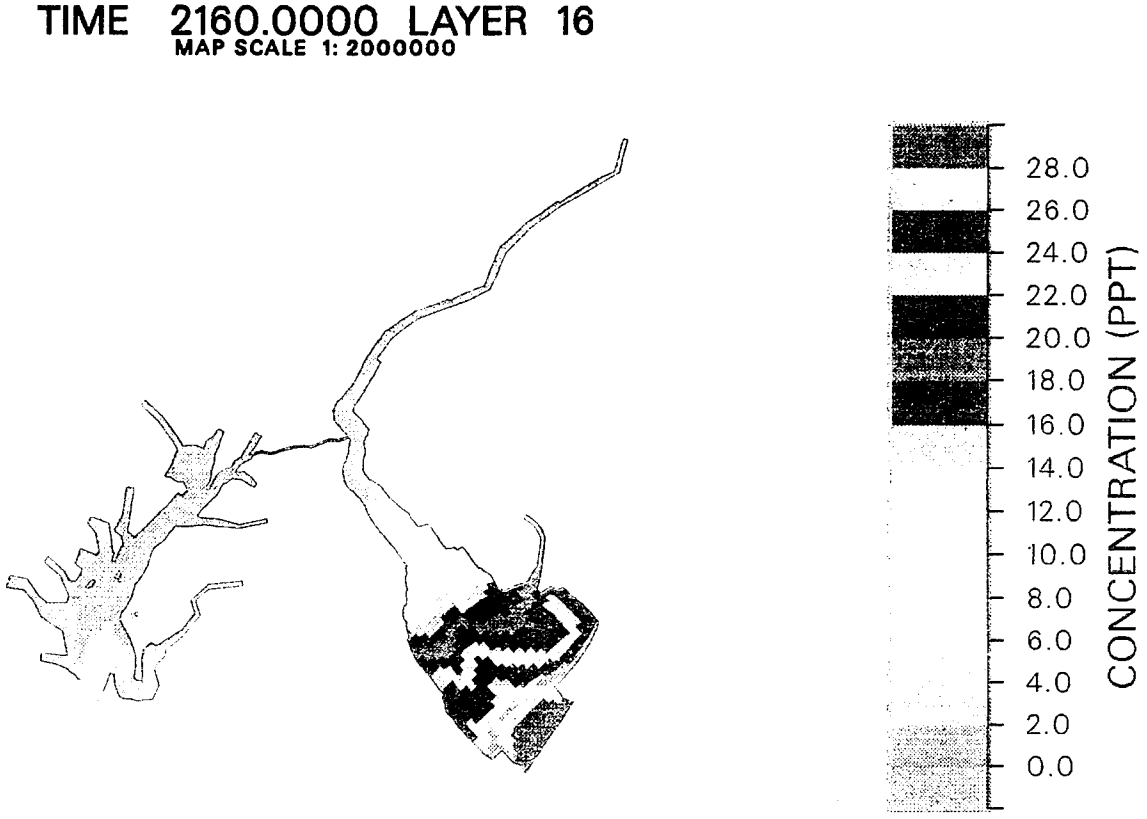

Figure 25b. Seasonal averaged salinity (highest-high flow, 1972) in layer 16 (0.8 m)

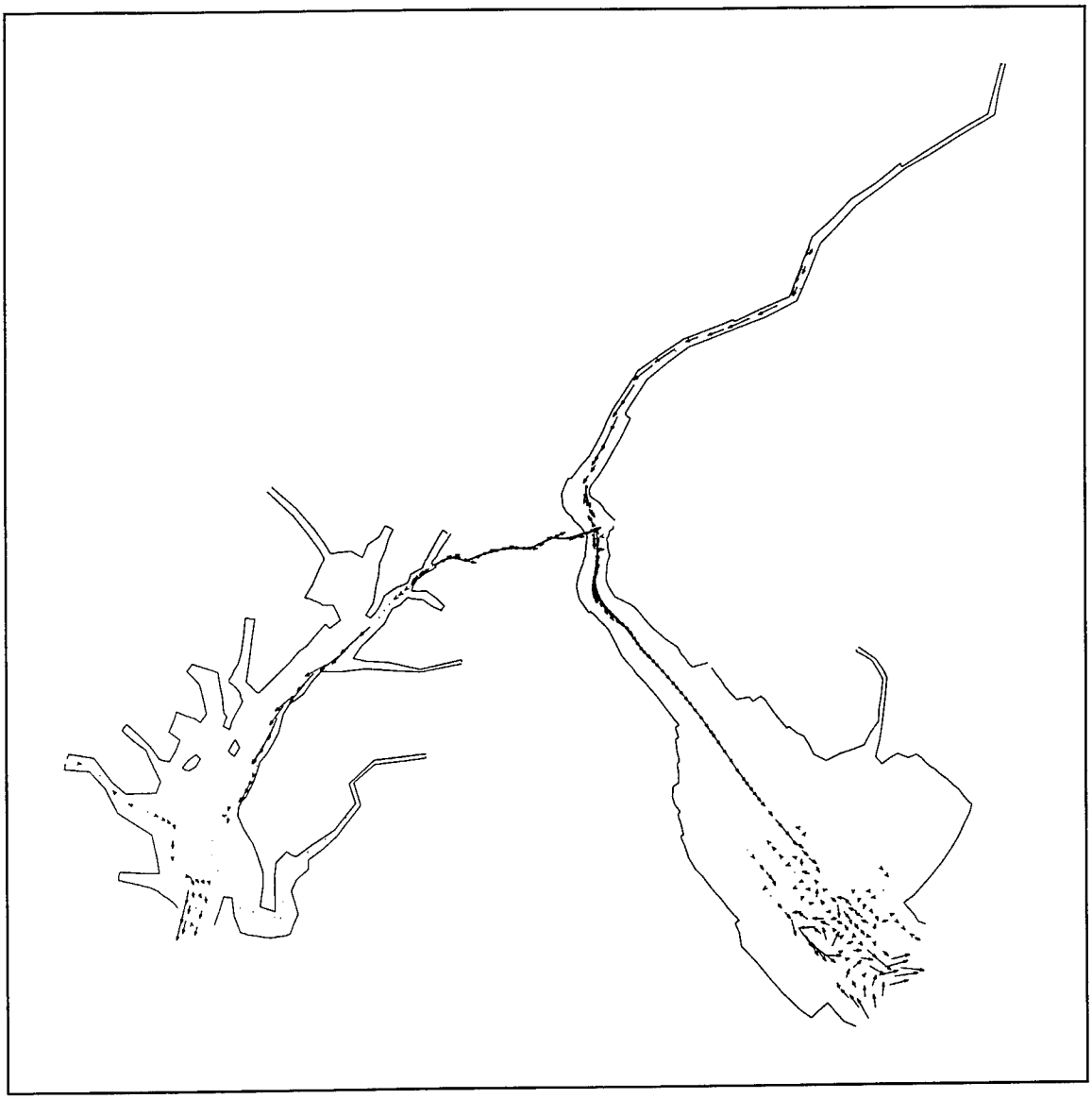

Figure 25c. Seasonal averaged flow (highest-high flow, 1972) in layer 10 (9.8 m)

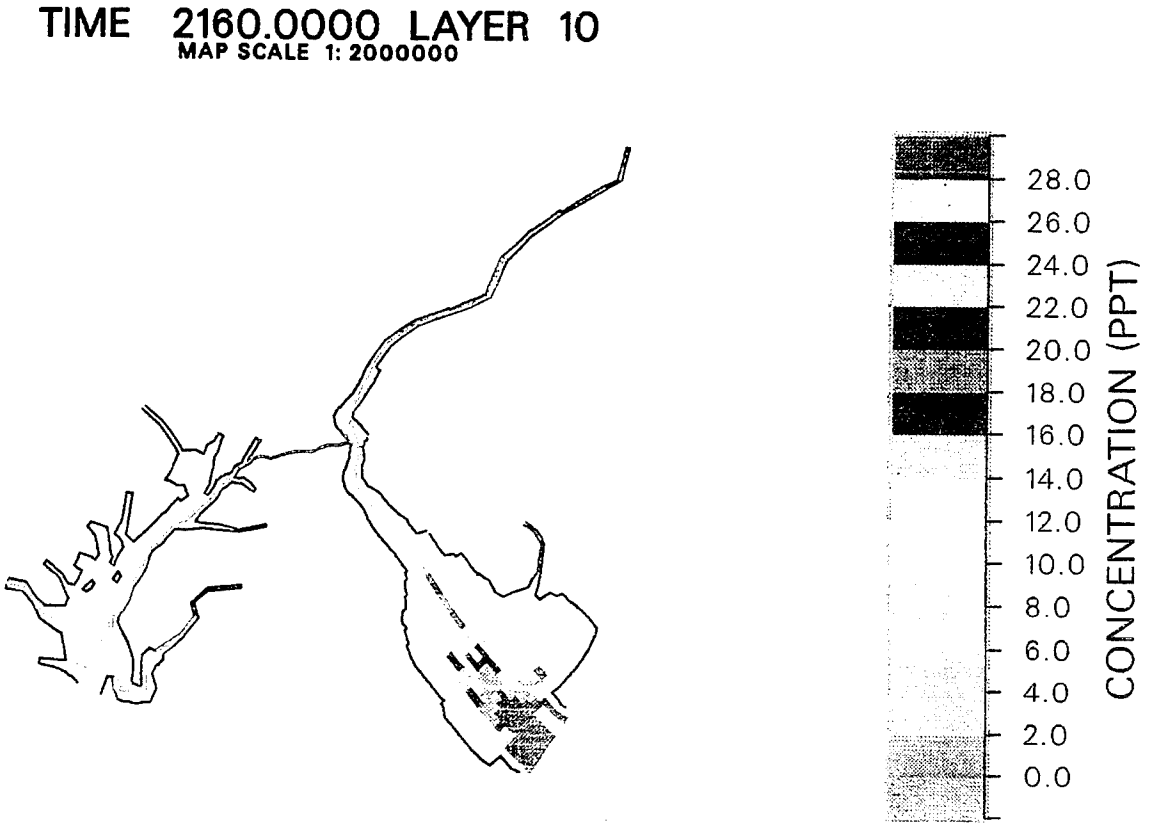

Figure 25d. Seasonal averaged salinity (highest-high flow, 1972) in layer 10 (9.8 m)

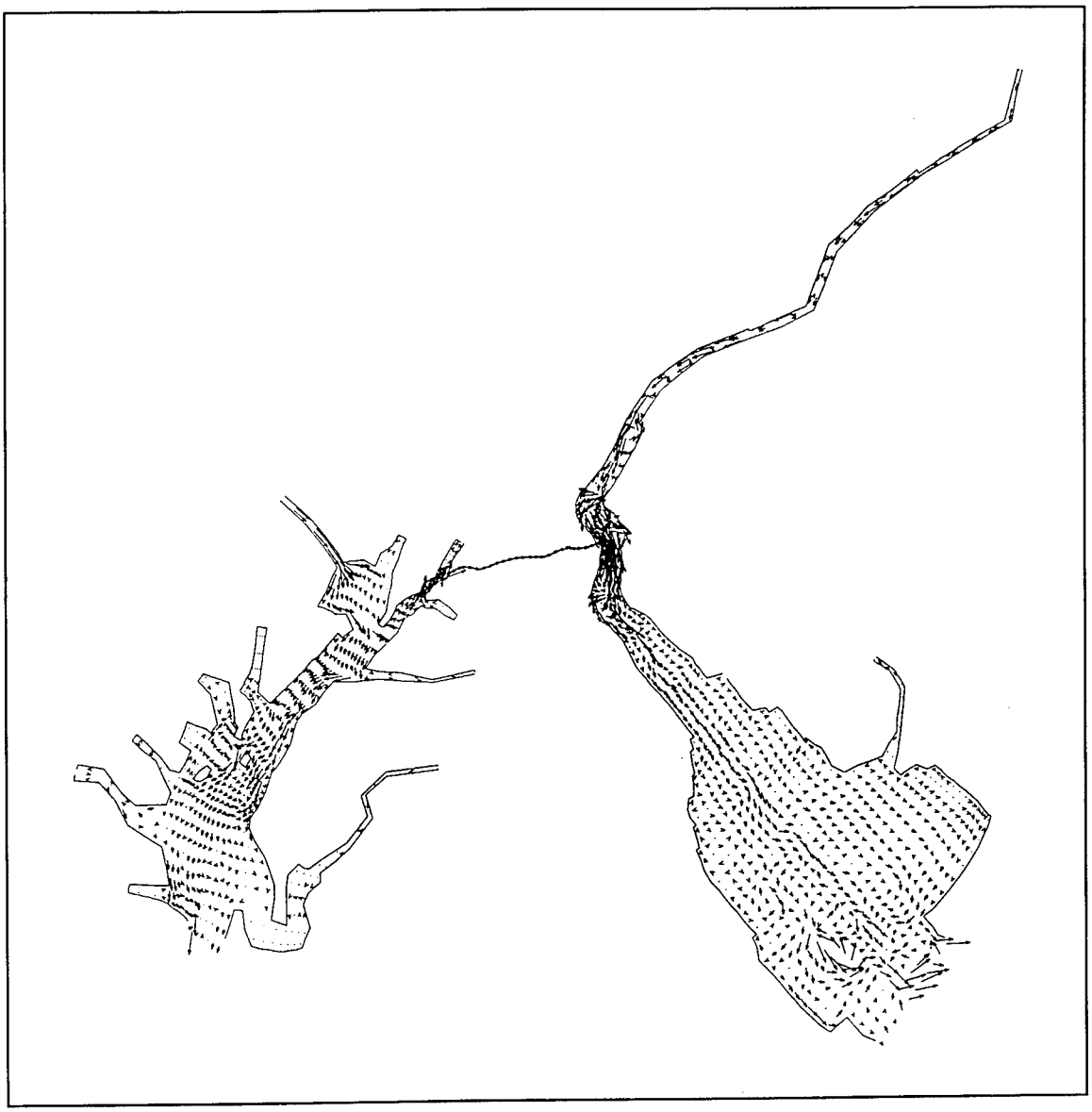

Figure 26a. Seasonal averaged flow (lowest-high flow, 1985) in layer 16 (0.8 m)

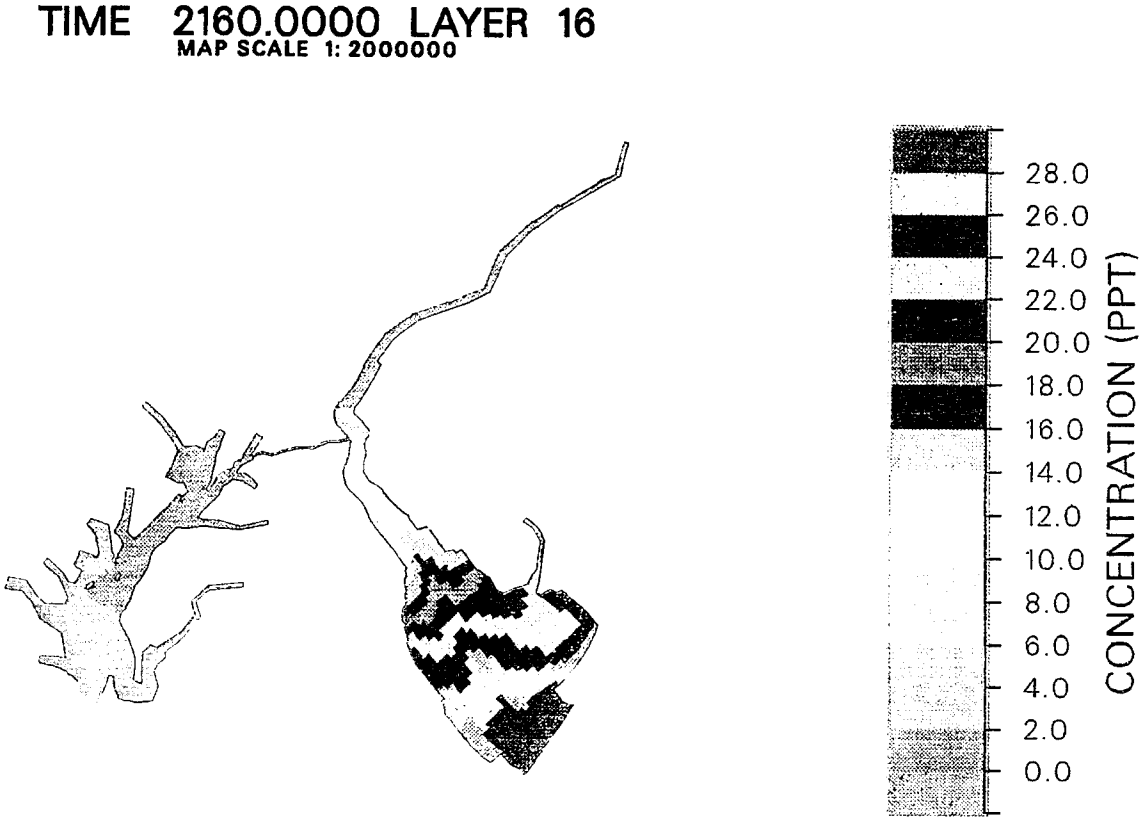

Figure 26b. Seasonal averaged salinity (lowest-high flow, 1985) in layer 16 (0.8 m)

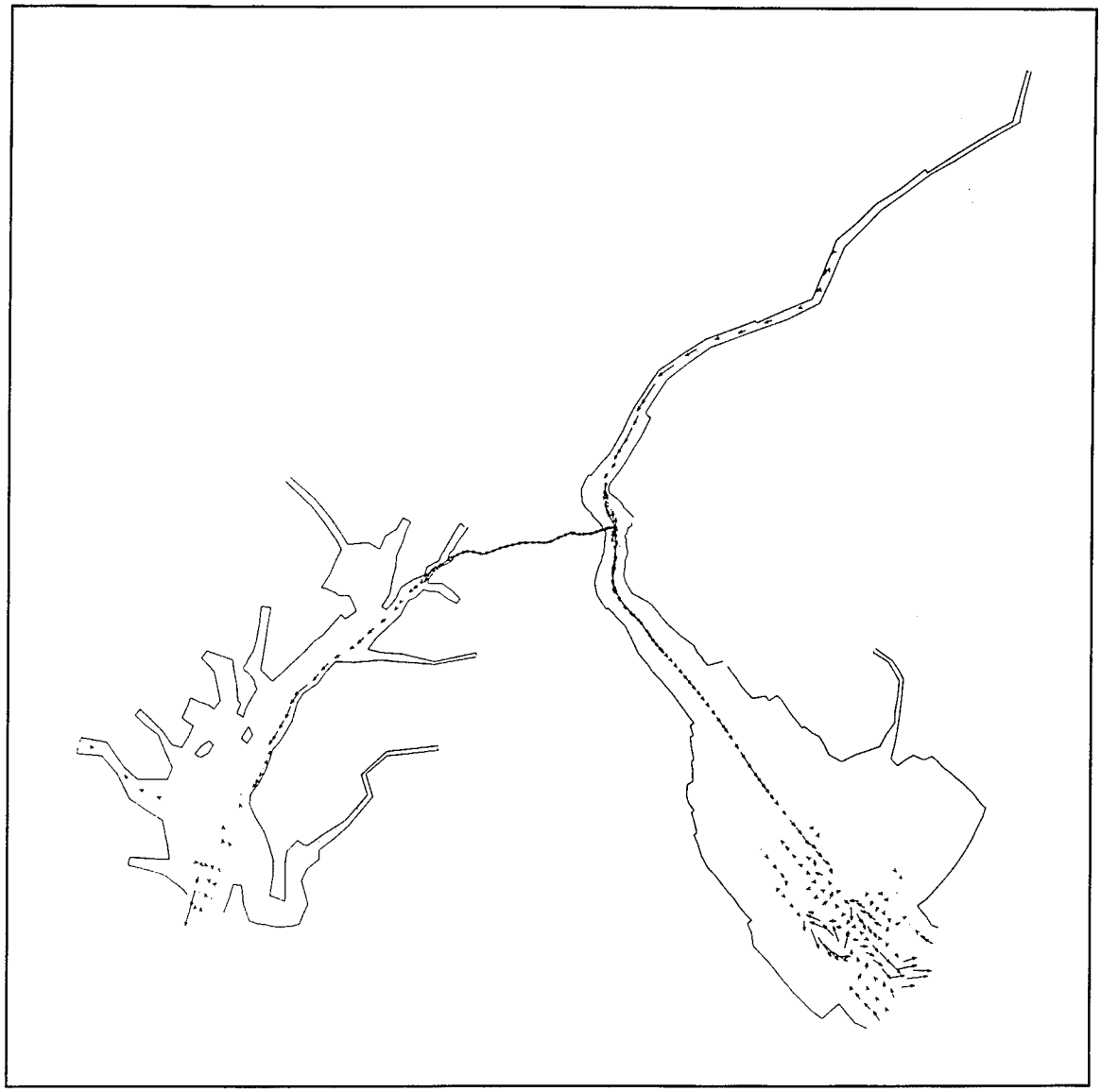

Figure 26c. Seasonal averaged flow (lowest-high flow, 1985) in layer 10 (9.8 m)

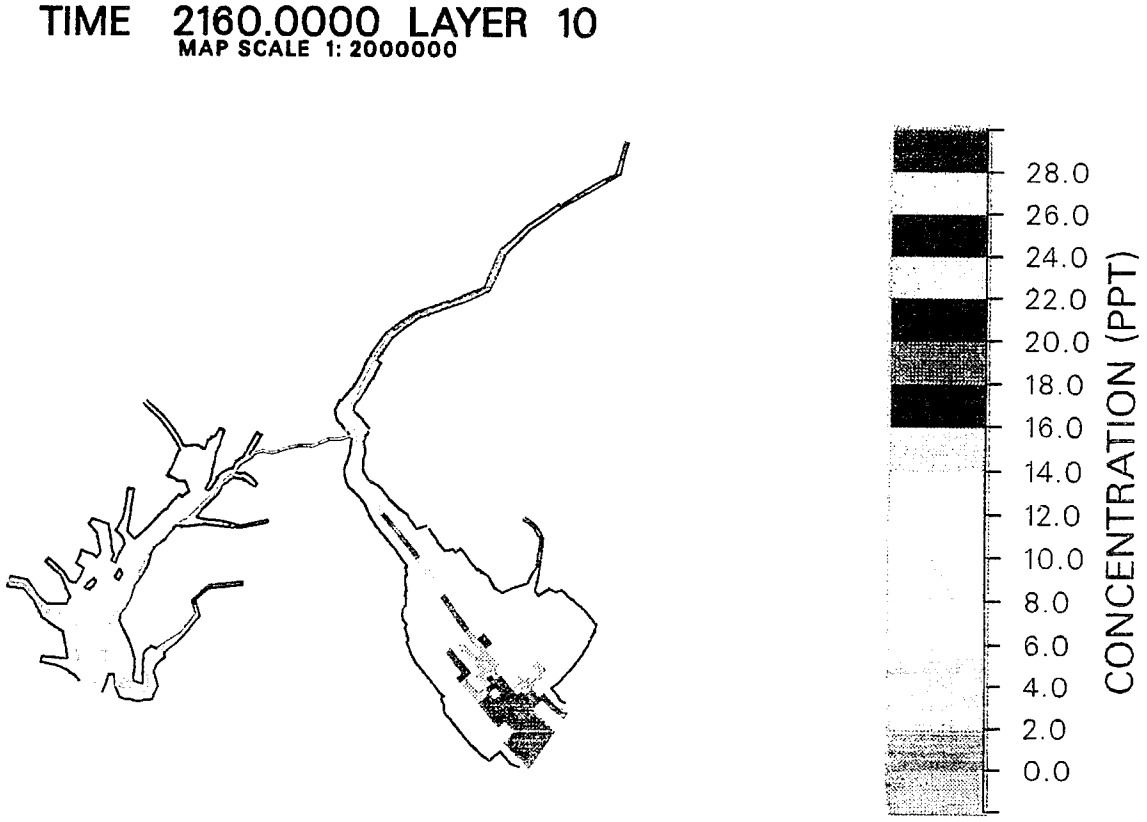

Figure 26d. Seasonal averaged salinity (lowest-high flow, 1985) in layer 10 (9.8 m)

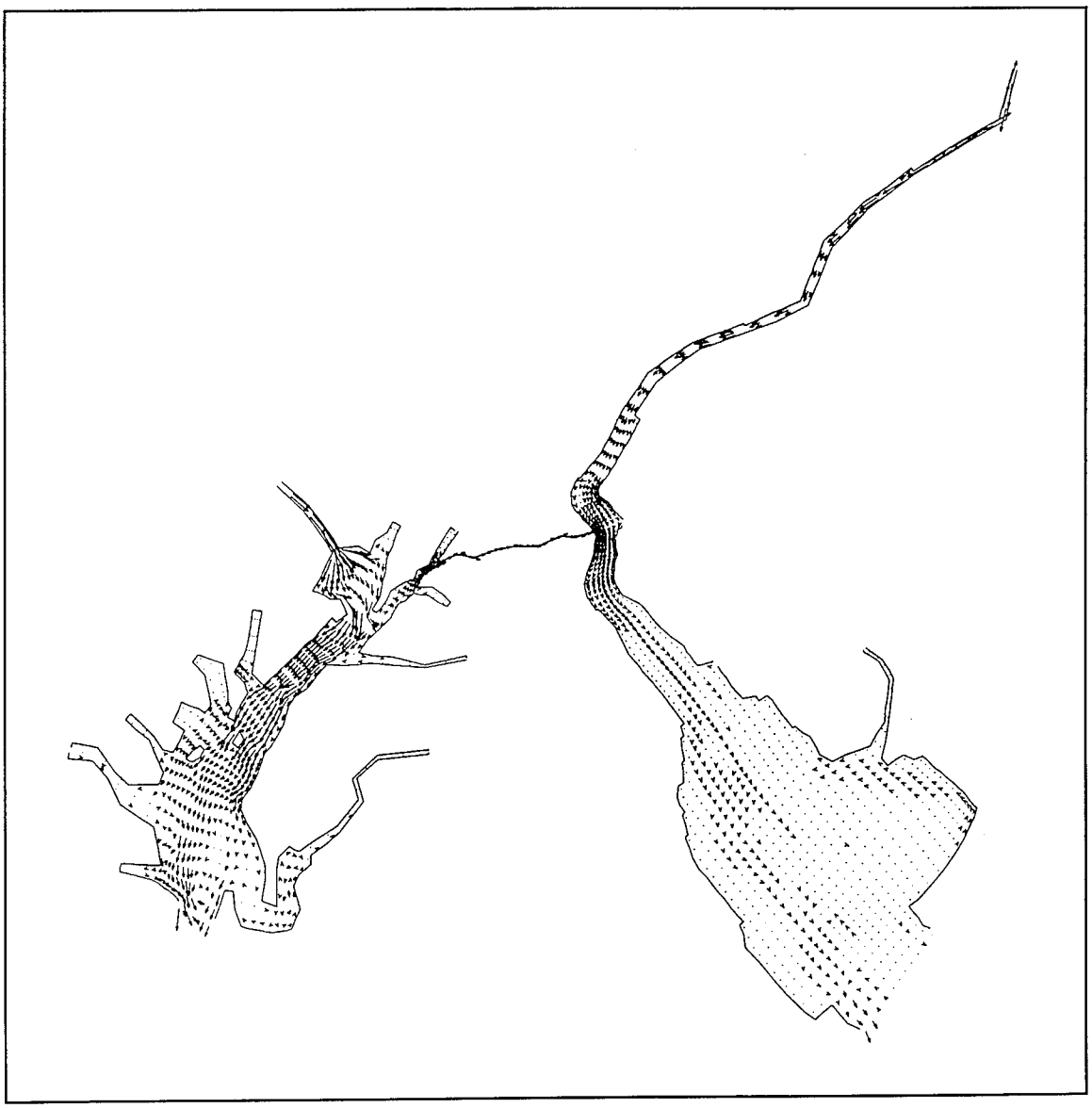

Figure 27a. Differences of seasonal averaged flow (1977 vs. 1964) in layer 16 (0.8 m)

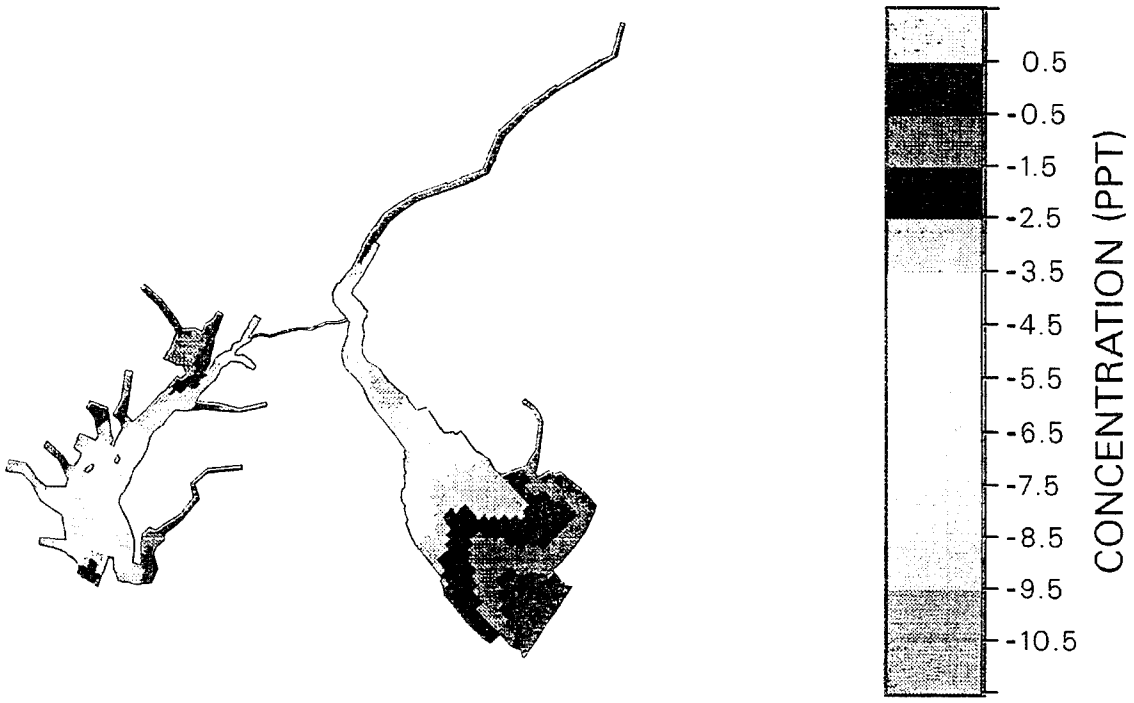

Figure 27b. Differences of seasonal averaged salinity (1977 vs 1964) in layer 16 (0.8 m)

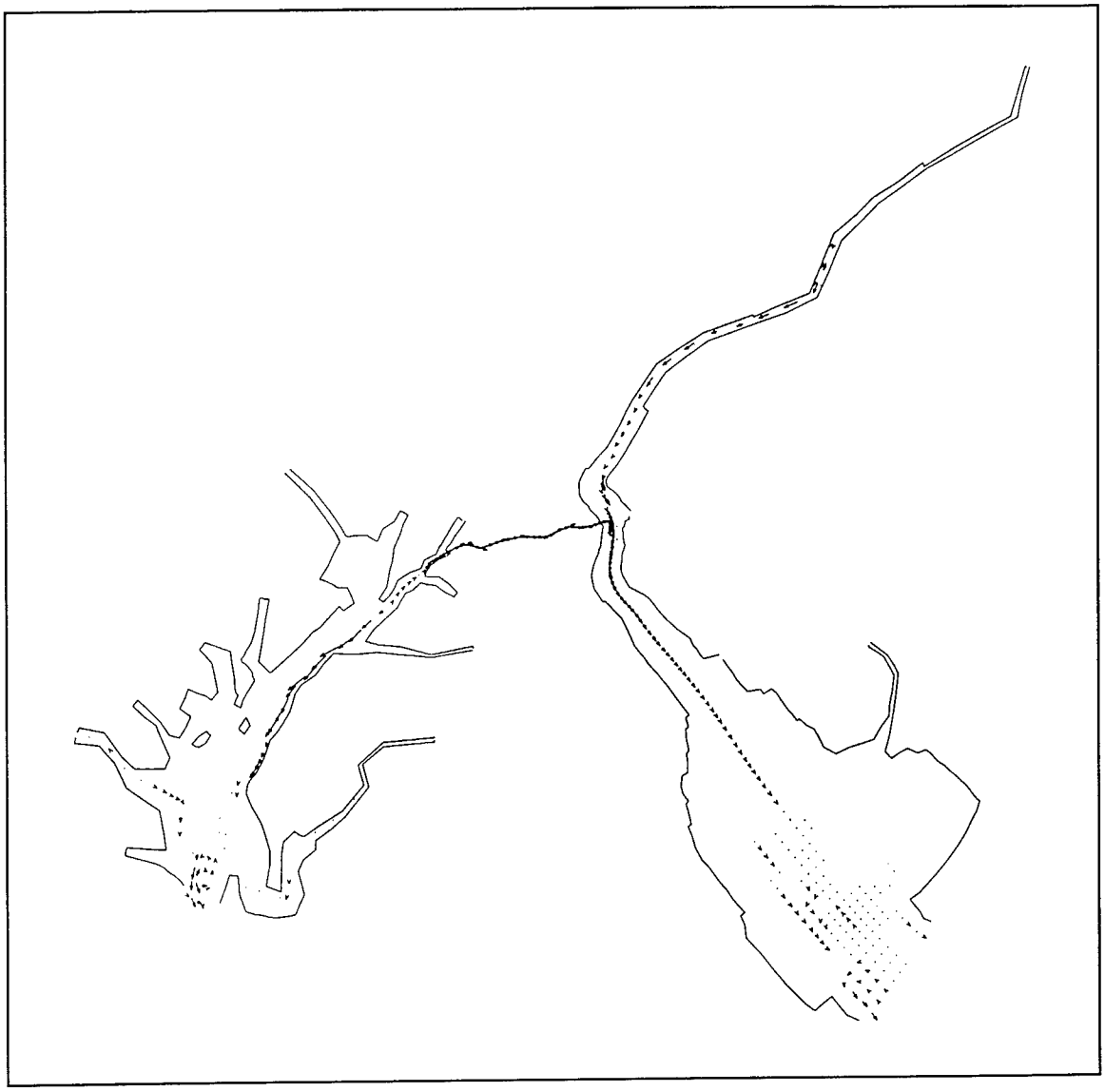

Figure 27c. Differences of seasonal averaged flow (1977 vs. 1964) in layer 10 (9.8 m)

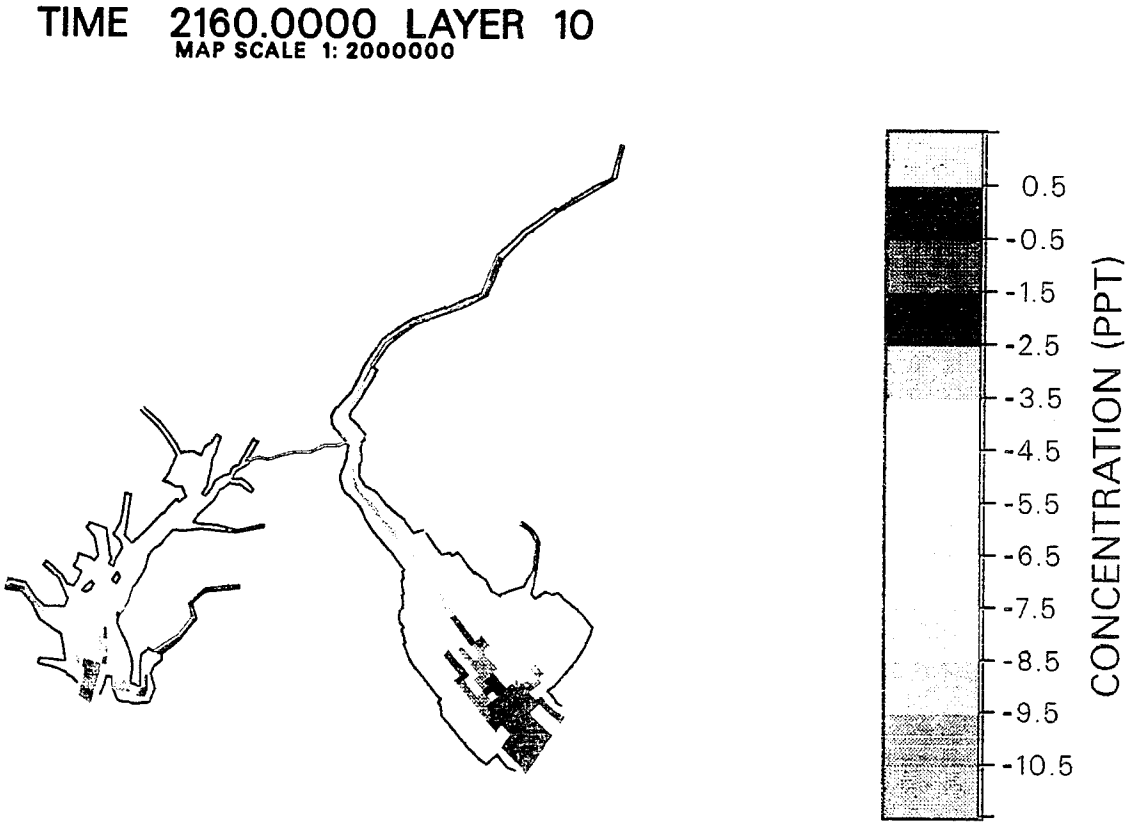

Figure 27d. Differences of seasonal averaged salinity (1977 vs 1964) in layer 10 (9.8 m)

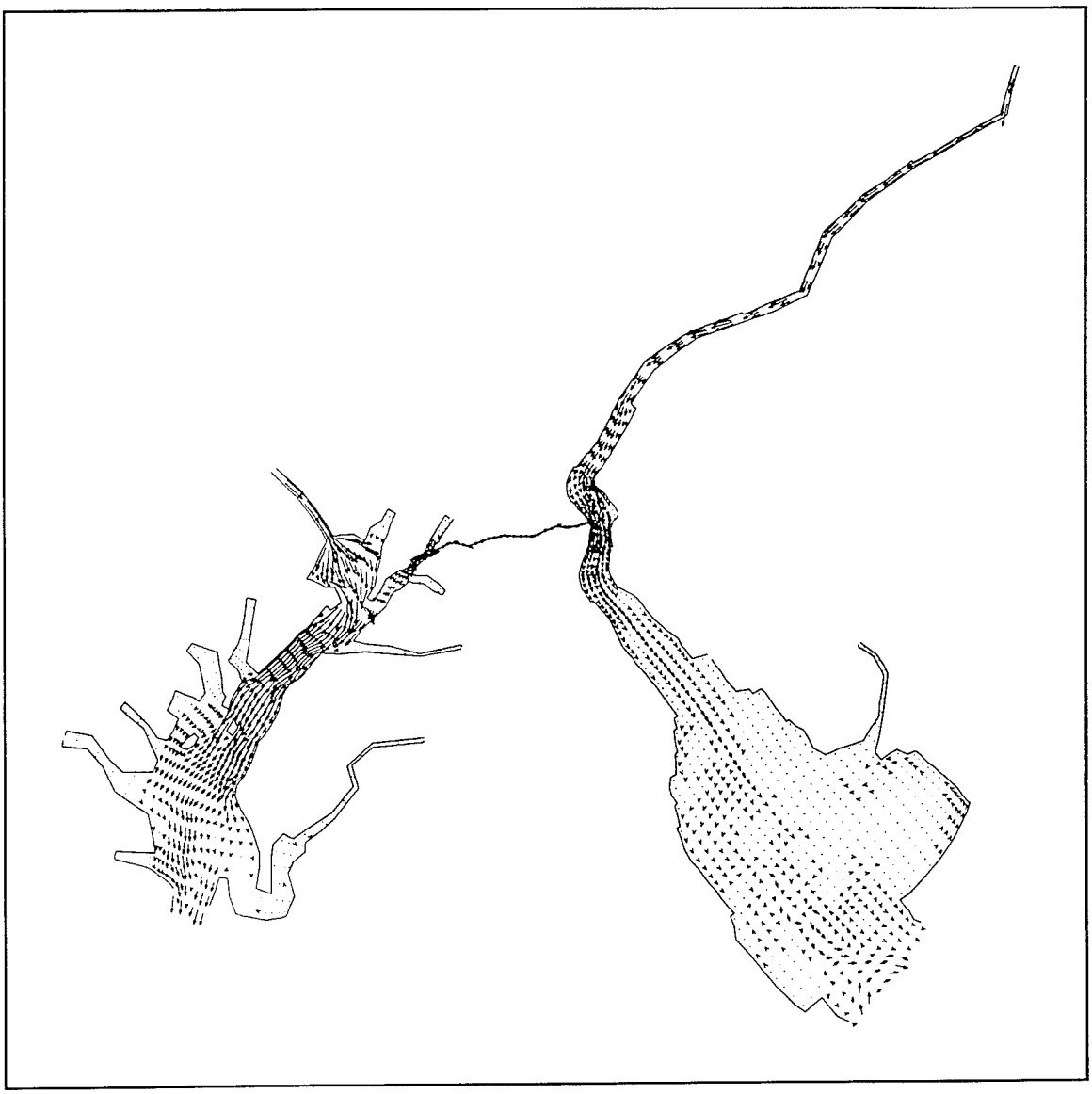

Figure 28a. Differences of seasonal averaged flow (1972 vs 1985) in layer 16 (0.8 m)

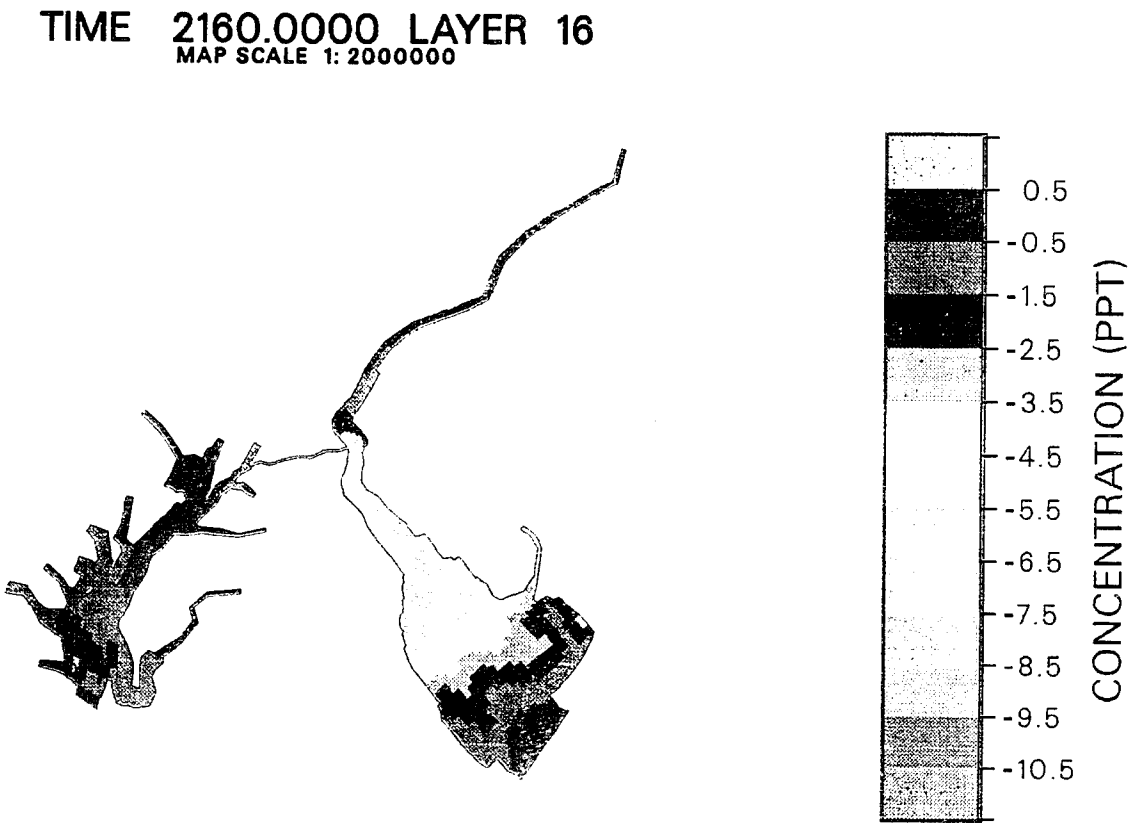

Figure 28b. Differences of seasonal averaged salinity (1972 vs 1985) in layer 16 (0.8 m)

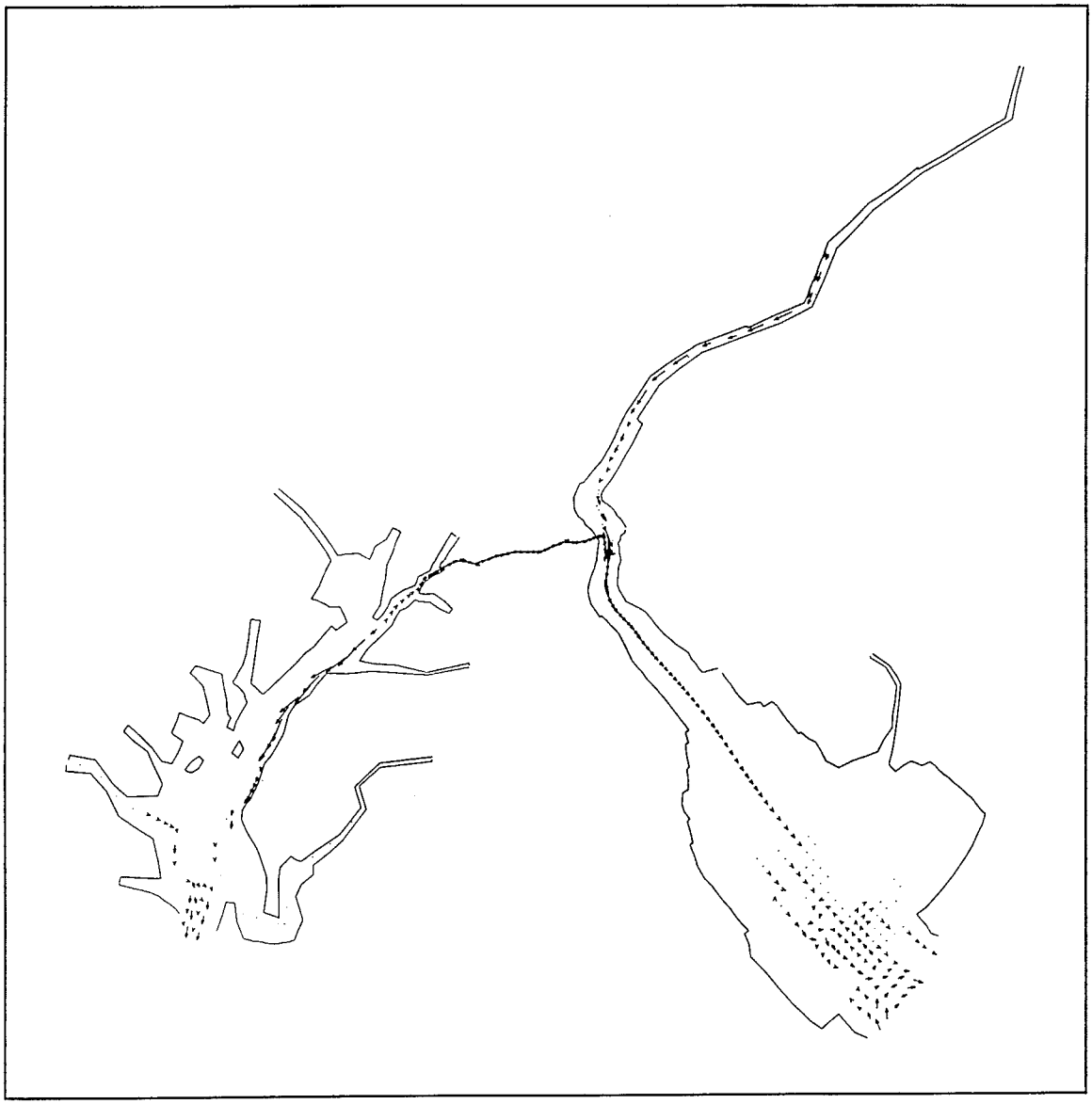

Figure 28c. Differences of seasonal averaged flow (1972 vs 1985) in layer 10 (9.8 m)

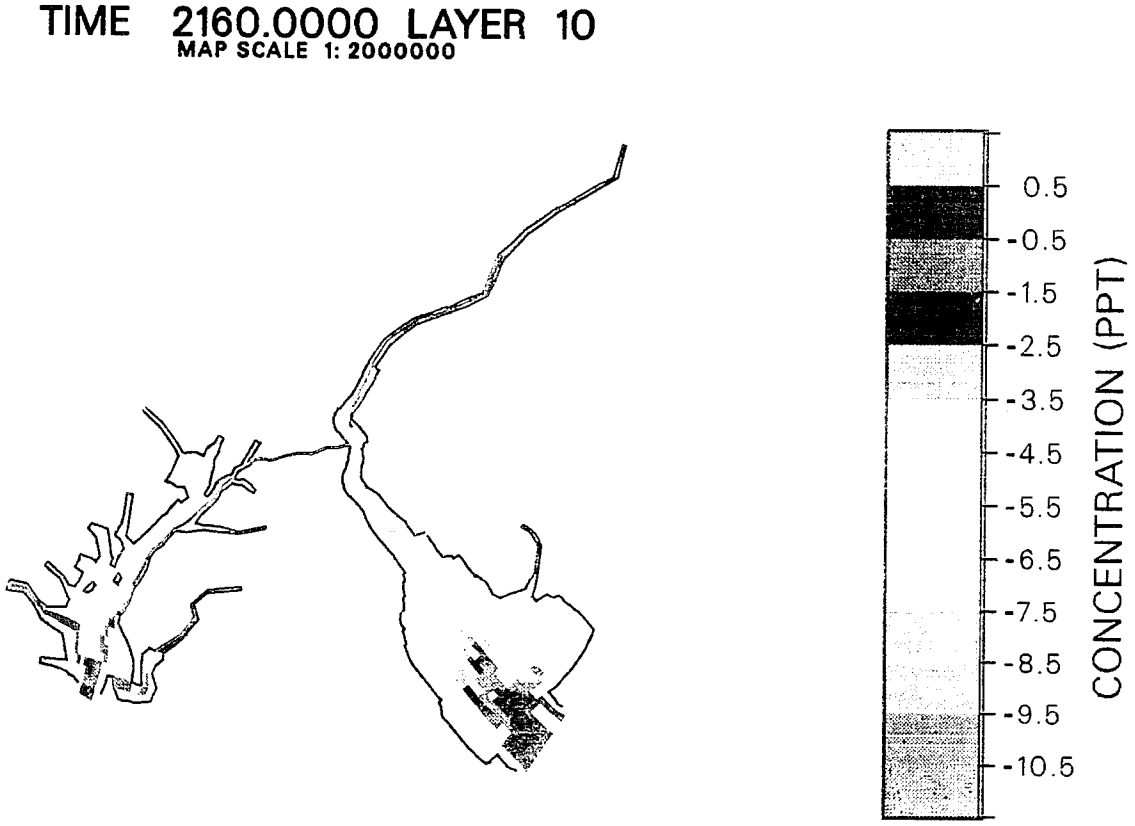

Figure 28d. Differences of seasonal averaged salinity (1972 vs 1985) in layer 10 (9.8 m)

Figure 29a. Differences of seasonal averaged flow (lowest-low, 1964) due to proposed channel deepening in layer 16 (0.8 m)

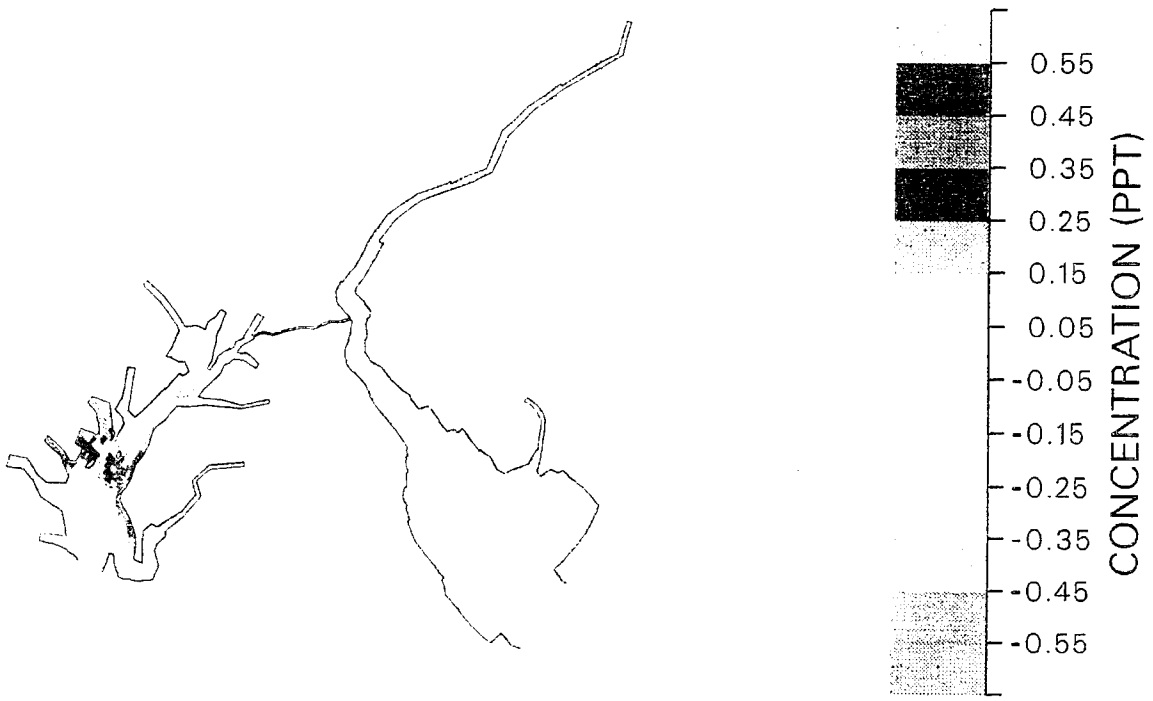

Figure 29b. Differences of seasonal averaged salinity (lowest-low, 1964) due to proposed channel deepening in layer 16 (0.8 m)

Figure 30a. Differences of seasonal averaged flow (highest-low, 1977) due to proposed channel deepening in layer 16 (0.8 m)

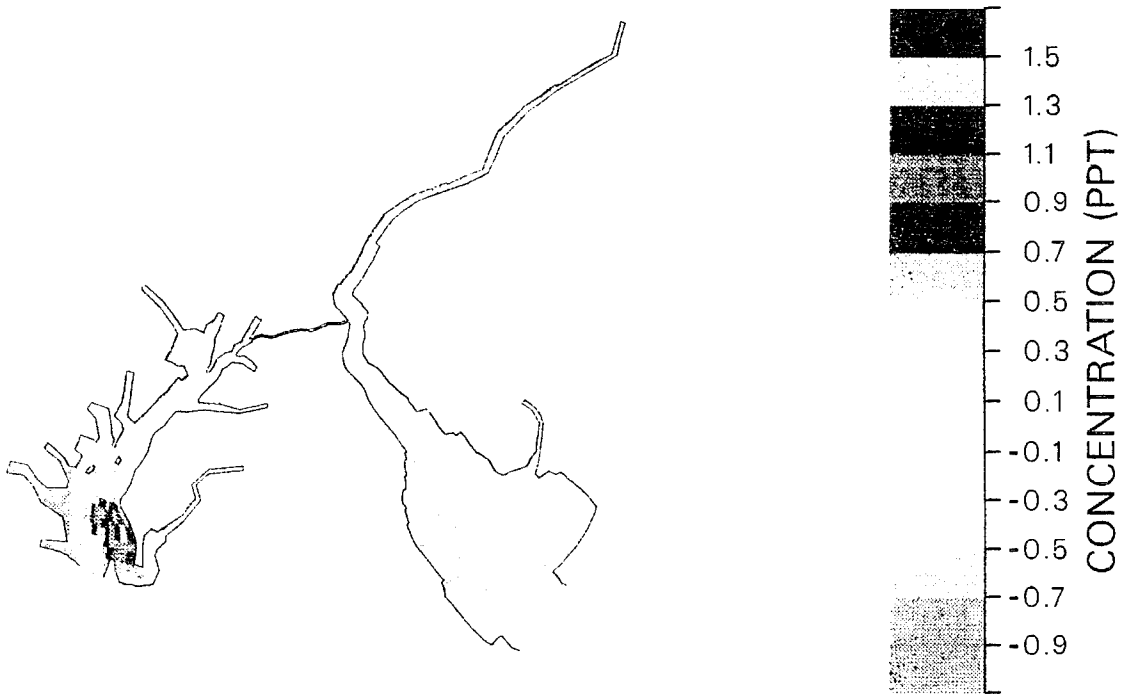

Figure 30b. Differences of seasonal averaged salinity (highest-low, 1977) due to proposed channel deepening in layer 16 (0.8 m)

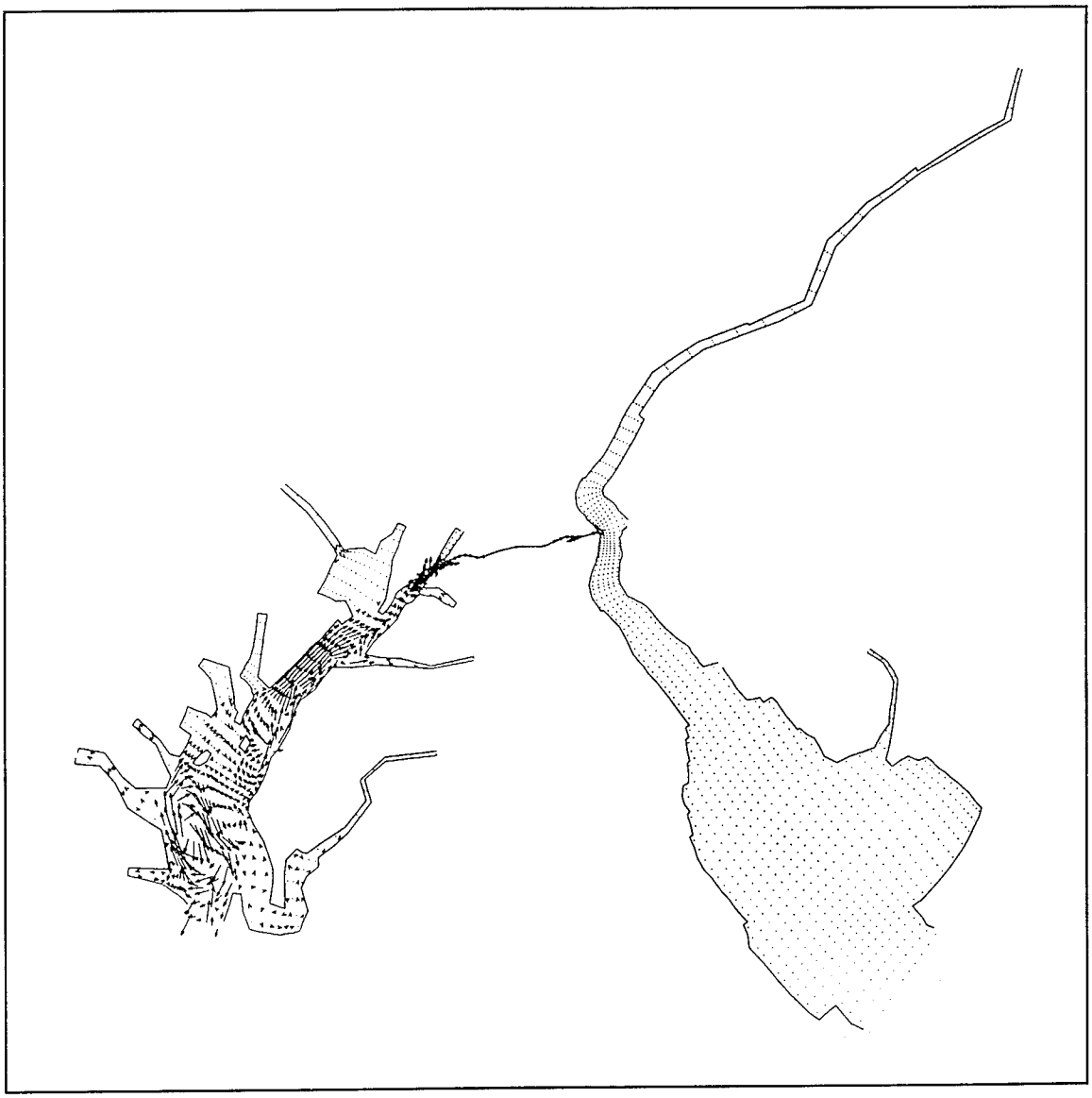

Figure 31a. Differences of seasonal averaged flow (highest-high, 1972) due to proposed channel deepening in layer 16 (0.8 m)

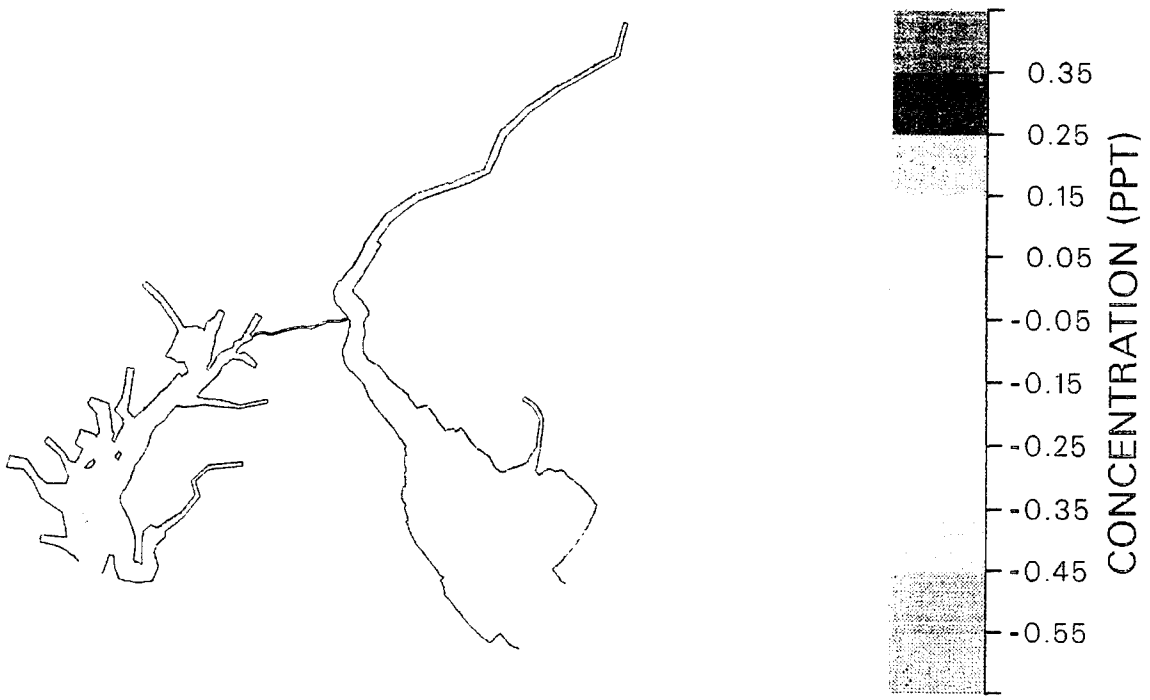

Figure 31b. Differences of seasonal averaged salinity (highest-high, 1972) due to proposed channel deepening in layer 16 (0.8 m)

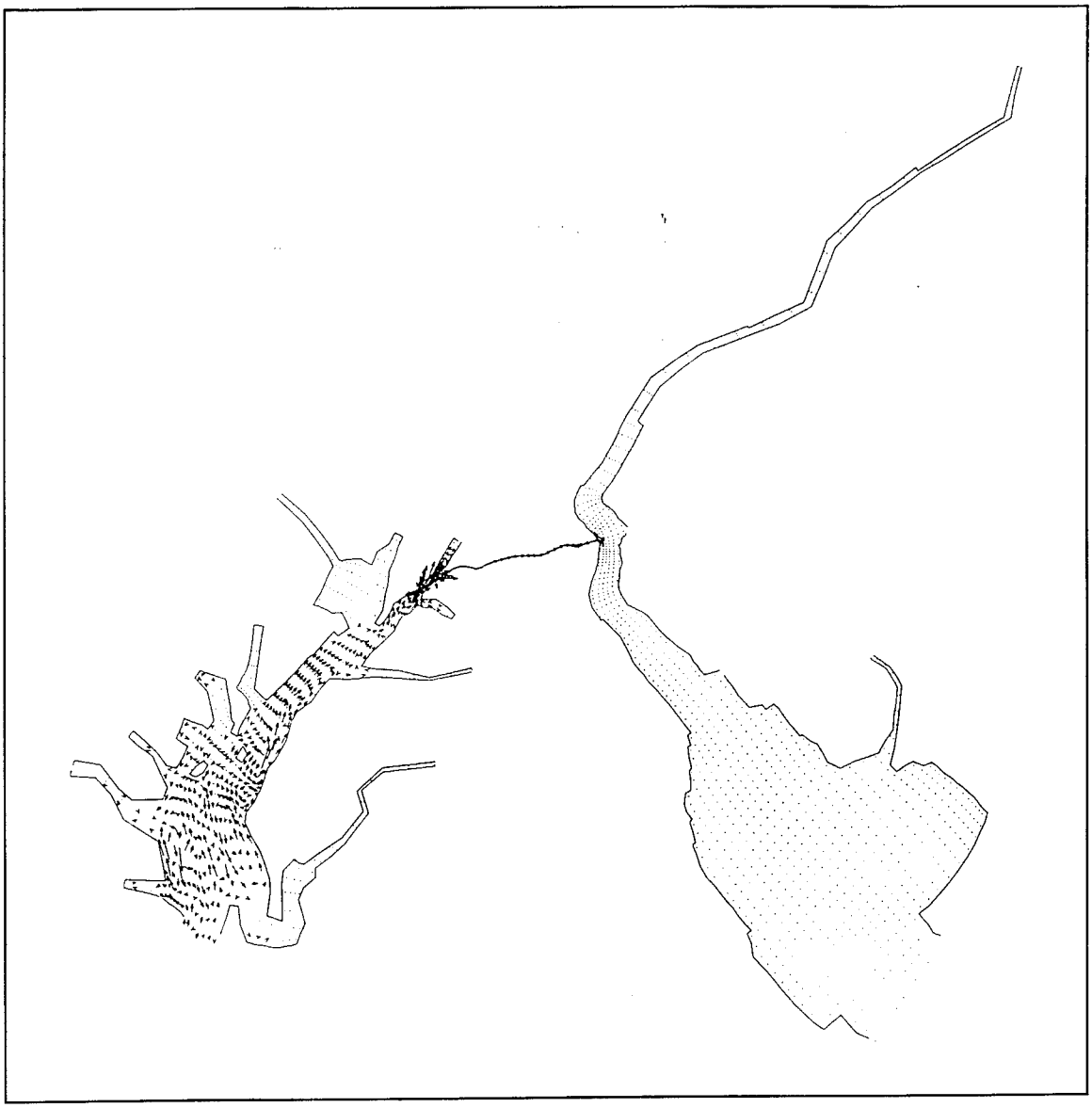

Figure 32a. Differences of seasonal averaged flow (lowest-high, 1985) due to proposed channel deepening in layer 16 (0.8 m)

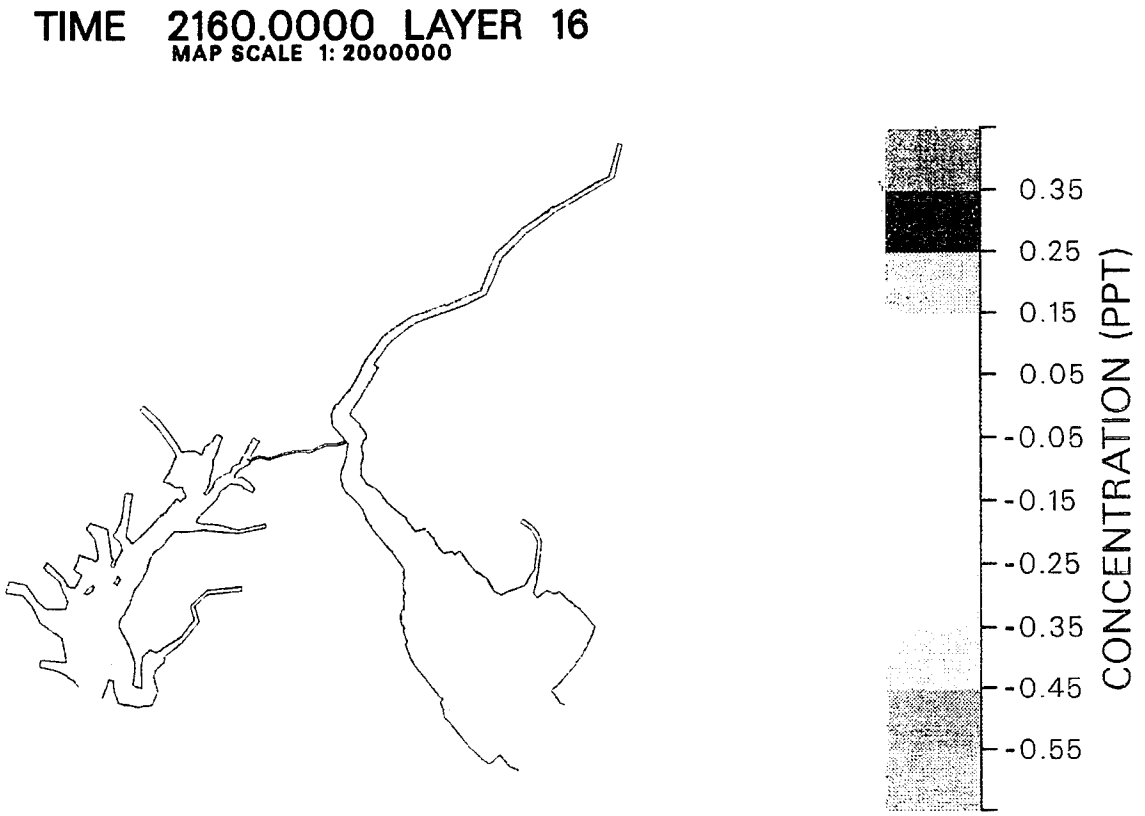

Figure 32b. Differences of seasonal averaged salinity (lowest-high, 1985) due to proposed channel deepening in layer 16 (0.8 m)

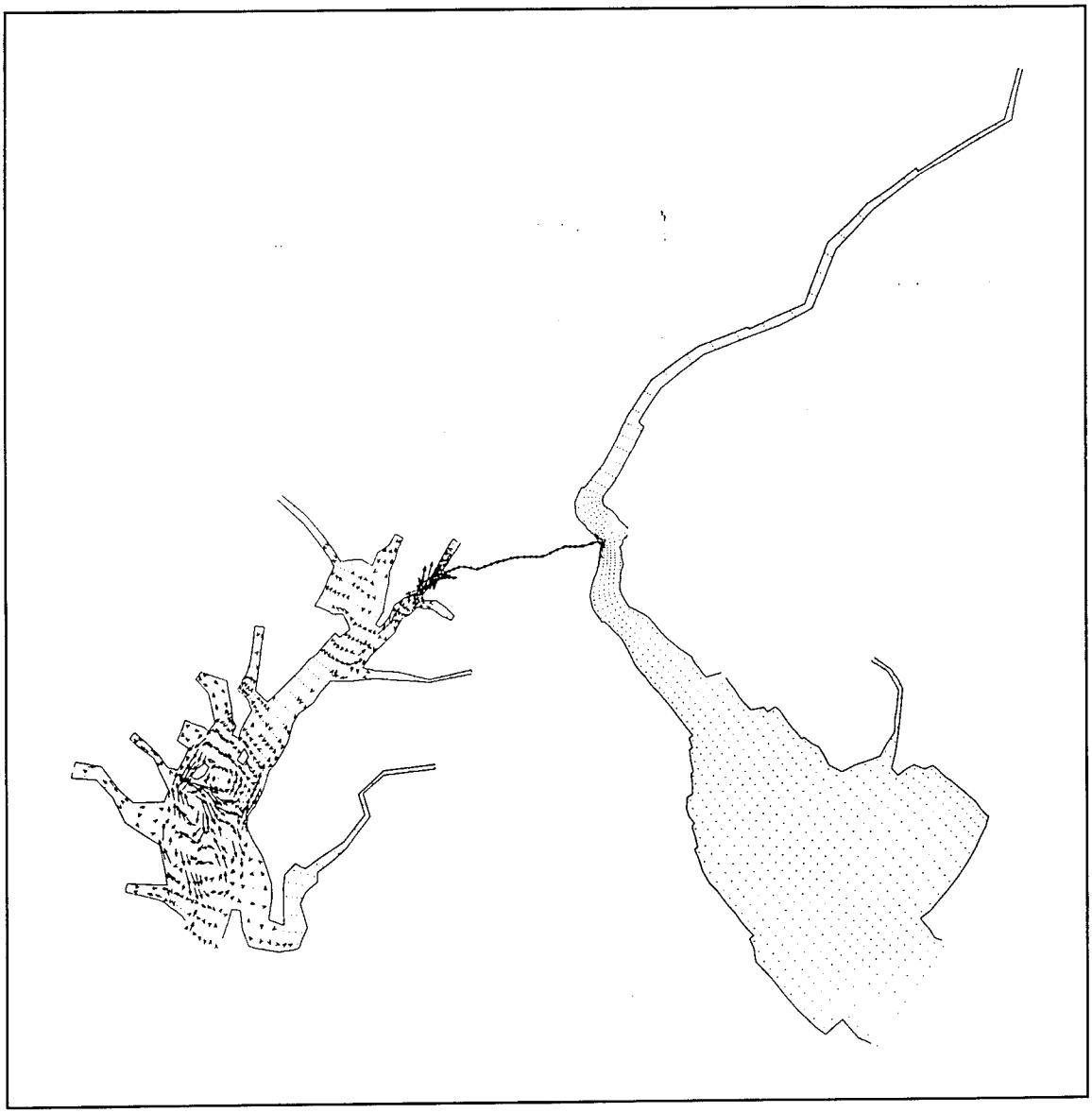

Figure 33a. Differences of seasonal averaged flow (lowest-low, 1964) due to channel deepening test 1 in layer 16 (0.8 m)

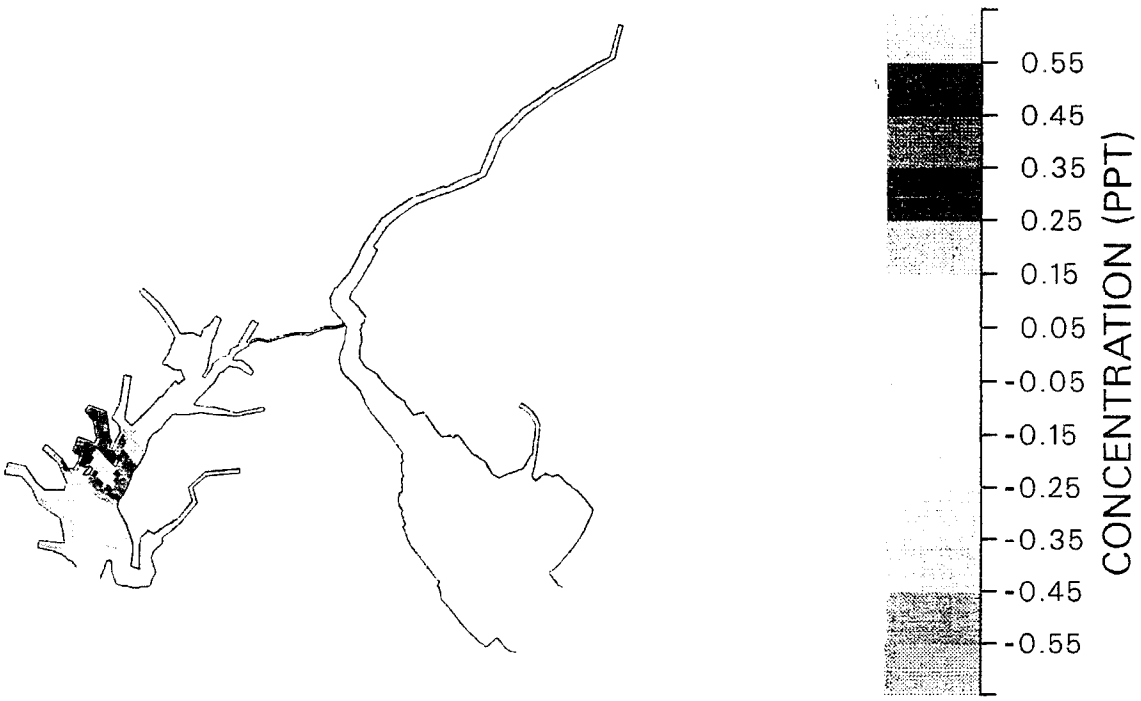

Figure 33b. Differences of seasonal averaged salinity (lowest-low, 1964) due to channel deepening test 1 in layer 16 (0.8 m)

Figure 33c. Differences of seasonal averaged flow (lowest-low, 1964) due to channel deepening test 2 in layer 16 (0.8 m)

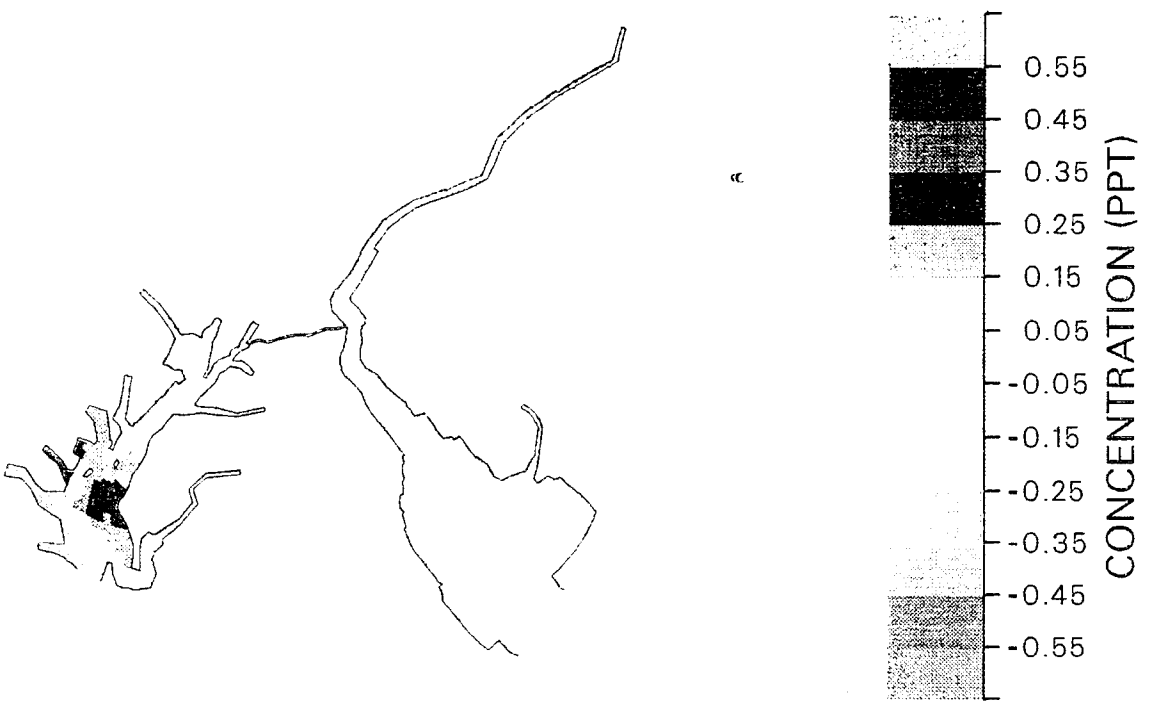

Figure 33d. Differences of seasonal averaged salinity (lowest-low, 1964) due to channel deepening test 2 in layer 16 (0.8 m)

Figure 34a. Differences of seasonal averaged flow (highest-low, 1977) due to channel deepening test 1 in layer 16 (0.8 m)

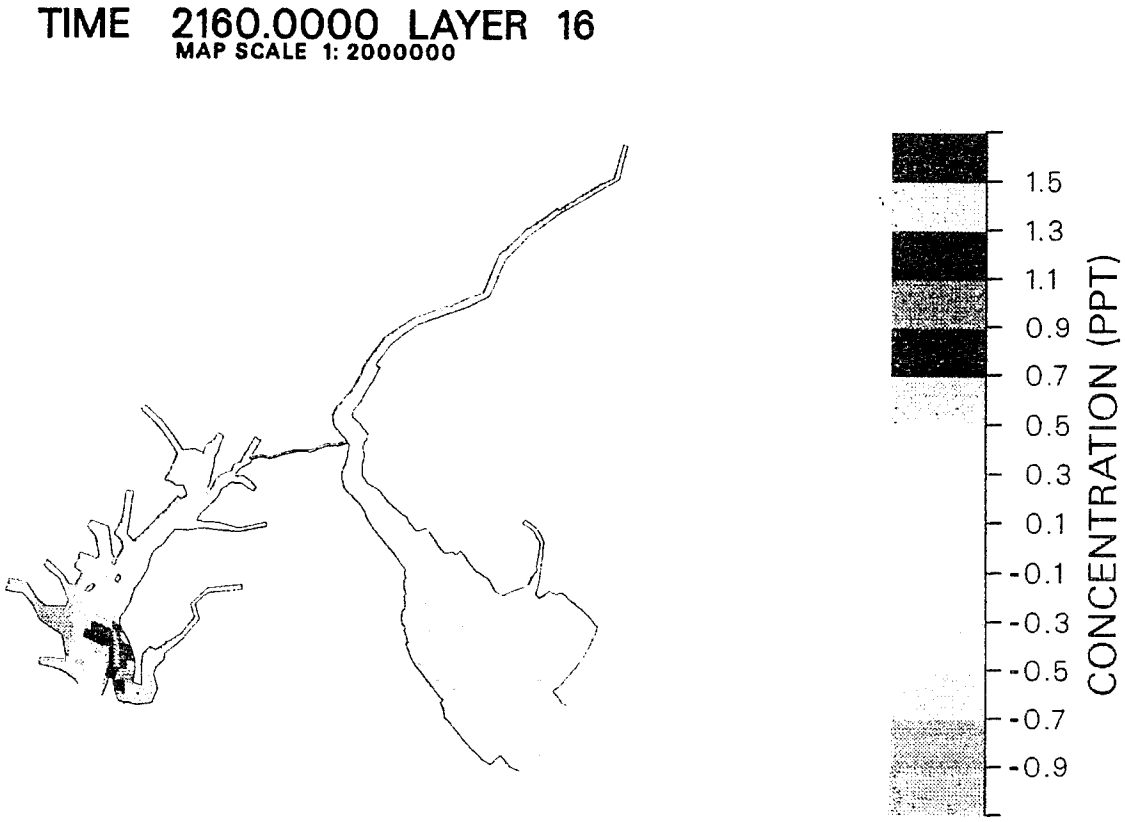

Figure 34b. Differences of seasonal averaged salinity (highest-low, 1977) due to channel deepening test 1 in layer 16 (0.8 m)

Figure 34c. Differences of seasonal averaged flow (highest-low, 1977) due to channel deepening test 2 in layer 16 (0.8 m)

Figure 34d. Differences of seasonal averaged salinity (highest-low, 1977) due to channel deepening test 2 in layer 16 (0.8 m)

Figure 35a. Differences of seasonal averaged flow (highest-high, 1972) due to channel deepening test 1 in layer 16 (0.8 m)

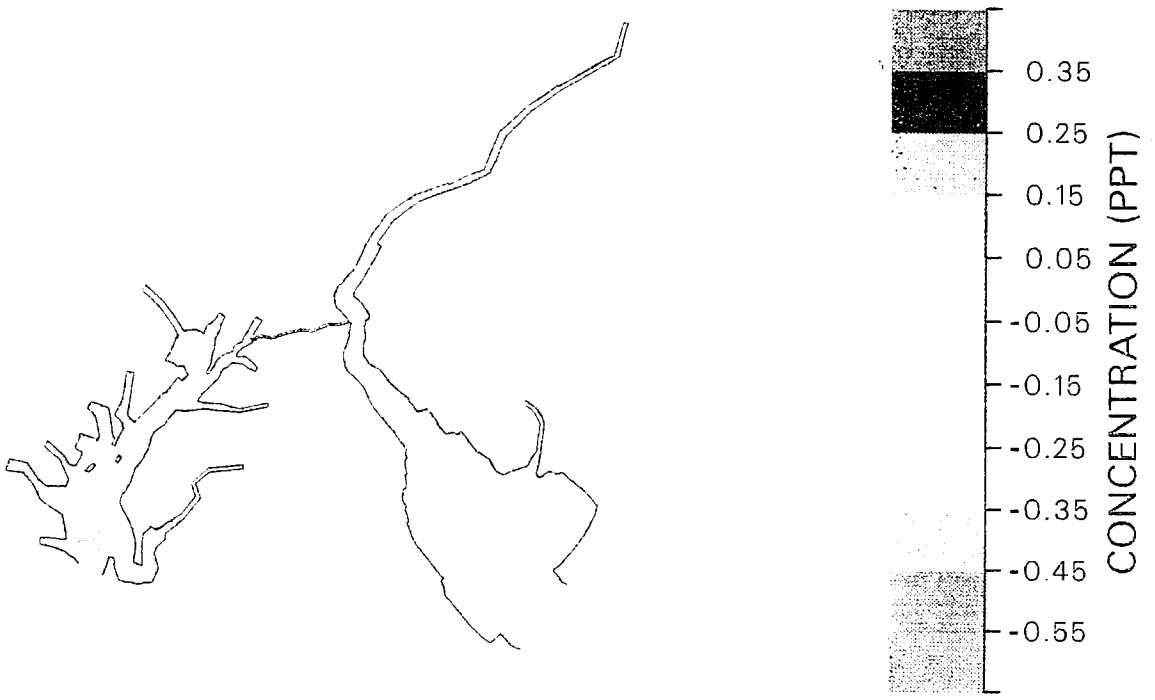

Figure 35b. Differences of seasonal averaged salinity (highest-high, 1972) due to channel deepening test 1 in layer 16 (0.8 m)

Figure 35c. Differences of seasonal averaged flow (highest-high, 1972) due to channel deepening test 2 in layer 16 (0.8 m)

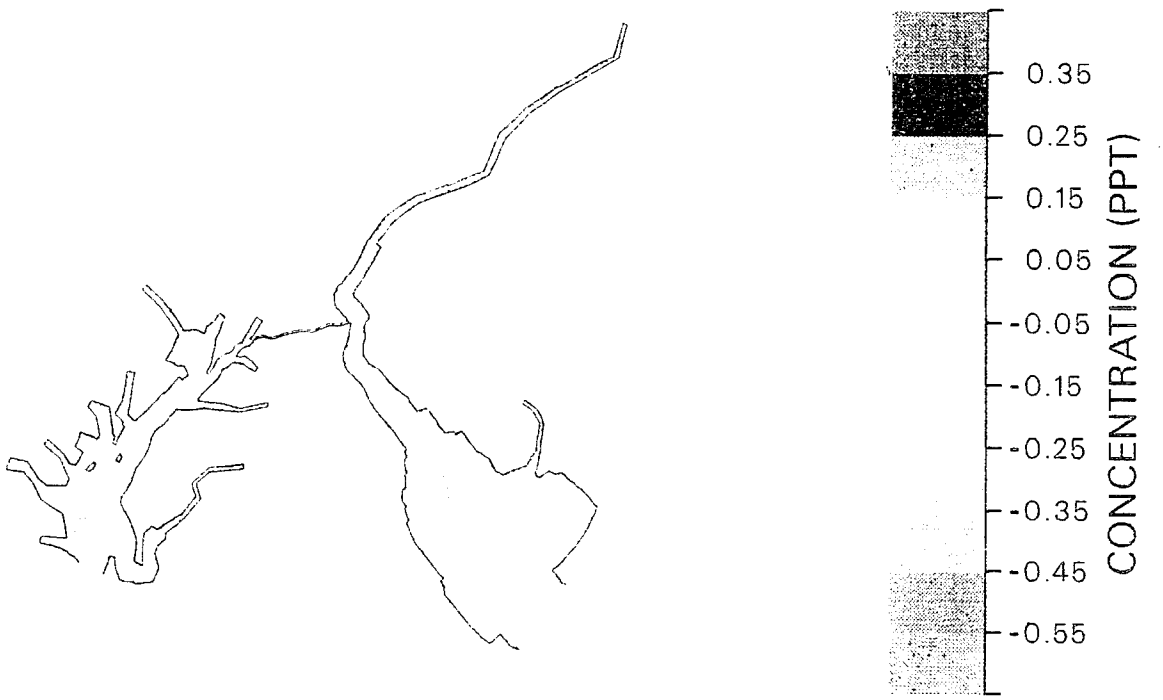

Figure 35d. Differences of seasonal averaged salinity (highest-high, 1977) due to channel deepening test 2 in layer 16 (0.8 m)

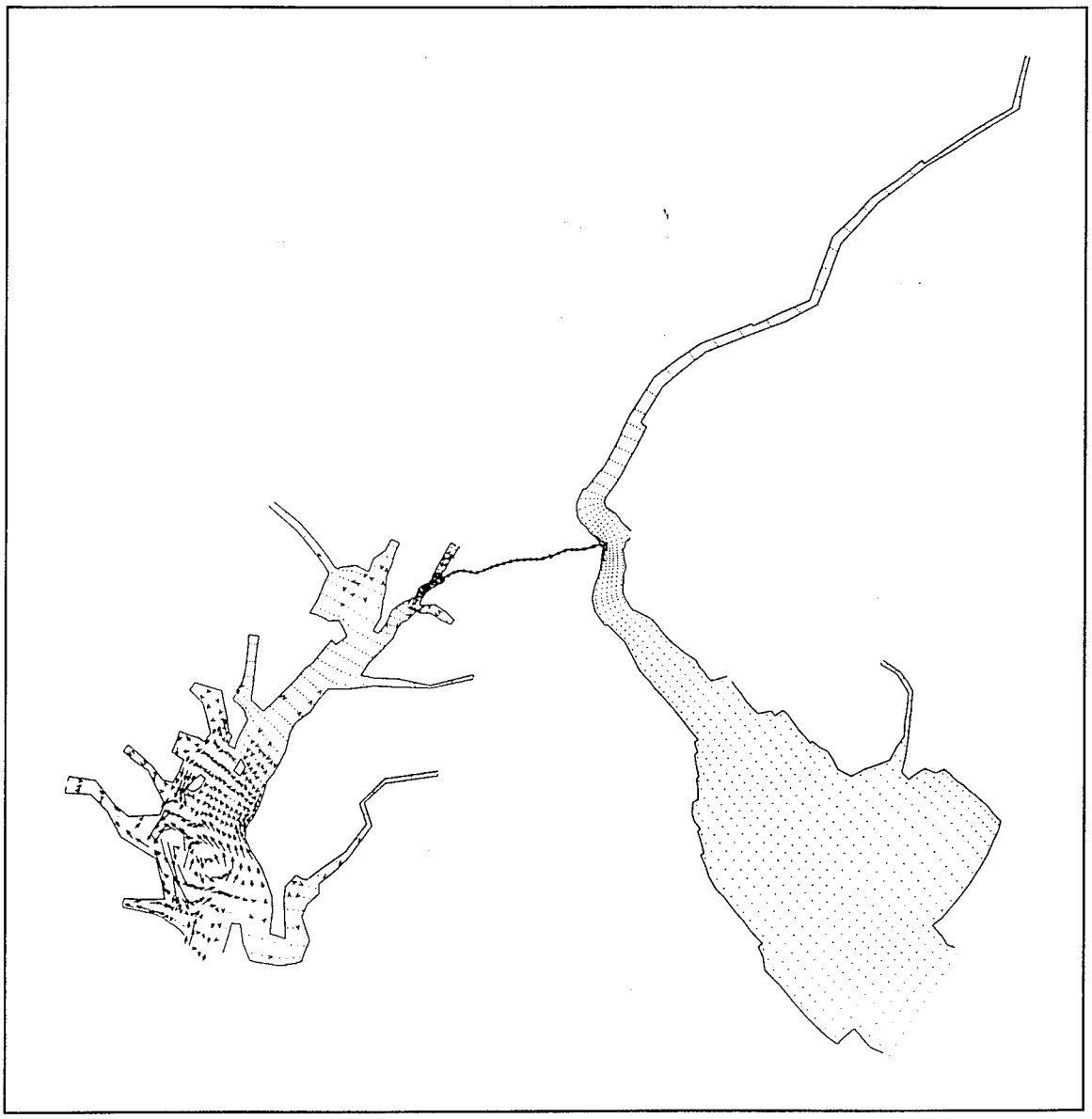

Figure 36a. Differences of seasonal averaged flow (lowest-high, 1985) due to channel deepening test 1 in layer 16 (0.8 m)

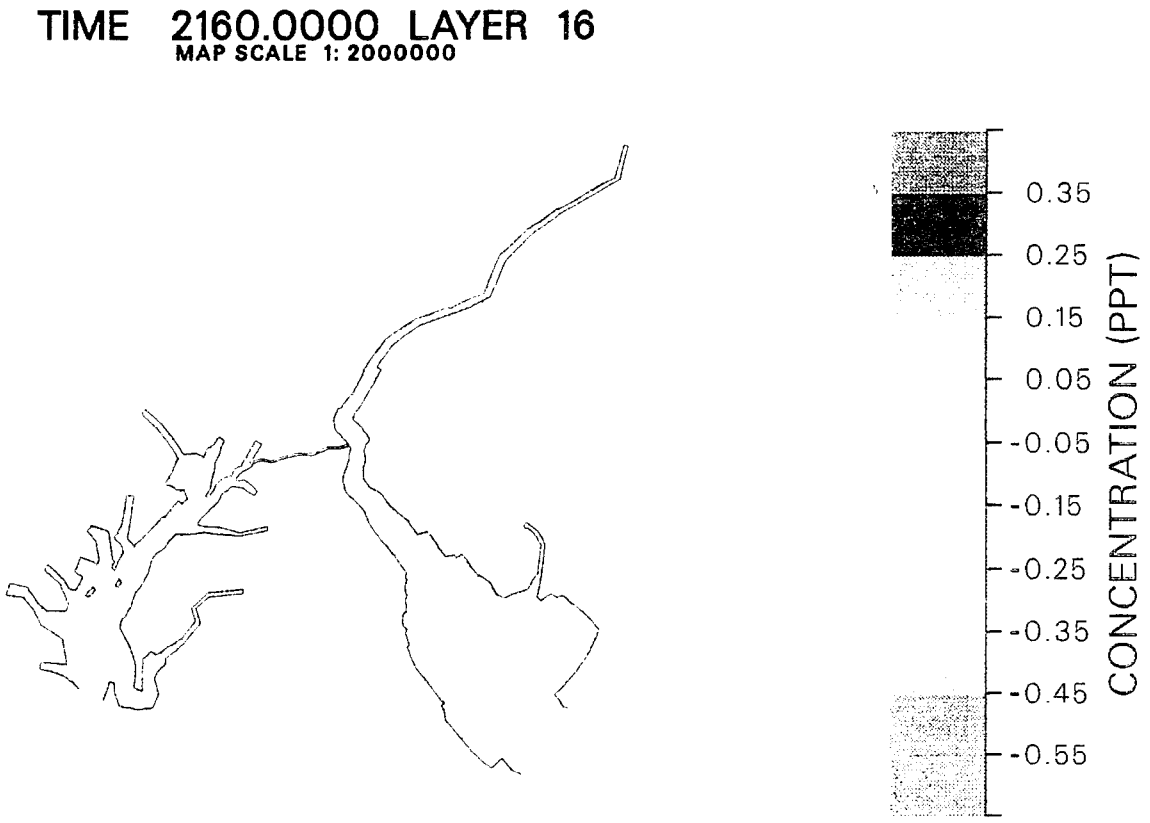

Figure 36b. Differences of seasonal averaged salinity (lowest-high, 1985) due to channel deepening test 1 in layer 16 (0.8 m)

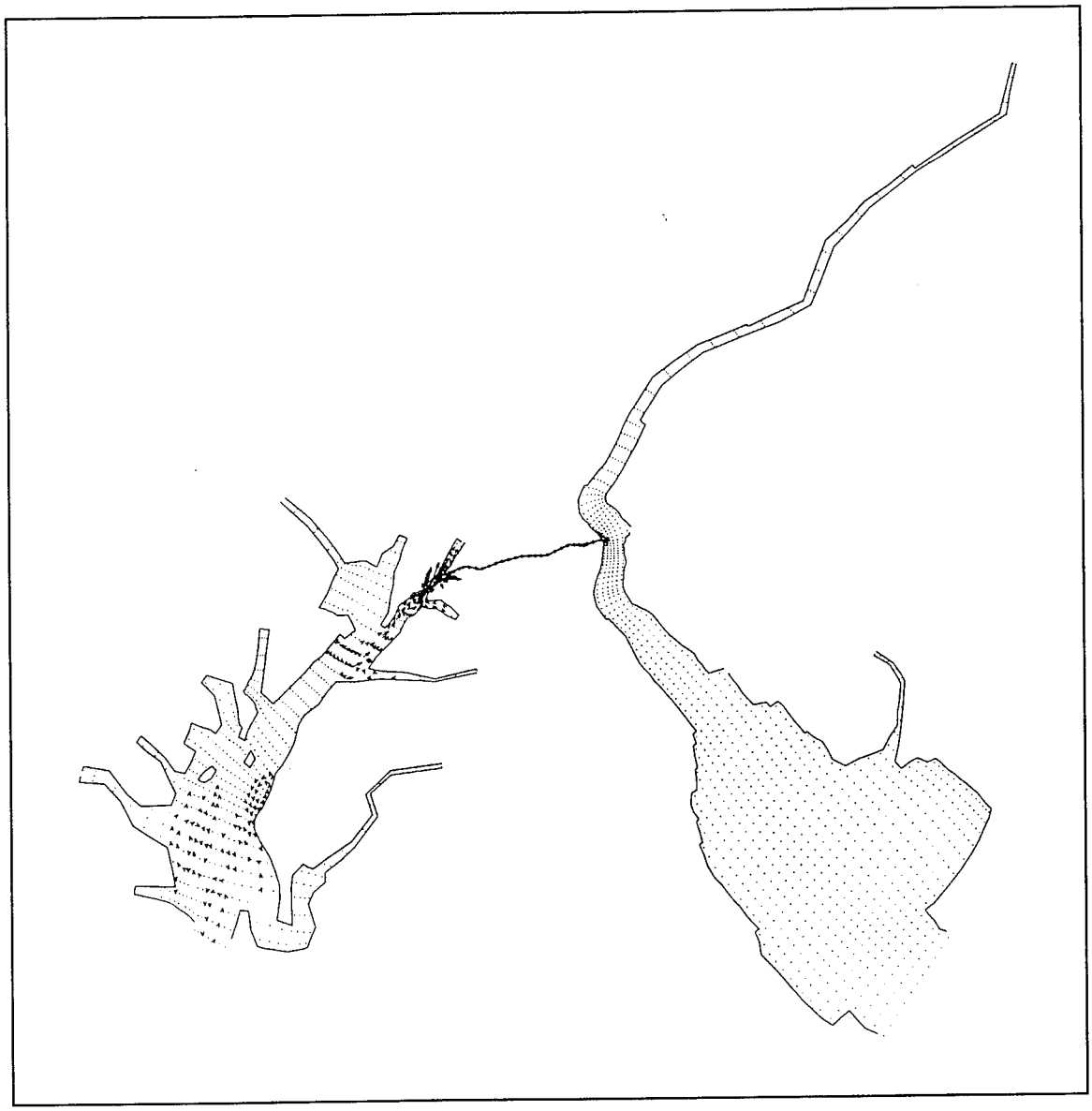

Figure 36c. Differences of seasonal averaged flow (lowest-high, 1985) due to channel deepening test 2 in layer 16 (0.8 m)

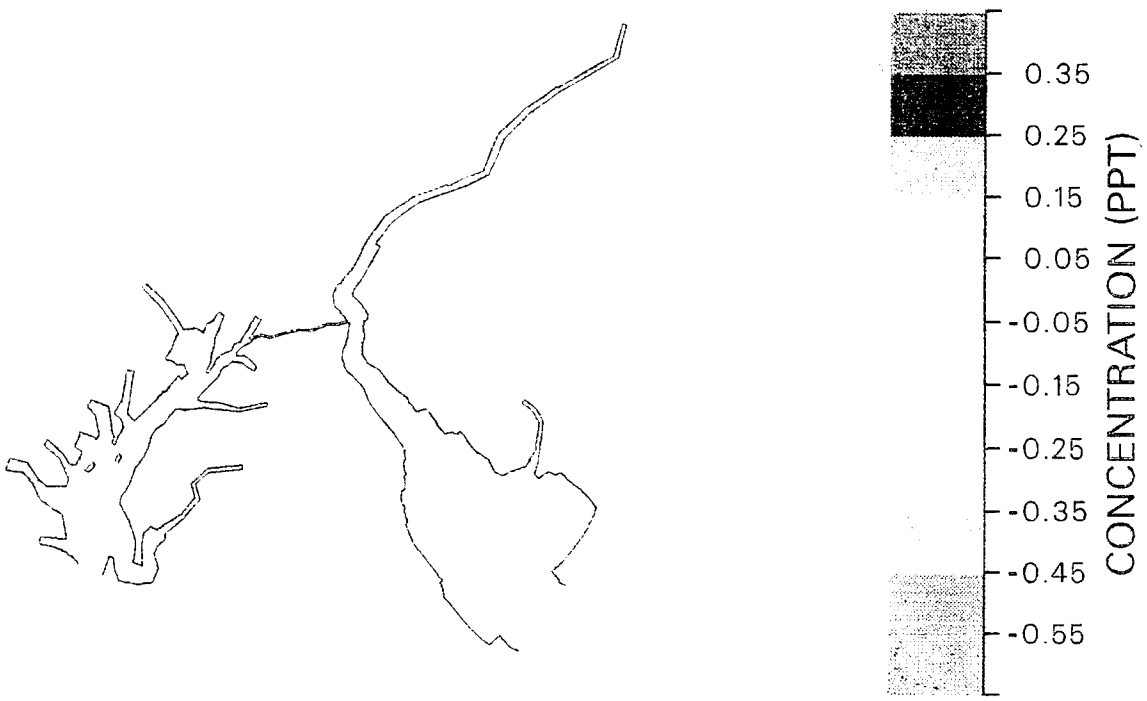

Figure 36d. Differences of seasonal averaged salinity (lowest-high, 1985) due to channel deepening test 2 in layer 16 (0.8 m)

REPORT DOCUMENTATION PAGE

Form Approved
OMB No. 0704-0188

1. AGENCY USE ONLY *(Leave blank)*	2. REPORT DATE	3. REPORT TYPE AND DATES COVERED
	April 1996	Final report

4. TITLE AND SUBTITLE
Three-Dimensional Numerical Simulation of Seasonal Flow and Salt Transport for the C&D Canal

5. FUNDING NUMBERS

6. AUTHOR(S)
Bernard B. Hsieh, David R. Richards

7. PERFORMING ORGANIZATION NAME(S) AND ADDRESS(ES)
U.S. Army Engineer Waterways Experiment Station
3909 Halls Ferry Road, Vicksburg, MS 39180-6199

8. PERFORMING ORGANIZATION REPORT NUMBER
Technical Report HL-96-14

9. SPONSORING/MONITORING AGENCY NAME(S) AND ADDRESS(ES)
U.S. Army Engineer District, Philadelphia
Wanamaker Building
100 Penn Square East
Philadelphia, PA 19107-3390

10. SPONSORING/MONITORING AGENCY REPORT NUMBER

11. SUPPLEMENTARY NOTES
Available from National Technical Information Service, 5285 Port Royal Road, Springfield, VA 22161.

12a. DISTRIBUTION/AVAILABILITY STATEMENT
Approved for public release; distribution is unlimited.

12b. DISTRIBUTION CODE

13. ABSTRACT ***(Maximum 200 words)***

Three-dimensional flow and transport models were developed to study the impact of deepening the C&D Canal and approach channel in Chesapeake Bay from 35 ft to 40 ft. The area modelled included Delaware Bay from the Atlantic Ocean upstream to the head of tide, the C&D Canal, and the upper Chesapeake Bay from Annapolis, MD, upstream to the head of tide. The boundary conditions for the models were based on two 3-month seasonal periods. The models were verified with observed prototype data and found accurate for water-surface elevations, tidal currents, and salinity distributions. Twenty-four simulations were conducted with a wide range of boundary conditions and geometries, including combinations of freshwater inflow, tide, and salinity boundary conditions. The low-flow, medium-flow, and high-flow conditions were determined using a statistical analysis of the historical records.

14. SUBJECT TERMS
C&D Canal
Estuary
Flow and salt transport
Seasonal simulation
Three-dimensional hydrodynamic model

15. NUMBER OF PAGES
124

16. PRICE CODE

17. SECURITY CLASSIFICATION OF REPORT	18. SECURITY CLASSIFICATION OF THIS PAGE	19. SECURITY CLASSIFICATION OF ABSTRACT	20. LIMITATION OF ABSTRACT
UNCLASSIFIED	UNCLASSIFIED		